Application of an Equilibrium Coastline Position Prediction Technique

By

Brendan Dollard, MIEI

A thesis submitted in part fulfilment of the requirements for the degree of M.Eng.

Submitted to: **Dublin City University**

School of Mechanical and Manufacturing Engineering

Dublin 9

Research Supervisors: **Dr. Lisa Looney**

Professor Saleem Hashmi

June 1998

DECLARATION

I hereby certify that this material, which I now submit for assessment on the programme of study leading to the award of the degree of M.Eng. is entirely my own work and has not been taken from the work of others save and to the extent that such work has been cited and acknowledged within the text of my work.

Signed : Barl Dill Date : 16/6/98

Student Number : 94971587

ACKNOWLEDGEMENT

I wish to express my thanks to the all those who have provided me with guidance and the enthusiasm needed to complete this thesis, especially my research supervisors Dr. Lisa Looney and Professor Saleem Hashmi of the School of Mechanical and Manufacturing Engineering, Dublin City University. I would also like to express my gratitude to my understanding colleagues in the Offshore & Coastal Engineering Unit in Forbairt particularly my previous and present patient managers Frank Motherway and Neil Kerrigan, Forbairt's Staff Development section and to my wife Sheila for allowing me to excuse myself from many domestic projects to which I can now devote my full attention.

ABSTRACT

APPLICATION OF AN EQUILIBRIUM COASTLINE POSITION PREDICTION TECHNIQUE

Brendan Dollard, MIEI

Coastal erosion is of significant interest in Ireland where reliable prediction of erosion patterns would facilitate planning for development of coastal regions. In the past, uncertainty about erosion trends has led to decisions which had costly, and environmentally detrimental, effects. The modern approach is to try to accommodate erosion rather than to prevent it. One of the ways to limit the economic cost of surrendering land to the sea is to restrict developments in areas which are under threat. This approach however requires a reliable forecast of future erosion trends. Erosion is a complex process, involving interacting factors such as wind climate, wave transformation, current effects, sea level changes, etc. which contribute to sediment transport rates. Simulation models of the process are therefore very difficult to develop, and the unavailability or expense of collecting detailed input data required for such models often prohibit their use.

Empirical models are easier to apply, and in the current research one such recently developed model, the parabolic curve technique, is applied to investigate the stability of coastline position, and vulnerability to coastal erosion. It is the first application of the technique specifically to Irish sites, and considers three bays on the east coast in Co. Wexford. Use of the technique required the gathering of data on the dominant wave approach angle, and the location of bay headlands. The study has simplified the application of the technique by the use of standard spreadsheet and graphing software. Difficulties associated with locating control points are discussed. Two different methods are used to determine the dominant wave direction, one based on the current planform or shape of the bay, and the other based on wave energy calculations.

Results show that the present coastlines in two of the three bays do not follow the 'natural' curvature prescribed by present climatic and geographic conditions. All three bays will suffer significant further erosion before reaching a state of 'static' equilibrium. The technique is used to consider future evolution of the coast, by testing the effect of changes in current wind / wave climate brought about by global warming. Erosion is seen to increase, however as bays reorient themselves toward more easterly waves, the lee of headlands will become less vulnerable to erosion. The thesis concludes with remarks on the applicability of the methods, the usefulness of predictions, and makes recommendations for future investigations.

CONTENTS

1. INTRODUCTION AND LITERATURE SURVEY

1.1 Introduction

Coastal erosion is a natural process where land is eaten away by the sea. It is as natural as the weathering of mountains or the tectonic activity that created them. The driving force behind it is the sun's energy as it unevenly heats the earth creating the winds that drive the sea waves. The vast amount of energy stored in these waves is dissipated on the coast causing sands and gravel to move and land to be eroded. It has, historically, always been regarded as a personal insult to mankind and ingenious methods have been devised to counteract it. Only in the latter half of this century have efforts been made to understand it.

Coastal erosion in Ireland is widespread with natural erosion rates on the increase due to rising sea levels which are caused, in part at least, by global warming. In areas where waves approach the coast predominantly from a particular direction there is as a consequence a movement of sediment in that direction. These areas are most susceptible to erosion as the rate of this longshore drift of sediment can fluctuate. When the supply of sediment decreases, soft coast such as beaches and backing dunes or clay cliffs erode. This is the case along much of the east coast of Ireland and is a more serious problem than the more common in-out movement of sediment associated with storms on the more indented western and southern coasts.

Dealing with this problem by coastal protection measures is an expensive enterprise. Along the eastern seaboard the 7 county councils and city boroughs estimate that of the

total coastline length of 593 km almost 440 km is at risk of erosion with over 218 km requiring immediate attention [1]. The cost of the immediate measures was estimated at £45m in 1992. Any technique that could reduce these costs would be extremely valuable to the country and one of the methods currently being employed is to restrict developments in areas which are likely to erode. This is known as the 'set-back line' technique which is where a line is drawn on a map seaward of which new developments are either restricted or not permitted. This will reduce the need for coastal protection measures in the future.

The decision of where to draw this line is, at present, not scientifically based. In some counties it is the nearest road or railway in the belief that if a road or railway is threatened then the problem is, at least in part, a national one and central government funds are easier to acquire. In others the line is set at a specific distance from the sea. In some cases this is based on the local erosion rate and the typical life expectancy of developments in the area.

Both of these methods are open to criticism. In some cases the lines drawn are overly conservative and developments which the sea would not reach in hundreds of years are denied permission. In others the set back lines are too near the sea and could be reached in 20 or 30 years.

Essentially there have been two approaches to resolving the problem of predicting erosion. With the advent of computers one approach has been to attempt to simulate in a computer model the myriad of interacting coastal processes such as local wind climate effects, wave transformation, current effects, sediment movement, sea level

changes, etc. The aim of this is to calculate the long term sediment transport rates which will determine whether a coast recedes or advances seaward. With accurate and detailed input data these models can provide an accurate picture of the future evolution of the coast. Unfortunately, in Ireland as with most countries, there is a lack of such data and the cost of collecting it, in many cases, would make the investigation into the problem, let alone any solution, uneconomical.

The other approach is to use empirical formulae derived from wave tank experiments where waves were run up on an originally straight sandy shore [2]. As the coastline evolved between two artificial headlands the bay coastline position was noted. The final evolved position, known as the static equilibrium position (SEP) because there was no sediment entering or leaving the bay, was plotted for various wave approach angles and bay lengths. This data led to the development of a formula and set of curves which can be used to predict the SEP for any bay once the dominant wave approach angle and bay headlands (control points) are known. It can also be used to indicate whether the curvature of bays which are in a state of dynamic equilibrium (where sediment is passing through the bay) is following a 'natural' relatively stable curve.

This thesis examines the application of a recently developed parabolic curve technique which seeks to predict the limit of erosion within a bay. Here, it has been applied to three bays on the east coast of Ireland each of which suffers from severe marine erosion with localised erosion rates of up to 0.75m/year over the past 70 years.

1.2 Coastal engineering

Coastal Engineering as a term used to define a specific field of engineering has its origin in a meeting held in Long Beach, California in 1950 entitled 'The First Conference in Coastal Engineering'. The concept of trying to control the sea, however dates from much earlier. Inman [3] when examining harbour construction in the Mediterranean Sea as early as 1000-2000 BC commented on the 'very superior lay understanding' that these untutored developers showed in working with the natural forces of waves and tides. Brunn [4] discussed some of the early coastal erosion control methods used in England, Holland and Denmark starting in the 10^{th} century. In the 11^{th} century, the Danish King of England, King Canute, is reputed to have used the disobedient flowing tide as evidence of the limitation of his mortal powers.

Coastal Engineering is primarily a branch of Civil Engineering which involves the sciences of oceanography, meteorology, fluid mechanics, structural mechanics, geology and geomorphology. A good practical understanding of mathematics and statistics as well as computer modelling techniques is also required. Coastal Engineering covers a number of activities such as;

- nearshore wave climate analysis
- design of coastal protection works
- harbour design
- prediction of water levels
- stabilisation of tidal entrances by dredging and/or training walls
- control and collection of oil spills

- navigation channel dredging
- control of marine erosion

Of these it is the latter activity which mainly concerns this research.

The coast is where water, land and air meet. It is where vast amounts of energy are dissipated on the shore through a series of complex coastal processes. Consequently, the coastal environment is one of the most changeable environments on the earth's surface and one which is also the most susceptible to damage from interference by man. Indeed it is this interference, through harbour developments and, ironically, coastal protection works, that have led to increased erosion rates at many points around Ireland [1].

Coastal protection measures attempt to prevent erosion of the land using either 'hard engineering' techniques such as seawalls and revetments (rock mounds) or by 'soft engineering' techniques such as beach nourishment (dredging offshore sediment and placing it on the shore), marram grass planting and sand trap fencing. Seawalls and revetments reflect and absorb wave energy thus protecting the coast. Soft engineering techniques try to emulate and speed up natural processes such as the creation of sand dunes by trapping wind blown sand, or by directly placing dredged sand on a beach in order to build up the coastal mass and better enable it to withstand storms. These measures also help sandy coastlines to self repair in the aftermath of damaging storms.

With the advent of a better understanding of coastal processes and the rise of environmental concerns management of the coastal zone has become much more

important. The primary objectives of Coastal Zone Management (CZM) is that all developments (including coastal protection measures) should be sustainable [5]. This requires that developments should be, as far as possible, compatible with the immediate environment. On eroding coast this management will include soft engineering techniques (with perhaps a minimum of hard engineering in the form of revetments and groynes) but mainly involves the control of man's interference through land use restrictions and planning controls. The overriding principal is that it is neither economic nor possible to hold the line everywhere against the sea.

1.3 Coastal erosion and sediment transport

Probably the most important question in eroding coastal areas is, will the erosion eventually stop if left alone, and if so where ? If this question could be accurately answered then the decision coastal engineers face on whether to adopt coastal protection measures could be taken against a background of knowing what the consequences of not doing so would be. In areas of low development it may prove far more economic to surrender land to the sea and to compensate the owner than to try to protect the coast. Indeed prevention of erosion in many instances may deprive areas downcoast of much needed sediment. These areas may be more economically valuable.

In dealing with the problem of coastal erosion it is convenient to divide the coast into 'coastal cells'. Over the past 20 years attempts have been made to 'compartmentalise' the coast in order to put a practical limit on the area to be studied. The main concern is the transport of sediment. A coastal cell can be defined as 'the area in which sediment

transport is confined' (Fig. 1.1). This is relatively easy on indented coasts, where prominent headlands prevent sediment moving along the coast but on open coast such as the east coast of Ireland the problem is far more difficult [6].

By far, the most dominant force in shaping coastlines is wave energy. Waves cause sediment to move about the coast (Fig. 1.2). The direction of this movement is mainly from the beach to the nearshore in response to storms. This material is usually returned during calm periods. During winter, sediment is drawn down from the beach and sand dunes by storms to be deposited just offshore in the form of sand bars. These bars limit the amount of wave energy which impinges on the coast by causing waves to break further from the shore. During summer, the calmer seas move the sediment onshore to form beach berms (a raised area of beach) and much of this may be blown into the dune systems behind.

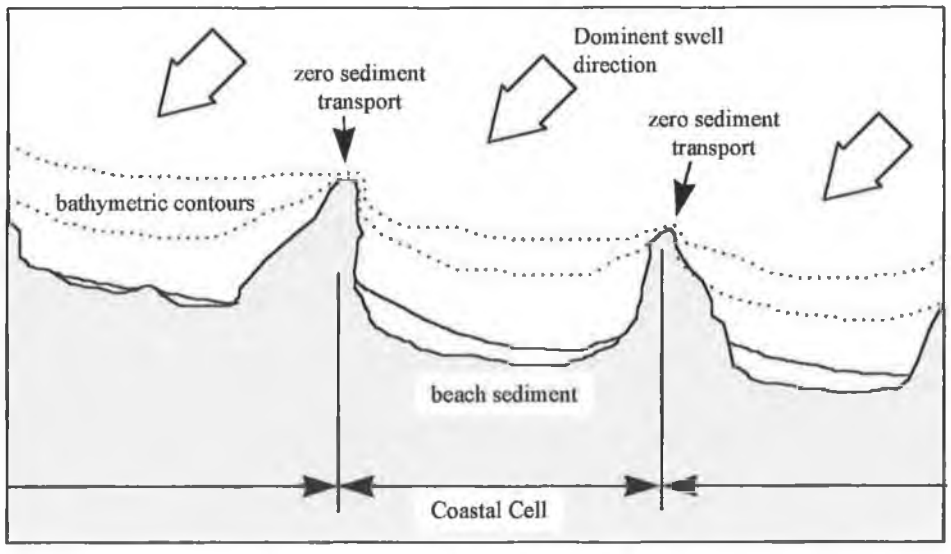

Fig. 1.1 - Idealised Coastal Cell

A more problematic form of sediment transport is longshore or littoral drift where sediment is moved along the coast. The direction and rate of littoral drift are directly

related to the amount of nearshore wave energy and particularly to the angle at which the waves strike the coast. This determines the longshore wave energy component of a wave field and this predominantly decides the speed and direction of the longshore current. The consequent movement of sediment alongshore, ultimately determines the shape of the coast. When this wave energy component is greater than zero, sediment will be moved along the coast until it reaches an area where the beach is more closely aligned to the waves. Here the longshore energy component drops to zero and the transport stops.

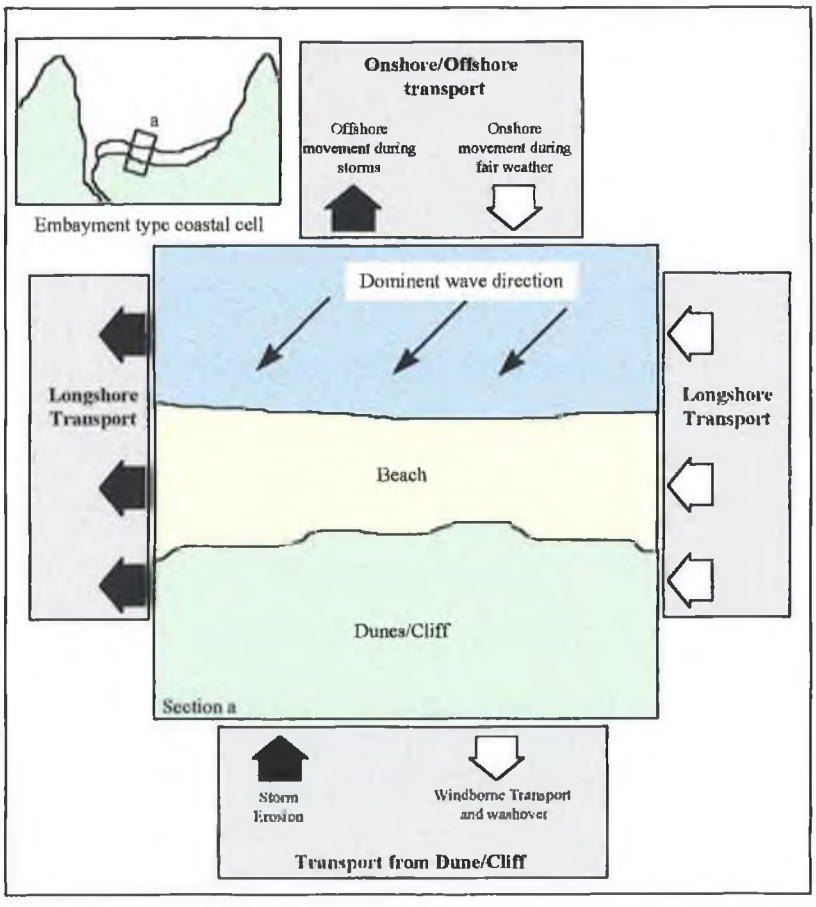

Fig. 1.2 - Sediment transport within a coastal cell [6].

As waves approach the coast the direction of their advance and the height of the waves is altered by wave refraction and, in the vicinity of headlands, wave diffraction.

Refraction is caused by the reduction in water depths as the wave moves shorewards. The velocity of the wave is reduced through the influence of the seabed on the orbital motion of the water particles within the wave. In Fig. 1.3 a simple illustration of wave refraction is given. The wave crest A_0-B_0 is entering shallower water. The water depth at point B_0 is greater than that at point A_0 and, from linear wave theory, the wave velocity is found to be greater at point B_0 than at point A_0. Thus the wave at A_0 is slower moving than at B_0. The result of this difference is to bend the wave towards the bathymetric contours. It can also be seen from the diagram that the wave rays, i.e. lines drawn at right angles to wave crests , are diverging as the wave crest moves shorewards. This divergence of the rays results in a spreading of wave energy leading to a reduction in wave height with the height of the wave crest A_1-B_1 being lower than A_0-B_0.

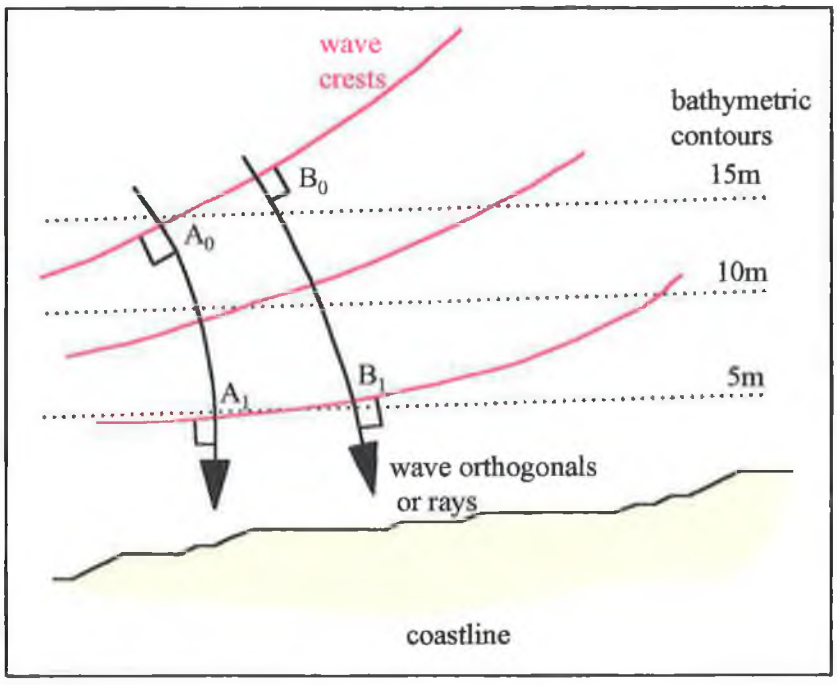

Fig. 1.3 - Wave refraction

Wave diffraction is a result of the diffusion of wave energy into areas behind headlands, breakwaters, etc. When part of a wave front is blocked by a barrier, wave energy will

spill laterally along the wave crests into the shadow area created by the obstruction. As seen in Fig. 1.4 when waves pass a barrier, i.e. the jetty in this example, wave energy will dissipate laterally along the wave crest into the area behind the obstruction. Due to this spreading of wave energy the resultant wave height of the diffracted waves are lower than that of the incident wave.

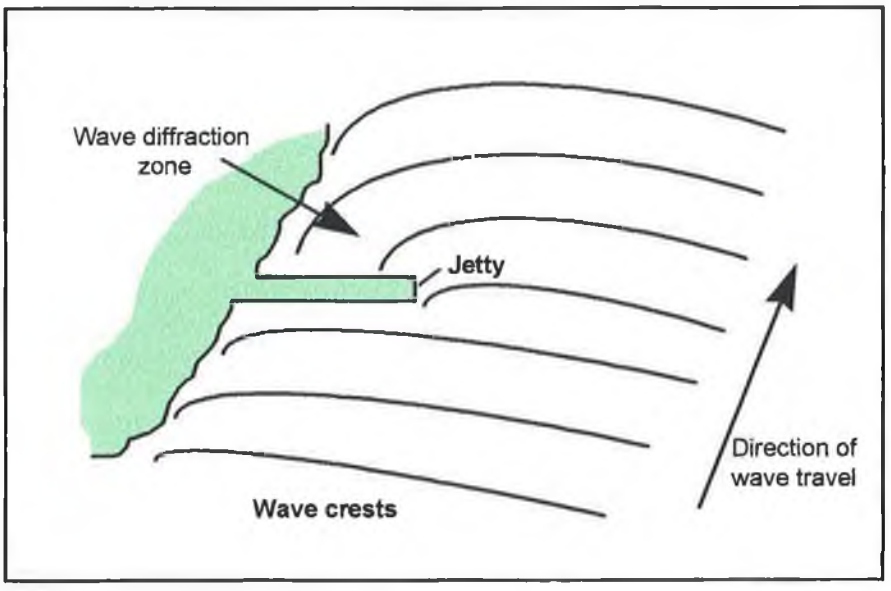

Fig. 1.4 - Wave diffraction

The relationship between sediment transport and longshore wave energy is described by the CERC (Coastal Engineering Research Centre, a division of the US Army Corps of Engineers) [7] as the equation shown in Fig. 1.5. This equation emerged from fundamental research on sediment drift rates and wave energy carried out on the Californian coast between 1950 and 1970. Although widely used, it has been criticised by Carter [6] and others for not making allowances for sediment size and texture and for not considering beach slope. These are potentially very important in accurately determining sediment transport rates.

Efforts to improve the situation have resulted in a number of variations of the CERC formula. Kamphuis et al [8] and Van Hijum and Pilarcyzk [9] included the effects of different grain size and beach slope. However, the complex nature of the processes involved, the number of feed back mechanisms that exist and the difficulty of obtaining accurate wave and nearshore bathymetric data means the formula gives, at best, only an order-of-magnitude estimate of volumetric transport rates. Calibration of the formula against site measurements helps to reduce the uncertainty.

The CERC formula relates the potential longshore sediment transport rate with the longshore component of the incident wave energy.

The immersed weight potential longshore sediment transport rate (I) can be calculated using;

$$I = \frac{K}{16\sqrt{\gamma_{br}}} \rho_w g^{\frac{3}{2}} H_b^{\frac{5}{2}} \sin(2\theta_b)$$

where
- K = empirical coefficient of proportionality (for typical sandy beaches, if wave height used is H_{rms} then this value is 0.77, if H_s then the value is 0.32)
- ρ_w = fluid density (kg/m^3)
- g = gravitational acceleration (m/s2)
- H_b = breaking wave height (m)
- θ_b = breaking wave angle (deg)
- γ_{br} = H_b/h_b where h_b is the water depth at breaking

The volumetric longshore sediment transport rate is calculated using;

$$Q = \frac{I}{(s-1)\rho_w g d'}$$

where
- s = specific density of sediment relative to density of fluid medium (usually taken as 2.65)
- d' = ratio of solid volume to total volume of sediment (usually taken as 0.6)

Fig. 1.5 - The Coastal Engineering Research Centre formula on longshore drift rates

Coastal cells come in many forms. Carter [6] cited three main types, the embayment, the spit and lake cell. This thesis deals with embayment cells which are possibly the most common type of coastal cell in Ireland. May and Tanner [10] designated key points within the cell with the letters A to E each identifying areas of particular

morphology such as the start of the erosion cell, the area of maximum erosion, equilibrium area, etc. Lowry and Carter [11] defined two types of cell boundaries, a fixed, and a free comprising of three different configurations (Fig. 1.6) each formed by variations in wave direction or wave energy:

1. Sediment transported away from boundary, upcoast and downcoast (divide)
2. Sediment transported towards boundary from both directions (meet)
3. Sediment transported up to boundary at a different rate than the rate that sediment leaves the boundary (pulse).

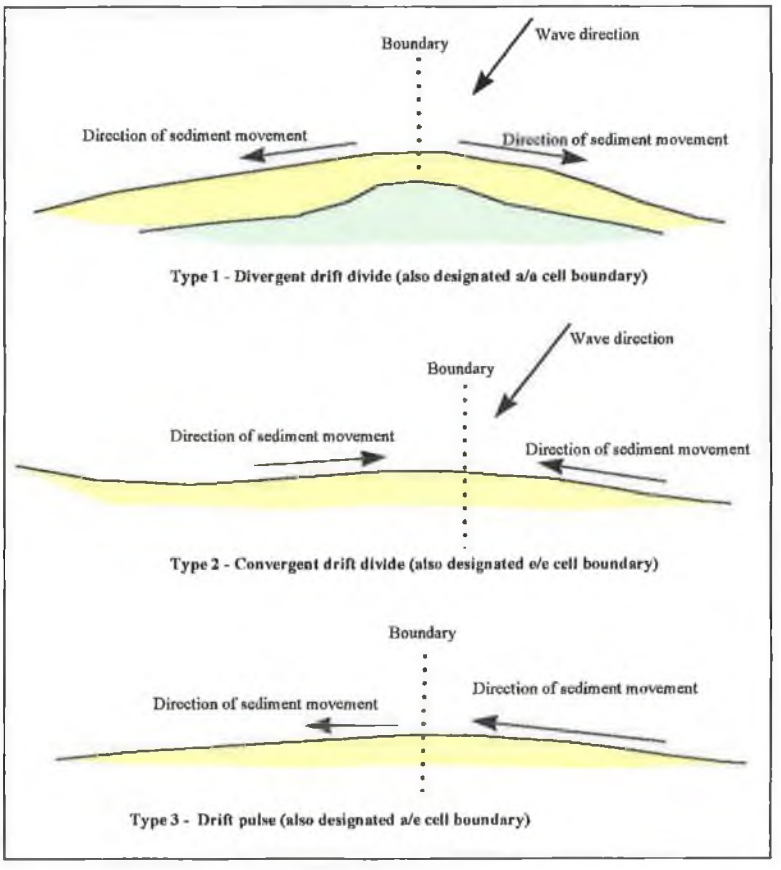

Fig. 1.6 - Classifications of coastal cell boundaries [6]

The fixed boundaries are usually headlands or structures on the coast, the free boundaries are however much harder to locate as their position depends on the wave field being experienced at a particular time . Using wave refraction models, Johnson

[12] showed that the location of coastal cells on the east Wexford coast changed with altering wave direction (Fig. 1.7).

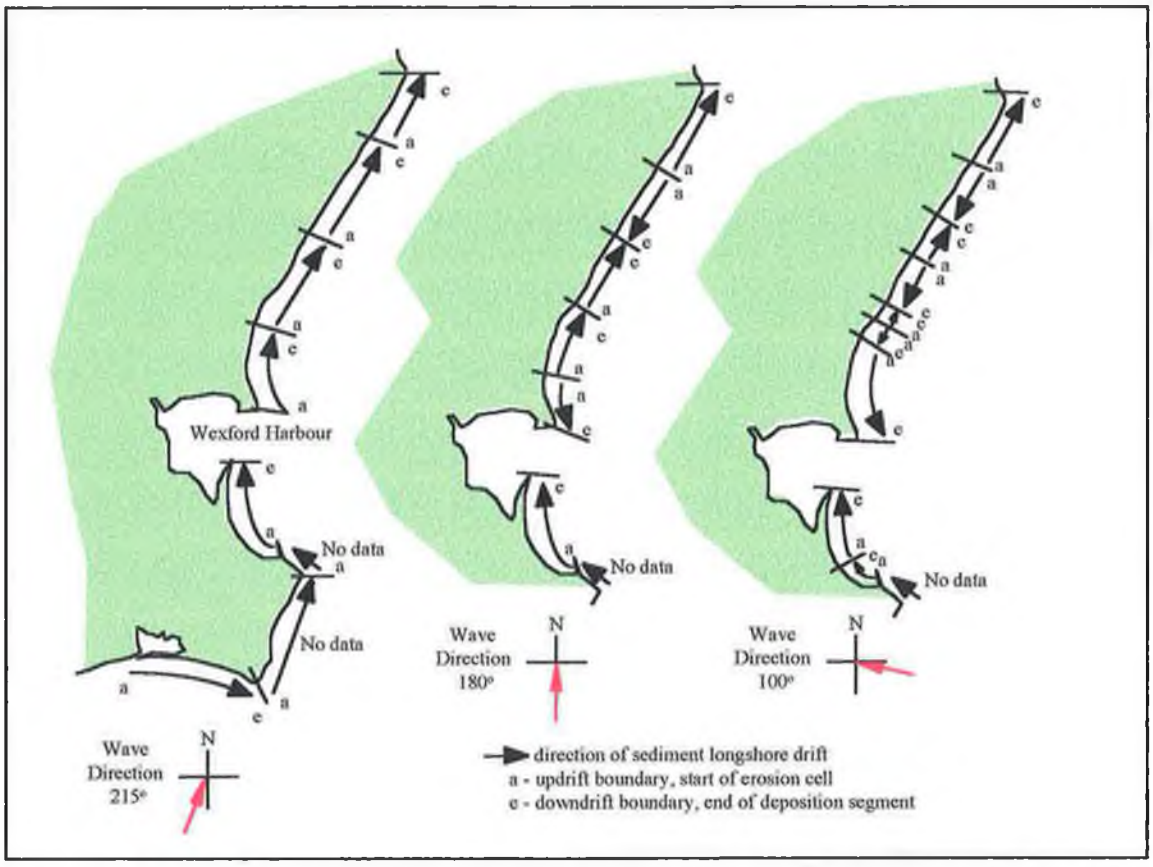

Fig. 1.7 - Sediment cell boundaries for various wave approach directions, south-east Wexford coast [12]

The position of the coastline within a cell is also influenced by the texture of the sediment, Davies [13], Harlow [14], McCave [15]. Depending on its size and texture, sediment moves at different rates within the cell. This means that the sediment becomes sorted, reflecting variations in the transport processes. Because of this it is possible to identify cells and their boundaries from sediment patterns on the beach, rather than by the more complex and error prone method of wave refraction. Stapor and May [16] used both wave refraction methods and sediment sampling to identify cell positions along the east coast of Florida. It was the sediment sampling that gave the truer picture of cell positions. This may be explained by the fact that the location of

sediment types within a cell is the practical result of a sorting process which is affected by each and every wave, whereas wave refraction by necessity can only deal with summarised wave statistics.

1.4 Coastal cell equilibrium

Cell equilibrium can be either static or dynamic [6]. Dynamic equilibrium applies to a coastal cell in which there is a constant throughput of sediment. These cells exhibit an imbalance between the forces acting on them and the resisting structure of the coast. This imbalance is countered by sediment moving through the cell either to and from adjacent cells or from a sediment source, such as a river, within the cell.

Static equilibrium is where the coastline has reached an equilibrium state without any influx of sediment. Carter [6] identified three forms of static equilibrium (Fig. 1.8);

a) Graded: Here the refracted dominant wave direction is at an angle to the coast and there is a positive longshore component of wave power. This is, however, countered by a natural sorting of sediment on the coast so that, in all places, the sediment size is such that the longshore energy is unable to move it.

b) Current: The refracted dominant wave is at an angle to the coast but the longshore energy component is reduced to zero by a counteracting current

caused, for example, by a strong wave height gradient or by an intersection of wave trains.

c) Swash alignment: Here the dominant wave is refracted so that the beach is at all times and, in all places, parallel to the approaching wave crests [17].

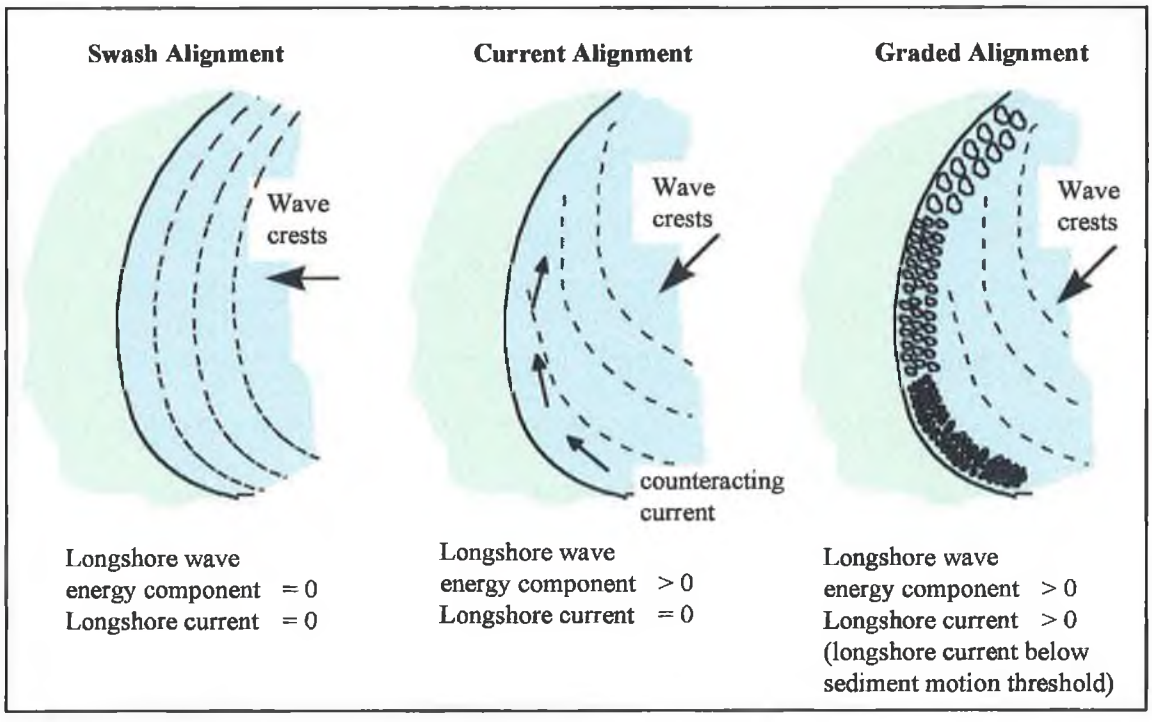

Fig. 1.8 - Types of static equilibrium [6]

In many cases equilibrium may be reached by a combination of two or all three of these options however Carter [6] states that.....

'It may be prudent to consider the swash alignment model as the ultimate expression of cell development as in this mode, somewhat paradoxically, the cell vanishes'.

He adds that the graded form is simply an 'arrested form of equilibrium'. Johnson [12], showed that all three types are common along the north west coast of Ireland with swash alignment the most prevalent.

The concept that swash alignment is the ultimate aim of coastline development has its origins in the work of Lewis [18]. This was elaborated on by Jennings [19] without full knowledge of wave transformation. Davis [20] later realised the importance of wave refraction in swash alignment.

1.5 Predicting the position of the coastline

Many attempts have been made to use longshore wave energy equations such as the CERC formula [7] and wave refraction/diffraction to predict the shape of the shore. Komar [21] developed an analytical technique in which the rate of change of beach width was related to the rate of change of sediment transport. He calculated the susceptibility of segments of coast to longshore energy input and using a computer model, these were subjected to typical waves. As the segments displayed differing transport rates over a time unit, the beach width was reduced by a proportional amount and the model adjusted the coastline. The resultant beach shape was fed back into the model to enable changes through time to be simulated and eventually a swash aligned, stable coastline emerged. This method, although mathematically proving the relationship between waves and bay shapes, proved impractical to use as it relies heavily on accurate wave data, sediment data and bathymetric measurements.

Simple models dealing with the evolution of a 'nearly straight' coast were developed in the early 1970's. These were called 'one line models' and predicted the change in a single representative beach contour (Fig. 1.9). Improvements were made to these over the years and the model developed by Hanson and Kraus [22] was able to allow for the effects of structures such as groynes and breakwaters.

If there is a change in the longshore transport rate along the coast, then the cross-sectional area (A) of the beach at any position (x) will change. This is expressed as;

$$\frac{\delta Q}{\delta x} = \frac{\delta A}{\delta t}$$

This change in area will cause the beach to advance or retreat. The change in beach contours (δy), mulitplied by a representative depth (D), will also be equal to the change in cross-sectional area, thus;

$$\frac{\delta Q}{\delta x} = D\frac{\delta y}{\delta t}$$

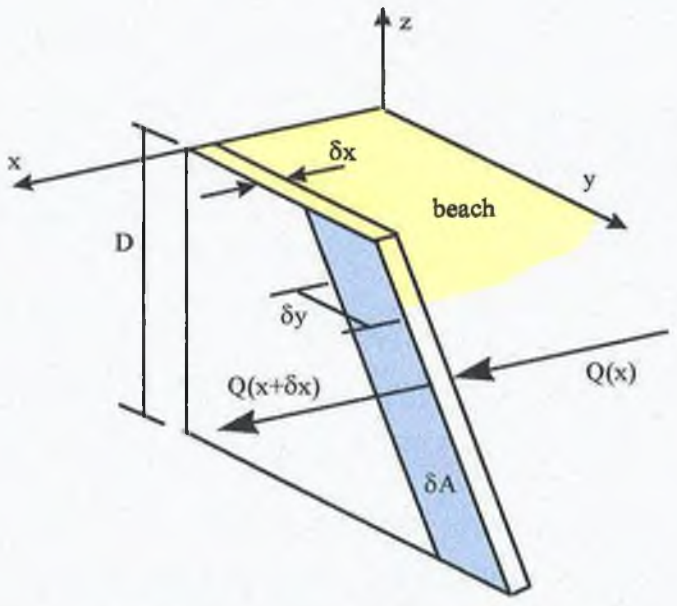

Fig. 1.9 - 'One line' model to predict coastline change

The main problem with applying this technique lies with the representative depth. This is known as the 'closure depth' and should ideally be the depth within which all beach

and nearshore slope changes occur (the nearshore active zone). This is difficult to determine accurately.

More sophisticated models able to predict the changes in more than one contour were also developed. These 2-line and multi-line models [23, 24] provide not only information on beach plan but also on beach profile. However, these models are limited to straight coasts and although they provide data on changes to a number of nearshore contours, the core calculations remained the same as the original One-Line models.

Currently 'Coastal Area' models which calculate wave, current and sediment transport parameters at grid points are being developed. These simulate changes in two dimensions using constituents from a number of modules describing various sediment transport components, such as complex current fields, tidal variations in water levels, offshore sand bar movement, etc. They contain a multitude of non-linear elements which when combined lead to instability in the numerical computation. These models although undoubtedly heralding the future of coastal engineering, require more sophisticated input data (e.g. waves, tides, sediment, bathymetry) than the earlier simpler models.

It is this complexity of processes that makes the accurate quantification of sediment transportation rates very difficult, especially on open coasts. It is somewhat analogous to long term weather forecasting in that at the micro scale a subtle change in one variable can have a dramatic effect. Empirical curve fitting models of cell equilibrium

on the other hand takes a simpler view, letting the shape of the bay show the result of the interactions of waves, tides, currents, storm surges, etc.

Three types of empirical models used to predict the evolution of beach plan shape exist

- the Spanish pocket beach model
- the log spiral model
- the parabolic curve model

The Spanish pocket beach model developed by Berenguer and Enriques [25] provides a set of design equations which predict the stable position of the shoreline in the lee of offshore breakwaters. These breakwaters have been used in many coastal resorts and have created many fine amenity beaches in areas previously suffering from erosion. The equations are limited to pocket beaches in their application and the tidal range for the location must be less than one metre.

1.6 The log spiral bay shape

Where bays are subjected to a dominant wave direction at an angle to the coast, the resultant shape of the coastline is characterised by an upcoast hook which passes laterally through a tangential section of coastline to the downcoast headland (Fig. 1.10). These bays have been variously described as a crenellate, spiral, zeta, half heart or headland-bays. They are especially common around Ireland where there is a

preponderance of south-westerly to westerly winds and consequently waves from these directions.

Krumbein [26] examined beach processes on a single beach near San Francisco, California, and suggested the approximation of the log spiral shape (Fig. 1.11). Silvester, Ho, Tsuchiya and Shibano [2, 27] carried out physical tests in a wave basin using obliquely approaching waves on a straight sandy beach with a number of hard points (headlands). After a number of hours the coastline had adopted the log spiral curve shape. He also observed that the coastlines in the model tests had three distinct curvature zones, a purely circular section in the lee of the upcoast headland, a curved mid section and a tangential section connecting this with the downcoast headland.

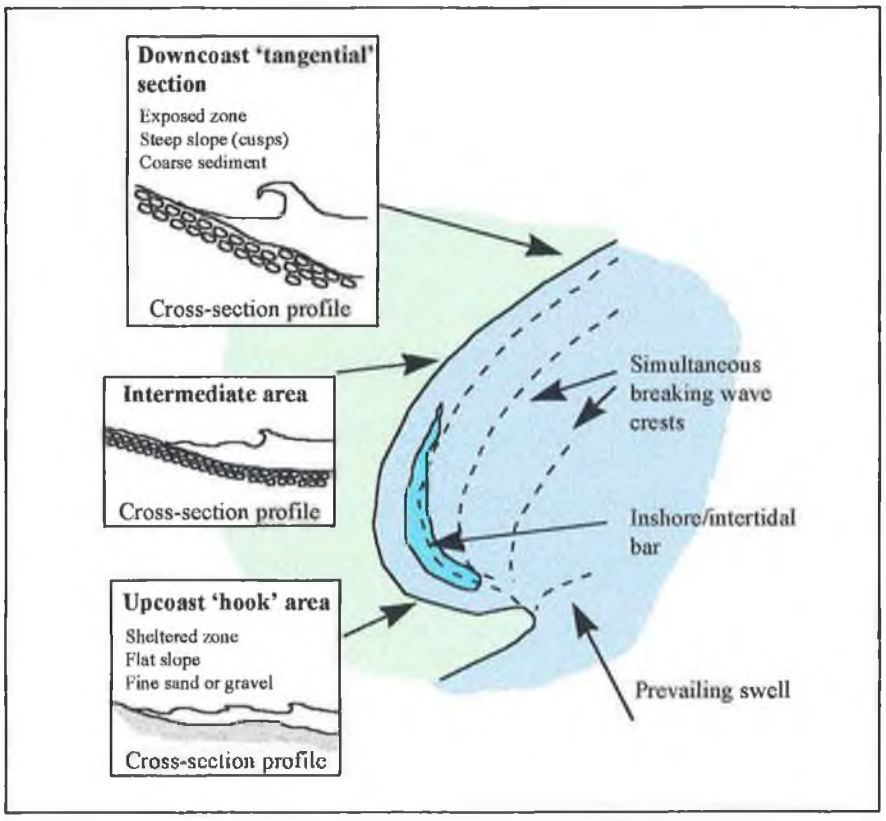

Fig. 1.10 - Log spiral curve bay for obliquely approaching dominant wave

Yasso [28] analysed this shape and approximated the form of the curved upcoast section to that of a log spiral. Carter [6] and Yasso [28] identified sand spit cells as being the inverse of the log spiral curve. Silvester and Ho [2] derived values for the spiral constant for equilibrium bays given the approaching wave direction. This work was based on comparisons between varying spiral constants for crennelate curve bays which were known to be in static equilibrium. This was presented by Silvester [29] as a tool by which the stability of a bay could be judged.

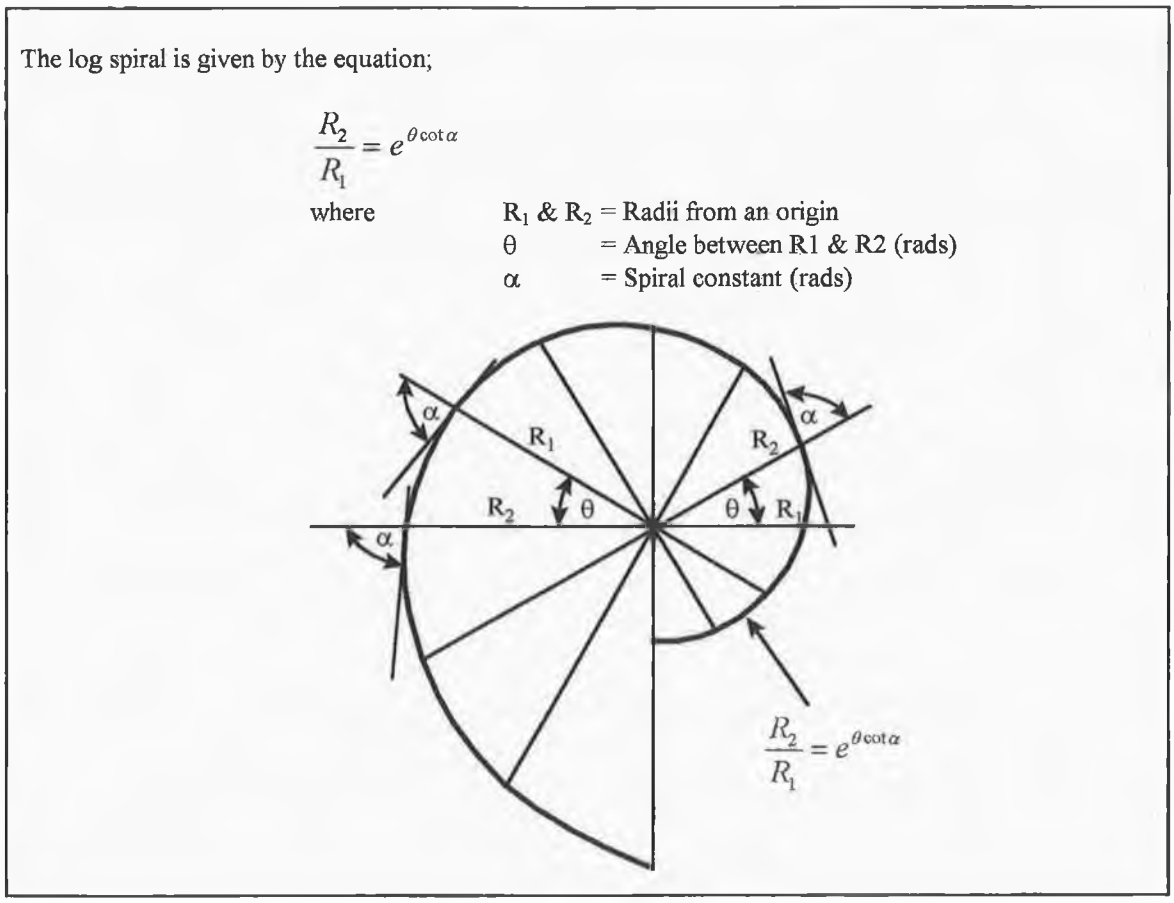

Fig. 1.11 Definition sketch of the log spiral

In practice, however, the technique proved unwieldy because of difficulties in identifying the centre point of the spiral and drawing the spiral itself. In order to try to rectify this, Sylvester, Tsuchiya and Shibano [27] produced a simplified version which utilised an 'indentation ratio' which was extracted from the spiral curves. Graphs were

presented from which this ratio could be read for a particular wave approach angle. This allowed the user to predict the maximum indentation distance measured from a straight line between the upcoast and downcoast headlands for a bay in static equilibrium. This test of stability proved much easier to use but difficulties remained. The single value of indentation meant that the coastline had to be drawn by hand to the half-heart planform and while the upcoast headland was easily identified, locating the downcoast headland was more difficult. Silvester and Hsu tackled these problems in a later book [30] on equilibrium bay shapes.

At least four different mathematical/physical models have been derived to explain the log spiral configuration. Rea and Komar [31] presented a numerical simulation of the evolution of a beach in the lee of a headland and, by an appropriate choice of the form of wave energy flux, succeeded in generating beach configurations which closely approximated the log spiral. Walton [32] also used changes in wave energy caused by wave diffraction to create the log spiral.

LeBlond [33] presented a detailed explanation for the log spiral plan form. By combining basic rules of wave refraction and diffraction along with empirical formulae on the relationship between wave energy, grain size and beach slope, he derived curves which closely matched both the natural planform of a number of sample equilibrium bays and curves produced by the log spiral method. The conclusion from this work is that the log spiral coastline shape is mainly the result of the effect of nearshore wave transformation (refraction from the seabed and diffraction from the headland). This effect is further refined by the reaction of beach slope (flatter near the headland) and sediment sorting (finer sediment near headland) caused by the resultant variance in the

longshore wave energy component along the coast. Later LeBlond [34] suggested that....

> '....what is thus significant about the shape of headland-bay beaches is the gradual decrease in curvature away from the headland, reflecting the decreasing influence of protection from wave action, and not the logarithmic spiral shape as such, which is merely a quantitative parameterisation of the qualitative behaviour.'

He further added that any model in which the effect of the headland on wave energy decreases with distance is bound to produce shapes of decreasing curvature which may be approximated by the log spiral. He concluded that the true test of a headland-bay model is whether it reproduces not only the log spiral planform but also the morphological and sedimentary characteristics (i.e. beach slope changes and sediment sorting).

Phillips [35] argued however, that from his studies using sediment/slope data collected at a small eroding area in the lee of the terminal of a seawall, there was no evidence of a systematic influence of the headland on wave energy. He suggested that the log spiral bay shape was the result of a variety of distance-decay functions (exponential or log) with the headland simply acting as the cell boundary. He concluded that wave energy was but one of these. Others might include:

- offshore bathymetry not-influenced by the headland
- decreased sediment supply to the area in the lee of the headland

- decreasing land height from the upcoast headland
- terrestrial environmental gradients (rainfall, vegetation type, etc.)

According to Carter, this concept agreed, to some extent, with the formation of sand spits [6].

1.7 The parabolic curve model

One of the many problems with applying the log-spiral curve method to predict the static equilibrium position of the coastline was that it gave only the curved portion of the bay. This had then to be connected to the downcoast headland or control point via the bay tangential section. This problem would not arise if a formula could be devised which would predict the entire bay shape.

Mishima's [36] bow shaped parabola uses the standard parabolic expression: $y = px^2 - b$

The constants p and b are as per the sketch below and are solved by iteration of the location of the centre of the parabola and solving the equation using the upcoast and downcoast fixed points. The true parabola was the one which most closely matched the present coastline.

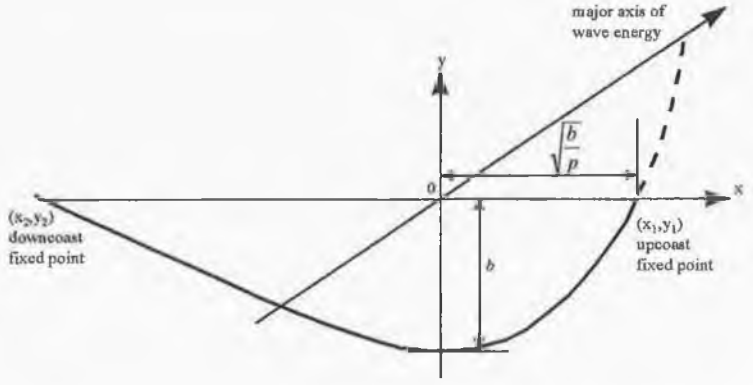

Fig. 1.12 - Parabolic formula used to predict bay shape

Mashima [36], noted that a close relationship existed between wind and wave energy roses (which were semi-elliptical in shape) and the planform of the bay. He used a simple parabolic formula to determine bay shape (Fig. 1.12). However there were complications with finding the centre of the parabola and the technique did not take into account the effects of wave diffraction or the wave obliquity.

Silvester and Hsu [30] progressed the idea of developing a simple technique of predicting the entire bay coastline by reanalysing the data from previous model tests carried out by Ho [37]. They plotted the dimensionless radii ratio ($\mathbf{R/R_0}$) against varying wave approach angles (β) for a range of radii angles (θ), Fig. 1.13. This resulted in a series of curves which could be used directly to determine the final static equilibrium shape of the bay. To make the technique easier to use, Hsu and Evans [38] developed a quadratic polynomial equation from these curves by a process of curve fitting. When applied, this formula predicted a coastline which closely matched the model test results. This formula was also applied to a number of log spiral bays around the world, some of which were known to be in static equilibrium, others not so. The results were very encouraging and the authors confidently presented the method as a validated technique in their book [30].

They did however acknowledge that here were still difficulties with its application although they addressed many of these. Firstly, the technique is dependent on the measurement of the angle between the direction of approach of the dominant waves and a line joining the headlands at the bay extremities. Secondly, it also requires measurement of the distance between the controlling headlands or points. It is with the accurate measurement of these that the difficulties lie.

The curves developed by Ho [37] from physical model test data related the coastline shape to wave approach angle. They were computerised by Hsu and Evans[38] to derive a polynomial in the form of;

$$\frac{R}{R_0} = C_0 + C_1\left(\frac{\beta}{\theta}\right) + C_2\left(\frac{\beta}{\theta}\right)^2$$

R, R_0, β and θ are shown in the sketch below. The coefficients C_0, C_1 and C_2 vary with β. Although this formula is strictly a quadratic because of the linear term of β/θ it is usually referred to as parabolic.

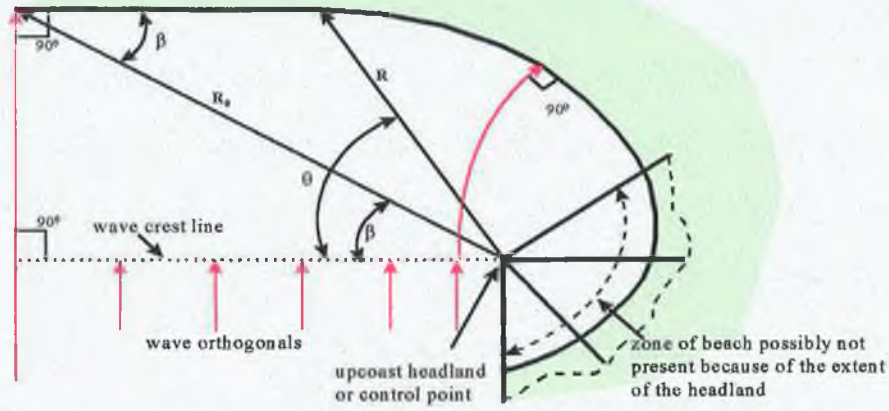

Fig. 1.13 - New 'parabolic' formula

From their model tests, Silvester [29] noted that the straight section of coastline adjacent to the upcoast headland achieved relative stability long before the hooked end of the bay. The angle this adopted was at 90° to the incident wave. He concluded that this was also true in reality and that this could be used as an indicator of the persistent or dominant swell wave direction, especially in bays at, or approaching, static equilibrium. He suggested that....

> '....prior to this [the equilibrium state] the angle so measured may be smaller than actual, due to changing orientation of this section with time.'

Even in these cases he maintained that this section of the bay would give a good indication of the closeness to full stability. In order to help confirm the angle measurements made, he suggested that.....

> '....assistance in this respect can be had by noting the tangential alignments of several adjacent bays. If the headlands are more or less aligned and the nearshore bathymetry relatively uniform then the dominant swell direction should be the same for each bay.'

The distance between controlling headlands or points proved difficult to measure because of the problem in identifying the downcoast control point. The upcoast headland is usually a prominent headland, with the hooked part of the bay to leeward. However, the downcoast headland is more difficult to locate especially on long bays. Often the control point is not the downcoast headland but may be some point along the tangential curve of the bay. In their book Silvester and Hsu [30] devote an entire section to this problem arguing that selecting different control points along this tangential section does not dramatically change the predicted static equilibrium shape of the bay. This is because with each change in the length of the control line between the upcoast headland and the downcoast control point there is a commensurate increase in the angle between the tangential section and the control line.

As this technique is relatively new (1993) there has not been any published feedback on its application to existing coastal erosion problems. If it is as successful as the log spiral method, despite its difficulties, then it is to be expected that the parabolic curve method will receive widespread use, particularly as a realistic method of determining

the location of coastal setback lines. These are lines drawn inland of the shoreline which predict the possible future position of the coastline. They are used by local authorities to restrict or prevent developments taking place in areas sensitive to coastal erosion. In Ireland, at the moment, in the few counties where these lines are used, they are arbitrarily drawn at a standard distance from the shore (typically 50m for soft coast), or along the nearest public road or railway to the coast.

2. AIMS OF THE PRESENT STUDY AND WORK PROGRAMME

2.1 Aims

The aims of the present work were to investigate the application of a recently developed technique which predicts the eventual static equilibrium position of the coastline. The effect of alternatives methods to obtain the input parameters for this technique was also examined.

The detailed objectives were:

1. To examine different methods of determining the dominant wave direction and control points for a number of bays on the east coast of Ireland.
2. To use this data in the application of the new parabolic curve technique to predict the current natural curvature of the bays along with the eventual static equilibrium position of the coastline
3. To investigate the implications of climate change and coastal protection measures on coastline evolution

2.2 Work Programme

For this study a work programme was drawn up which can be divided into a number of distinct stages.

Stage 1 - The new parabolic curve technique of predicting coastline position is reliant on the identification of the dominant wave approach angle. In the case of bays where their is little longshore drift of sediment this is accurately indicated by the orientation of the tangential section of the bay.

As the bays being studied experience a substantial longshore drift of sediment a more appropriate method of obtaining the dominant wave direction is to analyse a time history of nearshore wave data. This, however, required a considerable amount of effort involving water depth digitising, wave refraction / diffraction computer simulation and data analysis. This formed a substantial part of this study.

Stage 2 - Applying the technique and drawing the equilibrium coastline position entailed the scanning of maps and aerial photographs, photograph rectification and digitising coastlines. Drawing the equilibrium coastline involved digitising and extrapolating curves and coding a graphing spreadsheet.

Stage 3 - As the coastal environment is continually being altered by man it was decided to investigate how two specific impacts, climate change and hard coastal protection measures, might affect the future evolution of the coast. This work involved redrawing the equilibrium coastline position for altered wave conditions and examining the implications of artificially hardening an inherently unstable coastline.

Stage 4 - The suitability of the technique as an overall predictor of coastline stability was examined and commented on. This involved studying the historical evolution of the coastline, noting the difficulties encountered with the technique and making recommendations for further investigations.

These stages are shown in Fig. 2.1 and are further detailed in Chapter 3 - Methodology.

Stage 1

OFFSHORE WAVE DATA ANALYSIS
1. Obtain offshore wave data
2. Create Hs / Tz scatter plots

REFRACT/DIFFRACT OFFSHORE WAVE
1. Create bathymetric grid file and control file as required
2. Run refraction / diffraction computer model
3. Extract & format inshore wave data
4. Draw vector plot energy
5. Note dominant wave direction

Stage 2

EQUILIBRIUM COASTLINE PREDICTION
1. Obtain dominant wave direction from bay planforms
2. Identify the control points for each bays
3. Draw the static equilibrium position for both dominant wave directions
4. Compare equilibrium position with present position of the coastline

Stage 3

EXAMINE IMPACT OF CHANGE
1 Translate global warming predictions into wave climate change
2. Redraw equilibrium coastline position
3. Examine impact of hard coastal protection measures

Stage 4

EXAMINE SUITABILITY OF TECHNIQUE
1. Obtain historical coastline data
2. Plot historical coastline positions & compare with present & equilibrium positions
3. Identify difficulties with the technique
4. Make recommendations on suitability and further study

Fig. 2.1 - Study work programme

3. METHODOLOGY

3.1 Introduction

This study seeks to test the validity of the new parabolic curve method developed by Hsu and Evans [38] to predict the static equilibrium position of the coastline of headland controlled bays. It is applied to three bays on the east coast of Ireland. These bays are not in static equilibrium as there is evidence that sediment is passing along the coast [39]. However the exercise of predicting the static equilibrium position (SEP) of the coastline is very important as the rate of longshore drift is known to fluctuate [39]. The SEP of the coastline would represent the worse case condition as it would indicate the future position of the coastline should this longshore drift of sediment cease completely. The SEP is the result of gradual evolution over thousands of years. There will be many changes in erosion rate during this time as stormy periods give way to calmer intervals and sediment drift rates fluctuate.

The section of the coastline selected for study is a 6 km stretch between Duffcarrick Rocks and Pollshone Head on the east coast of County Wexford which consists of three bays and a number of headlands (Fig. 3.1). The bays in this region, Courtown North Beach, Ardamine and Pollshone, all exhibit the crenellate curve. This area has suffered and continues to suffer from erosion which may be in response to anthropogenic factors such as harbour development or removal of beach sediment but is more likely the result of changes in sediment supply rates [39, 40].

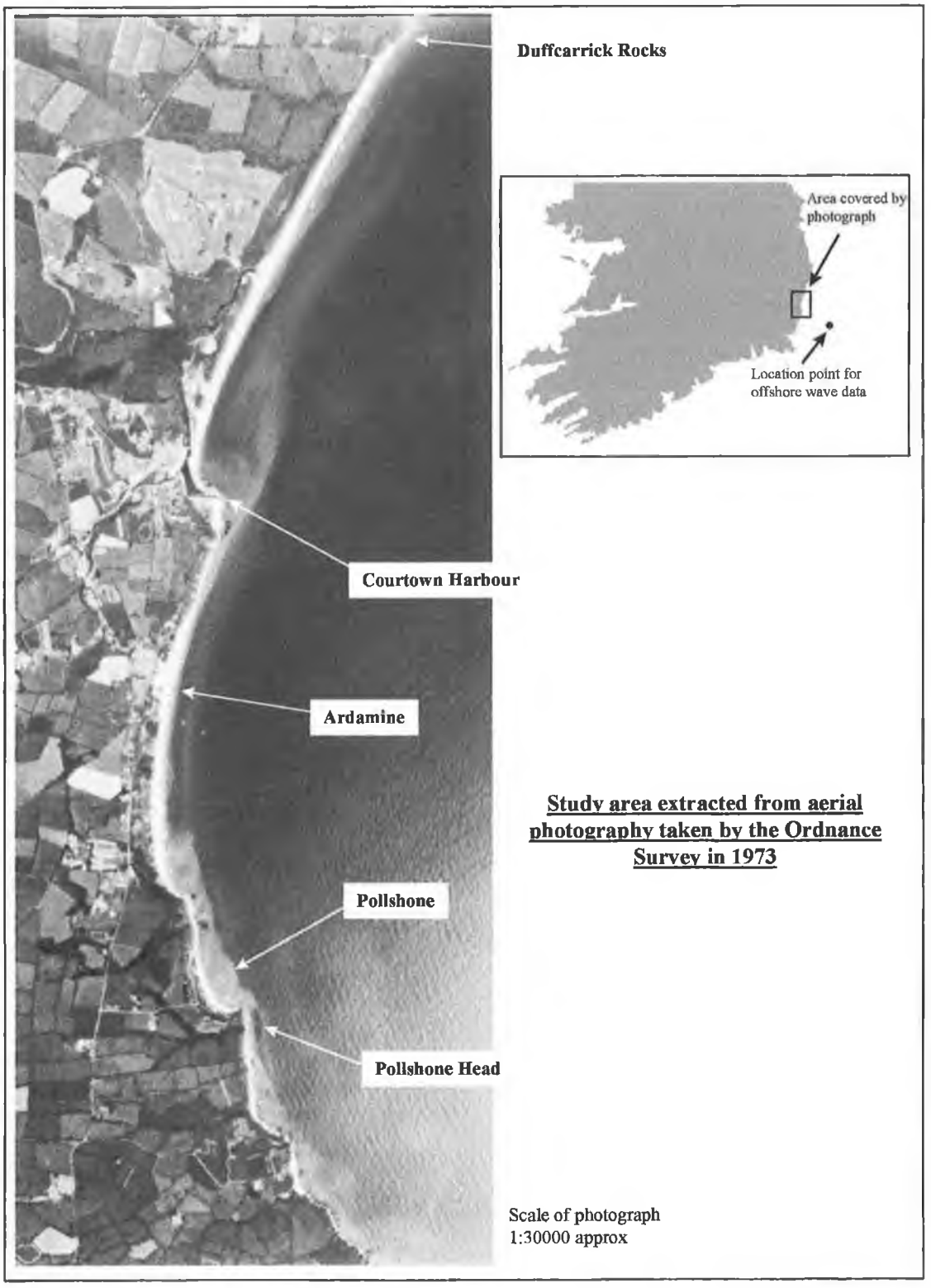

Fig. 3.1 - Location map of study areas

The methodology adopted to testing the application of the new parabolic curve method were to:

- **Ascertain the domination wave direction**. Two methods were used to determining this critical parameter. Firstly, the wave direction was determined from offshore wave data. Secondly this direction was independently obtained from the orientation (planform) of each bay. The results of both methods were compared and commented on.

- **Plot the predicted static equilibrium position** for the coastline of each bay. The SEP was plotted for the two dominant wave directions obtained. Differences between the coastlines are commented on.

- **Consider the effect of climate change and the impact of coastal protection measures**. The effect of changes in the dominant wave direction brought about by changes in the wind climate were examined. The impact of the current policy of installing rock revetments to prevent erosion the coast were also examined.

3.2 Ascertaining the dominant wave direction

This section examines one of the main problems identified by Silvester and Hsu [30] in applying either the old or new parabolic curve techniques: the accurate determination of the dominant wave direction. Two methods to solve this problem were investigated. It

should be noted that this is not, in fact, a direction of a single wave or wave train but the result of the effect of the total wave climate within the bay.

Firstly, the dominant wave direction was obtained from vectorised plots of the incident wave energy at each of the three bays. Since there have not been any wave recordings made in the area, the most appropriate source of information is offshore wave data generated by computer models using wind field information. These waves may then be propagated inshore using a computer wave refraction / diffraction model [41]. This is a complex method but has the potential to be very accurate.

The second method uses the simplified approach suggested by Silvester and Hsu [30]. This requires the measurement of the angle between the tangential end of the bay and a control line drawn between the upcoast and downcoast control points. This, he maintains, provides practical evidence of the persistent or dominant swell wave direction. Swell waves are long period waves which, along with containing the most wave energy, are most efficient at transporting sediment. These he considers most important in determining the overall shape or 'planform' of the bay. The swell waves which occur in the immediate aftermath of a storm are particularly important as much of the sediment disturbed is still in a state of flux and is available for transport to new (or recently vacated) locations.

Both these methods are detailed below and comparison of the results should give an indication of the overall stability of the bays by showing how much further the bay needs to adjust to align itself with the oncoming waves (i.e. swash alignment).

3.2.1 Dominant wave direction from wave data

The offshore wave data used was obtained from the British Meteorological Office fine mesh wave model (BMO model) [42]. Contemporary ocean wave prediction models use the wind field as the input to a spectral energy balance equation where the energy balance of the wave field is described as a function of frequency, direction, position and time combined with the wave field velocity in deep water. This energy is balanced by a source function (S) which represents the physical processes that transfer energy to and from the wave spectrum. It can be symbolically written as:

$$S = S_{in} + S_{nl} + S_{ds} \qquad (1)$$

where S_{in} = energy input to the wave field from the atmosphere (linear and exponential growth terms)

S_{nl} = transfer of energy associated with non linear wave interactions

S_{ds} = energy dissipation in both deep and shallow water

The BMO wave model is a second generation model and is classed as a Coupled Discrete (CD) model [43]. 'Discrete' refers to the fact that it represents the directional energy spectrum by a discrete number of finite bandwidth spectral components travelling in a specified number of directions. This provides detailed sea-state information at a given location in terms of a two-dimensional (frequency-direction) spectrum. From research of wave energy spectrums carried out on wave recordings made in the North Sea it was found that the spectra could be more accurately described

using parameters derived from the recorded spectra shape. Although this parametric wave model was a significant advance in wave modelling techniques because it allows the non-linear wave-wave interactions to be easily computed it had limited applicability. In view of this, combined parametric-discrete models were developed and these have been classified as Coupled Hybrid and Coupled Discrete models [43].

The BMO wave model is routinely verified against wave measurements at oil company platforms, fixed data buoys and weather ships. Winds from the atmospheric models used as the input data are also verified in the same way [42]. The model was also one of ten examined under the Sea Wave Modelling Project (SWAMP) [44] carried out by nine wave modelling groups from Europe, the United States and Japan. In this study it showed close agreement with the other models for typical wind conditions. While more complex and more accurate third generation models, where no ad hoc assumptions on wave spectral shape are made, are now available, most notably the WAM model [45], these currently operate on grid points which are spatially further apart. This limits their effectiveness especially in areas where land masses play an important role in determining sea state.

Data was obtained from the BMO model for the years 1994 and 1995 and the data format is shown in Fig. 3.2. The location point for this data is shown in Fig. 3.1.

Time		Location		Depth			Wind		Result. Wave			Wind Wave			Swell Wave		
Hr	Date	Lat	Long		d		Sp	Dir	Hs	Tz	Dir	Hs	Tz	Dir	Hs	Tz	Dir
00	10 04 1994	52.50N	6.06W	2	45	1	27	327	2.4	5.9	305	2.4	6.0	305	0.5	11.1	225
03	10 04 1994	52.50N	6.06W	2	45	1	26	343	2.3	5.8	343	2.3	5.9	343	0.4	11.1	187
06	10 04 1994	52.50N	6.06W	2	45	1	17	349	1.9	5.3	057	1.7	5.5	002	0.9	9.1	057
09	10 04 1994	52.50N	6.06W	2	45	1	15	006	1.5	5.1	034	1.4	4.6	034	0.6	9.3	070
12	10 04 1994	52.50N	6.06W	2	45	1	13	018	1.2	4.7	033	1.1	4.0	036	0.6	7.9	033
15	10 04 1994	52.50N	6.06W	2	45	1	12	026	1.1	4.4	036	1.0	3.7	036	0.4	8.6	033
18	10 04 1994	52.50N	6.06W	2	45	1	6	019	0.9	4.3	034	0.4	0.1	029	0.8	4.9	034
21	10 04 1994	52.50N	6.06W	2	45	1	5	045	0.7	4.2	040	0.3	0.1	036	0.6	4.7	040
00	11 04 1994	52.50N	6.06W	2	45	1	3	159	0.6	4.2	039	0.0	0.0	000	0.6	4.2	039
03	11 04 1994	52.50N	6.06W	2	45	1	5	199	0.5	4.3	036	0.0	0.0	000	0.5	4.3	036
06	11 04 1994	52.50N	6.06W	2	45	1	9	194	0.5	4.3	188	0.3	2.0	189	0.4	5.3	188
09	11 04 1994	52.50N	6.06W	2	45	1	8	190	0.5	4.4	143	0.3	2.2	185	0.4	6.1	143
12	11 04 1994	52.50N	6.06W	2	45	1	10	190	0.6	4.3	144	0.4	2.3	185	0.4	7.1	144
15	11 04 1994	52.50N	6.06W	2	45	1	10	210	0.6	4.2	142	0.4	2.6	205	0.4	7.7	142
18	11 04 1994	52.50N	6.06W	2	45	1	13	217	0.7	3.7	142	0.5	2.9	212	0.4	9.2	142
21	11 04 1994	52.50N	6.06W	2	45	1	10	223	0.6	3.9	217	0.5	3.0	217	0.3	8.9	139
00	12 04 1994	52.50N	6.06W	2	45	1	9	233	0.6	3.8	223	0.5	2.8	223	0.3	7.8	156
03	12 04 1994	52.50N	6.06W	2	45	1	11	299	0.6	4.1	153	0.3	2.1	270	0.5	5.0	153
06	12 04 1994	52.50N	6.06W	2	45	1	14	334	0.6	3.9	152	0.5	2.7	329	0.4	7.3	152
09	12 04 1994	52.50N	6.06W	2	45	1	13	331	0.6	3.6	333	0.5	2.9	333	0.3	8.2	147
12	12 04 1994	52.50N	6.06W	2	45	1	14	341	0.6	3.5	342	0.6	2.9	342	0.2	9.5	150
15	12 04 1994	52.50N	6.06W	2	45	1	13	339	0.6	3.7	341	0.6	3.0	341	0.3	10.3	147
18	12 04 1994	52.50N	6.06W	2	45	1	14	342	0.7	3.8	342	0.6	3.0	342	0.3	11.7	147
21	12 04 1994	52.50N	6.06W	2	45	1	12	353	0.6	3.9	159	0.5	2.9	353	0.3	10.1	159
00	13 04 1994	52.50N	6.06W	2	45	1	16	347	0.7	4.0	160	0.6	3.0	353	0.4	8.0	160
03	13 04 1994	52.50N	6.06W	2	45	1	18	352	1.0	4.2	003	1.0	3.8	003	0.3	11.8	157
06	13 04 1994	52.50N	6.06W	2	45	1	15	356	1.1	4.4	019	1.0	4.1	019	0.3	10.4	160
09	13 04 1994	52.50N	6.06W	2	45	1	15	004	1.1	4.4	019	1.0	4.1	019	0.4	9.3	158
12	13 04 1994	52.50N	6.06W	2	45	1	17	011	1.1	4.4	023	1.1	4.1	023	0.3	9.6	162
15	13 04 1994	52.50N	6.06W	2	45	1	15	007	1.1	4.4	023	1.0	4.1	023	0.3	10.8	159
18	13 04 1994	52.50N	6.06W	2	45	1	14	019	1.0	4.3	022	0.9	3.9	022	0.4	11.4	158

Hr = hour; Lat = Latitude; Long = Longitude; d = depth (m); Sp = Wind Speed (m/s); Dir = Direction (degrees); Hs = Significant wave height (m); Tz = Wave period (sec)

Fig 3.2 - Offshore wave data format

In order to ascertain the dominant wave direction at each bay it was necessary to examine the effects of nearshore bathymetry and headlands by propagating these offshore waves shorewards using a wave refraction/diffraction computer model. The model used was RCPWAVE, originally developed by the US Corps of Engineers [41]. This was modified by Murphy and Walsh [46] who added a Graphic User Interface and named the new package ROWAVE. The model propagates linear, monochromatic waves using formulae based on a numerical solution to an elliptic equation which approximates the complete wave transformation process over bathymetry constrained only to have 'mild' bottom slopes (as computational refractive methods fail in regions of complex bathymetry). The main formulae used are the 'mild slope equation', originally developed by Smith and Sprinks [47] and Snell's Law [48]. The model also includes an algorithm which estimates wave conditions inside the surf zone (shoreward of the breaking waves).

RCPWAVE requires two input files, the control file and the bathymetric grid file. The control file contains information on both the bathymetric grid (number of grid points, distance between points, etc.) and on the input wave (wave height, period and direction). The bathymetric file contains the water depth data (Fig. 3.3). Water depths for an area 19.5km by 27.7km were digitised from Admiralty Chart no. 1727. The area close to shore (down to -6m water depth) is particularly important and accurate bathymetry for this area was obtained from measurements taken by the EROPRO project [49]. This file contains a total of 21,875 water depth measurements.

It was not practical to propagate every offshore wave ashore so scatter tables of the offshore wave (resultant) was firstly created using customised software. This

summarised the waves into usable blocks based on their wave direction, height and period. Each block was then brought ashore to obtain the altered wave at location points within each of the three bays.

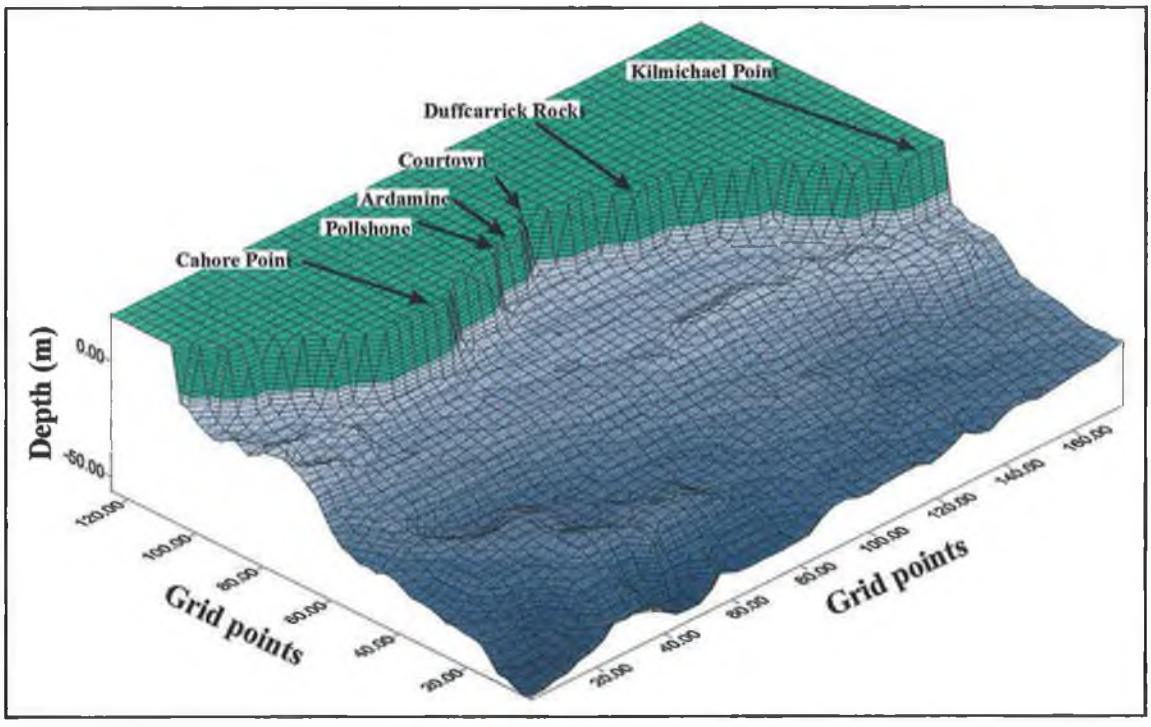

Fig 3.3 - Bathymetric grid of study area

These blocks of inshore wave data were then converted to directional wave energy using Airy theory [50]. This employs first order functions resulting in a linear approach. Unfortunately, since many non-linear processes exist in shallow waters this method is not particularly suited for nearshore work. More complex higher order theories such as Stokes II, III or IV, Cnoidal or Solitary would be more appropriate but these have the disadvantage of increased computational requirements and more detailed input data. For practical reasons and because of the fact that accurate information was not available on the non-linear nearshore processes it was decided to use the Airy wave approach.

The Airy wave energy formula is:

$$E = 0.5\rho g L\left(\frac{H}{2}\right)^2 \qquad (2)$$

Where E = Energy per wavelength for each metre of wave crest (Joules)

ρ = Density of sea water (kg/m^3)

g = Gravity (m/s^2)

L = Wave length (m) = $T(gd)^{2.5}$ Where T = Wave period (s)

d = Water depth (m)

H = Wave height (m)

The directional wave energy for each point was summated and plotted as a vector diagram. From this the resultant wave energy and direction was established. This direction was assumed to represent the dominant wave direction.

3.2.2 Dominant wave direction from coastal planform

This technique adopts the methodology proposed by Silvester and Hsu [30]. They suggest that the dominant wave direction is indicated by the tangent to the coastline drawn at the downcoast extremity of the bay. The angle this makes with the control line (the line joining the two control points) is designated β (Fig. 3.4).

The problems associated with this technique are the difficulty in identifying the downcoast control point, and the fact that the bays are not in a static equilibrium condition due to the longshore drift of sediment.

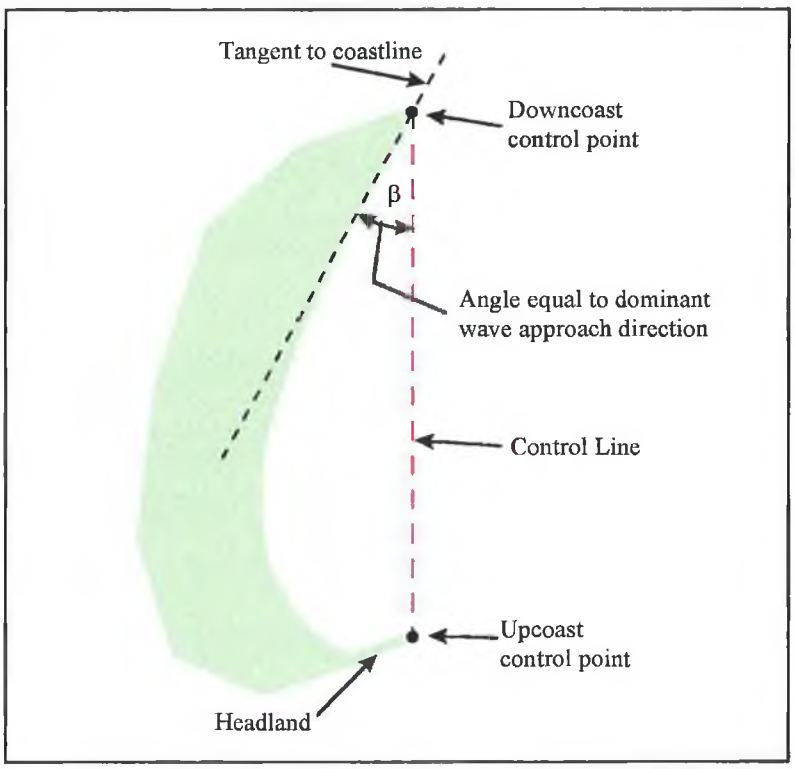

Fig. 3.4 - Sketch showing dominant wave approach angle as indicated by a bay in static equilibrium

3.2.2.1 The downcoast tangential section

This section of the bay is adjacent to the downcoast control point. The downcoast control point in small crenellate bays is usually located at a headland or rock outcrop. However, this point is more difficult to locate in longer bays as the controlling point may be reached before the downcoast headland. In this case the point will exist somewhere along the coastline within the bay and may not have any identifying features. Because of its length and the acute dominant wave approach angle one of the bays, Courtown North, was found to have this problem. It is only possible to solve this difficulty by selecting a number of control points within the bay and plotting the resultant SEP's. The tangent itself, however, is usually constant for all possible downcoast control point locations. Measuring the angle in relation to the 360^0 compass (with true north at 0^0) gives the dominant wave direction.

3.2.2.2 Crenellate Bays not in Static Equilibrium

Silvester and Hsu [30] suggested that when any reasonable length of coastline is being considered, the direction of the dominant wave should be sensibly constant, even when refracted across the continental shelf to the beach. If the headlands were aligned, the wave orthogonals would be parallel and hence the downcoast tangents of successive bays would be similarly oriented. Unfortunately however, this is not the case with the study area and as the three bays are not aligned and the angle measured would be expected to be different for each bay. They also observed that for a coastline curving away from the sea β would increase as one moved farther along the curve [30]. This means that the indentation of bays along it would also increase. Conversely, when the coast curves towards the sea the angle and the indentation should decrease. This is the case for the studied site.

The fact that the bays are not in static equilibrium leads to a smaller β being measured than would be the case had the longshore drift of sediment ceased. From laboratory tests carried out by Ho [37] it was noted that the downcoast tangential section of the bay reached a state of quasi-equilibrium long before the bay had eroded to its SEP. The technique is therefore usable on evolving bays although the final angle β may be larger for the final swash aligned beach.

A further point raised by Silvester and Hsu [30] in relation to β is if this angle is measured for a bay that exhibits a planform or shape that closely match the static equilibrium position then β for this bay is the true dominant wave angle for the area including nearby bays which may not be in static equilibrium. This wave angle can

then be refracted back into deep water to determine the dominant offshore wave approach angle. This can then be refracted shorewards into other bays to find the true dominant wave angle for these. This has implications for the present study as one of the bays, Pollshone, appears to be close to static equilibrium. It is postulated that this is because longshore drift is bypassing this small bay due to the prominence of the headland to the south (Fig. 3.1). This is further discussed in Chapter 4.

3.2.3 Comparison of the two techniques

The dominant wave angle obtained by the two techniques were compared and the differences for each bay noted. This comparison has a number of purposes. Firstly, differences between the two should indicate how far from static equilibrium is the current coastline. Secondly, they could also indicate a possible change in wave angle caused by changes in wind climate and thirdly, if the difference between angles varies between bays this could mean that the rate of longshore drift also varies from bay to bay.

3.3 Plotting the static equilibrium coastline

In order to plot the static equilibrium position of the coastline using the new parabolic curve method two input variables are required. The wave approach angle has been detailed above. The second variable is the control line.

3.3.1 The Control Points and Control Line

The control line or $\mathbf{R_0}$ is the line joining the upcoast and downcoast control points (Fig. 3.5). As discussed in section 3.1.2, in the case of small pocket bays, the downcoast control point is usually a headland or rock outcrop. However, for longer bays, the point may be located within the tangential section of the bay.

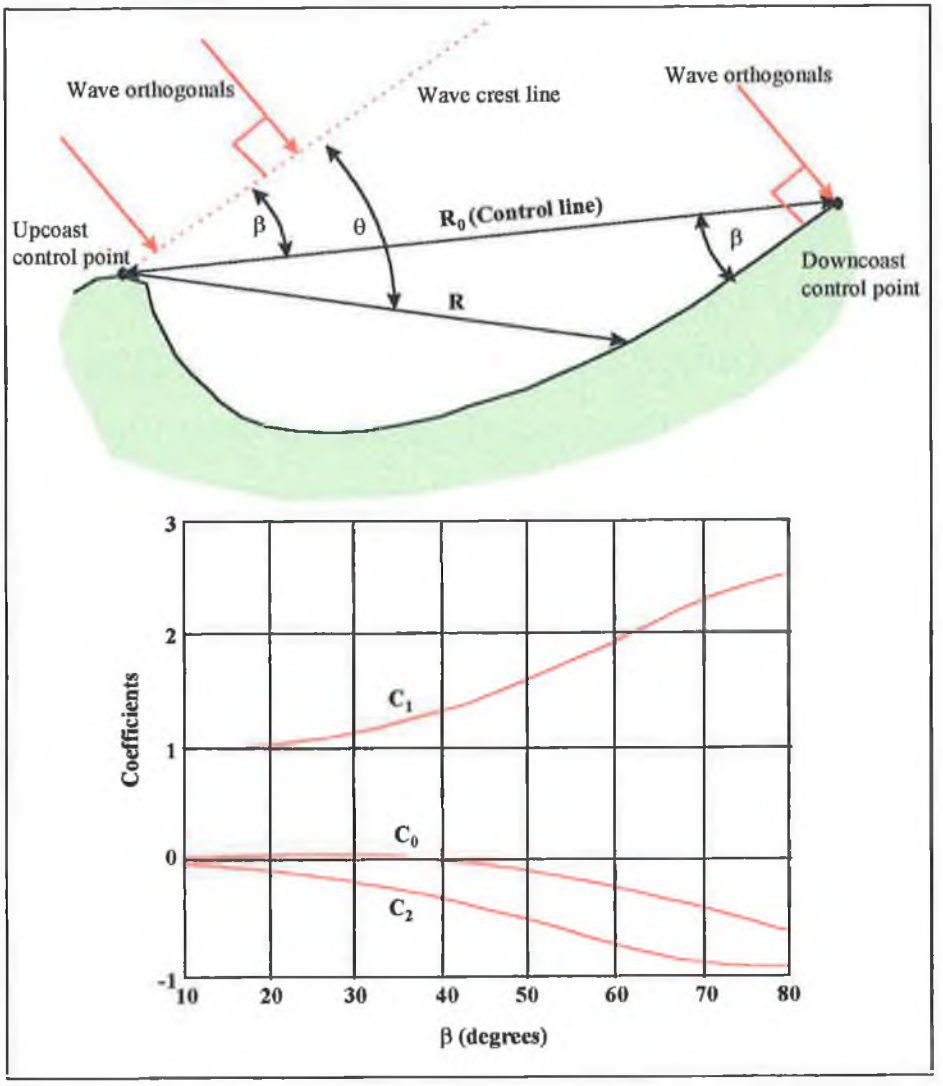

Fig. 3.5 - Definition sketch of the new parabolic curve method and graph showing C_0, C_1 and C_2 coefficients

Silvester and Hsu [30] examined the sensitivity of the bay shape to changes in location of the downcoast control point and the consequent changes in the length of the control line (Fig. 3.5). Even though this length was varied by ±15% there was little change in the static equilibrium position of the coastline mainly because the change in the control line caused a commensurate change in the angle β (by $\pm 5^0$). This technique was adopted for Courtown North and Ardamine where, by comparing a number of SEP's against the existing coastline, it was possible to determine the location of the downcoast control point with reasonable accuracy.

There is generally little difficulty in locating the upcoast control point as it is the point where wave diffraction takes place. This is usually at a headland, pier, reef or rocks. It is, however, unreliable identifying such a point from maps as they may not show rock outcrops or submerged reefs. For this study, aerial photographs showing wave crests were used to find this point for each of the studied bays. The photographs were from a series taken by the Ordnance Survey in 1990. The scale of the photographs is 1:10,000.

A complication arose in the case of Courtown North beach. The remains of an artificial breakwater constructed at the beginning of the 18^{th} century extends from a headland to the south giving two possible diffraction points. A third exists at the end of the harbour entrance walls. This problem of multiple upcoast control points had been discussed by Silvester and Hsu [30] who detailed a technique for plotting a coastline created by a number of upcoast control points. As shown in Fig. 3.6, the coastline is first plotted for the outermost control point using the measured values of the length of the control line **AD** and the wave approach angle β^1.

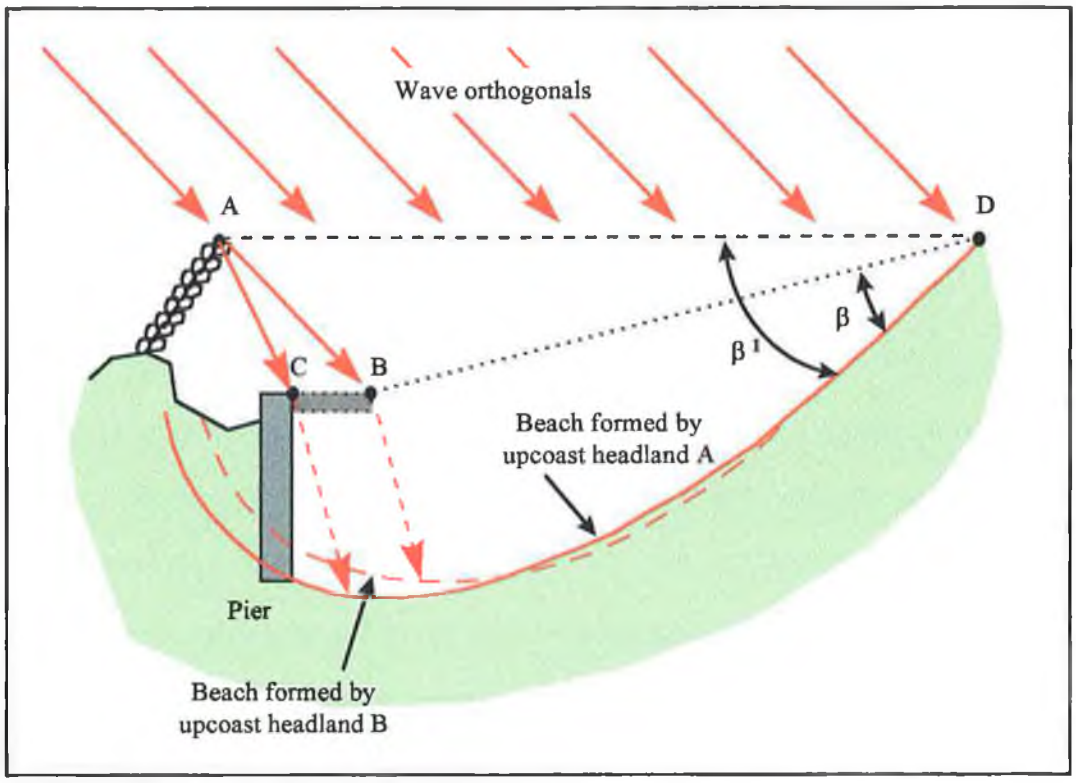

Fig. 3.6 - Bays formed by multiple headlands

The static equilibrium position for this situation is as shown in the figure up to the point where the wave orthogonal from **A** to **C** is diffracted. From this point to the lee of the pier there will be further diffraction causing greater curvature than is shown. If however the pier is extended to point **B** the original wave orthogonal will intersect both **A** and **B** so the line **BD** will become the new control line and the wave approach angle will have changed to β. The new beach will be as shown up to the point where the orthogonal from **A** to **B** is diffracted where there will, again, be additional curvature from here to the lee of the pier.

This technique was applied to the case of Courtown North where the harbour entrance walls were found to have the dominant effect on the bay shape.

3.3.2 Drawing the SEP

Having determined both the dominant wave approach angle and the control line it was then possible to draw the static equilibrium position for each of the three bays. The task itself is simply a matter of applying the polynomial developed by Hsu and Evans [38] i.e.

$$\frac{R}{R_0} = C_0 + C_1\left(\frac{\beta}{\theta}\right) + C_2\left(\frac{\beta}{\theta}\right)^2 \qquad (3)$$

where; **R, R_0,** β, θ are as shown in Fig. 3.5

C_0, C_1 and **C_2** are variables which change with β and are graphed in Fig. 3.5

An outline of the bay was traced from the aerial photographs of the area. This was then marked with the control points and the control line. The distance **R** was calculated for a number of selected values of θ (Silvester and Hsu [30] recommends steps of 15^0) and each of these lines were drawn on the trace. The endpoint of each of these lines marked the position of the coastline in static equilibrium conditions i.e. a swash aligned beach with zero transport of sediment into or out of the bay.

As this task was to be repeated many times it was decided to automate the process to some degree. Values for the coefficients were extracted from the curves given in Fig. 3.5 and were inputted into a standard spreadsheet computer package. The formula for calculating **R** was inserted into the programme and a graphing routine was developed which automatically created a radial plot of entered values of **R_0** and θ (Fig. 3.7). This was then pasted into a standard 2D drafting computer package where it was properly scaled and fitted as an overlay on the bay outline trace

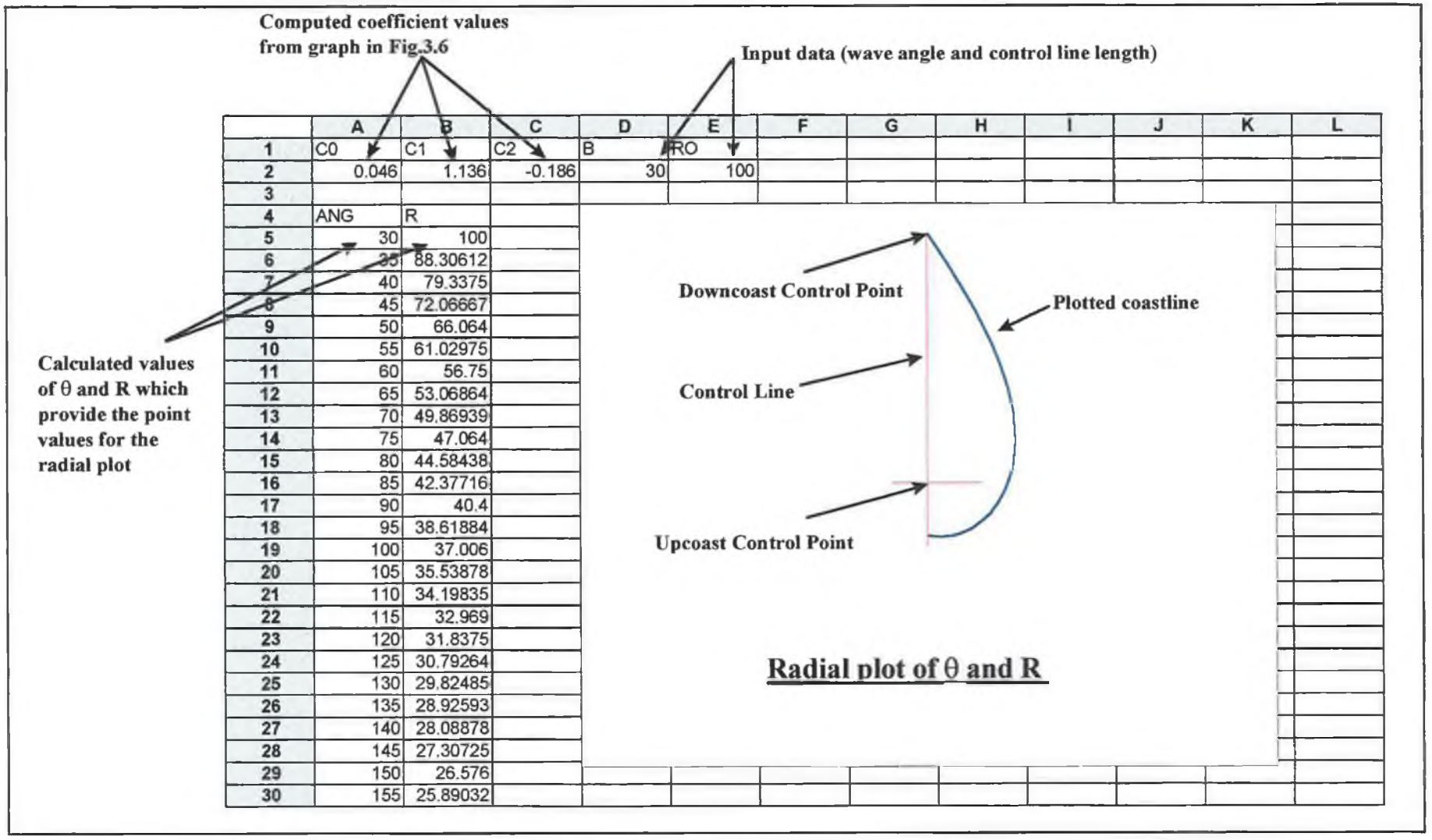

	A	B	C	D	E	F	G	H	I	J	K	L
1	C0	C1	C2	B	RO							
2	0.046	1.136	-0.186	30	100							
3												
4	ANG	R										
5	30	100										
6	35	88.30612										
7	40	79.3375										
8	45	72.06667										
9	50	66.064										
10	55	61.02975										
11	60	56.75										
12	65	53.06864										
13	70	49.86939										
14	75	47.064										
15	80	44.58438										
16	85	42.37716										
17	90	40.4										
18	95	38.61884										
19	100	37.006										
20	105	35.53878										
21	110	34.19835										
22	115	32.969										
23	120	31.8375										
24	125	30.79264										
25	130	29.82485										
26	135	28.92593										
27	140	28.08878										
28	145	27.30725										
29	150	26.576										
30	155	25.89032										

Fig. 3.7 - Display from spreadsheet used to draw radial plots

The SEP's for the three bays being studied were thus drawn for various control points and for the two wave approach angles as determined by the wave data and the bay planform methods.

3.2.3 Comparison of differing SEP's

The SEP's as drawn using the two wave approach angles were compared for each of the three bays by overlaying one on the other. Differences between the SEP's and the existing coastline were commented on and possible reasons for the variations were suggested.

3.3 Climate change and coastal protection measures

3.3.1 Climate change

Long term coastal change is primarily driven by changes in the climate. Global warming as a result of increasing levels of greenhouse gases in the atmosphere will have two major effects on the coast. It is anticipated that sea levels will rise by approximately 0.2m by the year 2030 [51] with the current rate of rise of about 1 to 2mm per year rising to 5mm per year [52]. The effect of this will be an increase in the erosion rate and recession of the coastline. However, the overall response of the coast to sea level rise is currently not fully understood with feedback mechanisms such as the development of offshore bars expected to play a major part. There is as yet little

evidence of this accelerated rise having started. Because of these uncertainties the effect of sea level rise on the coast is not investigated in this study.

The other effect of global warming is changes in storm patterns. There is strong evidence that this is presently underway with storm intensity, and consequently wave activity, on the increase since the 1950's [53, 54]. This has the potential to increase the amount of wave energy impinging on the coast and could change the direction of approach of the waves. If this happens all bays will be forced to adjust as beaches try to maintain swash alignment. It is this reaction that is investigated here.

The dominant wave approach direction β was varied to represent changes in storm pattern. It is considered more likely that there will be an increase in easterly winds which will cause β to decrease for the three bays and indeed all bays facing east. Step increases of two degree up to a maximum of 6 degrees were investigated and the realigned static equilibrium position coastlines are drawn for each.

3.3.2 Coastal protection measures

Man's development of the coastal zone has been a primary factor in increasing erosion rates [6]. Structures which interfere with the longshore drift of sediment such as piers, channel training walls, etc., have been a major factor as coastal areas downdrift have been starved of sediment. This effect is now well understood and developers of such structures in the future will be required to carry out an environmental impact assessment.

Coastal protection measures can, paradoxically, contribute to increased erosion rates. For example, waves impinging on the vertical face of a seawall are reflected back to sea. These can carry large amounts of sediment seaward, ultimately being deposited downdrift. The beach levels in front of these walls fall and remedial measures are required to prevent the walls being undermined. Because of this and their prohibitive cost, seawalls are now rarely built as coastal protection structures.

More common nowadays are coastal protection rock revetments. In the study area two have already been built, one is currently being extended and another is at the planning stage. Rock revetments provide a bulwark against the sea. Usually they are built at or above the high water mark and face wave attack only during storms or very high water levels. Their highly broken surface absorbs most of the wave energy with little being reflected back to the sea.

The problem with revetments is that they often try to maintain a coastline that is not in equilibrium with the forces of the sea. In the short term, it is the terminal points of the revetment that are problematic. Re-entries is a form of erosion where the soft coast at the end of the revetment is eroded into the crenellate curve, in effect a smaller version of the bay curve. This was investigated for each of the existing, extended and planned revetments within the study area.

In the long term, the artificial hardening of an unstable coastline will, without constant maintenance, eventually fail as structures become undermined. In areas which have little longshore sediment transport this can happen within a number of years. The study area is, however, fortunate to have a longshore transport rates of between 50,000 and

100,000 m^3 per year [39]. Therefore, it is likely that undermining of the revetment will be relatively slow even though the coastline is inherently unstable.

4. ANALYSIS AND DISCUSSION OF RESULTS

4.1 Ascertaining the Dominant Wave Direction

4.1.1 Dominant wave direction from wave data

Having obtained offshore hindcast wave data from the British Meteorological Office computer model for the selected point in the south Irish sea (Fig. 3.1), the first step was to group the two years of 'resultant wave' data into blocks which could be brought inshore using the wave refraction/diffraction computer model. This model requires input wave descriptors such as, wave height, wave period and wave direction. The wave data was analysed and tables created based on these parameters allowing the number of occurrences of each type of wave to be counted. As the entire data set contains 5840 lines of data each containing 20 variables, the only possible way of carrying out such analysis was by using a computer program. A customised program was written in BASIC and the listing is given in the Appendix.

4.1.1.1 Creation of scatter tables

The generated tables are called 'directional scatter tables' and have the wave period on the x-axis with wave height on the y-axis (plots 4.1 to 4.8). The term 'Zero Up-crossing Period' refers to the time taken for the wave to pass a fixed point. Each of the plots presented below cover a wave direction span of 22.5^0 starting at 0^0 and ending at 180^0. Waves approaching from the west are ignored as their contribution to inshore wave energy would be very difficult to ascertain and in any event is likely to be small.

Each value in the plots represent a period of 3 hours. Thus a value of 8 for a wave period of 6 seconds and a wave height of between 1.5 to 2m means that these waves occurred for a total duration of 24 hours over the years 1994-95. Since one such wave occurs every 6 seconds the total number of individual waves occurring over the 24 hours is 14,400.

		SCATTER TABLE FOR WAVE DIRECTION BETWEEN 0 - 22.5 DEG.															Total
SIG.	14 *	0	0	0	0	0	0	0	0	0	0	0	0	0	0	0	0
WAVE	13.5 *	0	0	0	0	0	0	0	0	0	0	0	0	0	0	0	0
HEIGHT	13 *	0	0	0	0	0	0	0	0	0	0	0	0	0	0	0	0
(metres)	12.5 *	0	0	0	0	0	0	0	0	0	0	0	0	0	0	0	0
	12 *	0	0	0	0	0	0	0	0	0	0	0	0	0	0	0	0
	11.5 *	0	0	0	0	0	0	0	0	0	0	0	0	0	0	0	0
	11 *	0	0	0	0	0	0	0	0	0	0	0	0	0	0	0	0
	10.5 *	0	0	0	0	0	0	0	0	0	0	0	0	0	0	0	0
	10 *	0	0	0	0	0	0	0	0	0	0	0	0	0	0	0	0
	9.5 *	0	0	0	0	0	0	0	0	0	0	0	0	0	0	0	0
	9 *	0	0	0	0	0	0	0	0	0	0	0	0	0	0	0	0
	8.5 *	0	0	0	0	0	0	0	0	0	0	0	0	0	0	0	0
	8 *	0	0	0	0	0	0	0	0	0	0	0	0	0	0	0	0
	7.5 *	0	0	0	0	0	0	0	0	0	0	0	0	0	0	0	0
	7 *	0	0	0	0	0	0	0	0	0	0	0	0	0	0	0	0
	6.5 *	0	0	0	0	0	0	0	0	0	0	0	0	0	0	0	0
	6 *	0	0	0	0	0	0	0	0	0	0	0	0	0	0	0	0
	5.5 *	0	0	0	0	0	0	0	0	0	0	0	0	0	0	0	0
	5 *	0	0	0	0	0	0	0	0	0	0	0	0	0	0	0	0
	4.5 *	0	0	0	0	0	0	0	0	0	0	0	0	0	0	0	0
	4 *	0	0	0	0	0	0	0	0	0	0	0	0	0	0	0	0
	3.5 *	0	0	0	0	0	0	0	0	0	0	0	0	0	0	0	0
	3 *	0	0	0	0	0	0	1	0	0	0	0	0	0	0	0	1
	2.5 *	0	0	0	0	0	0	2	0	0	0	0	0	0	0	0	2
	2 *	0	0	0	0	0	2	0	0	0	0	0	0	0	0	0	2
	1.5 *	0	0	0	0	1	8	0	0	0	0	0	0	0	0	0	9
	1 *	0	0	0	0	27	0	0	0	0	0	0	0	0	0	0	27
	0.5 *	0	0	0	21	14	0	0	0	0	0	0	0	0	0	0	35
	0 *	0	0	0	29	0	0	0	0	0	0	0	0	0	0	0	29
		1	2	3	4	5	6	7	8	9	10	11	12	13	14	15	
		ZERO UP-CROSSING PERIOD (seconds)															

Table 4.1 - Directional scatter table for waves between 0^0 - 22.5^0

SCATTER TABLE FOR WAVE DIRECTION BETWEEN 22.5 - 45 DEG.																	Total
SIG.	14 *	0	0	0	0	0	0	0	0	0	0	0	0	0	0	0	0
WAVE	13.5 *	0	0	0	0	0	0	0	0	0	0	0	0	0	0	0	0
HEIGHT	13 *	0	0	0	0	0	0	0	0	0	0	0	0	0	0	0	0
(metres)	12.5 *	0	0	0	0	0	0	0	0	0	0	0	0	0	0	0	0
	12 *	0	0	0	0	0	0	0	0	0	0	0	0	0	0	0	0
	11.5 *	0	0	0	0	0	0	0	0	0	0	0	0	0	0	0	0
	11 *	0	0	0	0	0	0	0	0	0	0	0	0	0	0	0	0
	10.5 *	0	0	0	0	0	0	0	0	0	0	0	0	0	0	0	0
	10 *	0	0	0	0	0	0	0	0	0	0	0	0	0	0	0	0
	9.5 *	0	0	0	0	0	0	0	0	0	0	0	0	0	0	0	0
	9 *	0	0	0	0	0	0	0	0	0	0	0	0	0	0	0	0
	8.5 *	0	0	0	0	0	0	0	0	0	0	0	0	0	0	0	0
	8 *	0	0	0	0	0	0	0	0	0	0	0	0	0	0	0	0
	7.5 *	0	0	0	0	0	0	0	0	0	0	0	0	0	0	0	0
	7 *	0	0	0	0	0	0	0	0	0	0	0	0	0	0	0	0
	6.5 *	0	0	0	0	0	0	0	0	0	0	0	0	0	0	0	0
	6 *	0	0	0	0	0	0	0	0	0	0	0	0	0	0	0	0
	5.5 *	0	0	0	0	0	0	0	0	0	0	0	0	0	0	0	0
	5 *	0	0	0	0	0	0	0	0	0	0	0	0	0	0	0	0
	4.5 *	0	0	0	0	0	0	0	0	0	0	0	0	0	0	0	0
	4 *	0	0	0	0	0	0	0	0	0	0	0	0	0	0	0	0
	3.5 *	0	0	0	0	0	0	1	1	0	0	0	0	0	0	0	2
	3 *	0	0	0	0	0	0	2	0	0	0	0	0	0	0	0	2
	2.5 *	0	0	0	0	0	0	3	0	0	0	0	0	0	0	0	3
	2 *	0	0	0	0	0	11	0	0	0	0	0	0	0	0	0	11
	1.5 *	0	0	0	0	17	35	1	0	0	0	0	0	0	0	0	53
	1 *	0	0	0	0	55	5	0	0	0	0	0	0	0	0	0	60
	0.5 *	0	0	0	39	38	4	0	0	0	0	0	0	0	0	0	81
	0 *	0	0	0	21	2	0	0	0	0	0	0	0	0	0	0	23
		1	2	3	4	5	6	7	8	9	10	11	12	13	14	15	
		ZERO UP-CROSSING PERIOD (seconds)															

Table 4.2 - Directional scatter table for waves between 22.5^0 - 45^0

SCATTER TABLE FOR WAVE DIRECTION BETWEEN 45 - 67.5 DEG.																	Total
SIG.	14 *	0	0	0	0	0	0	0	0	0	0	0	0	0	0	0	0
WAVE	13.5 *	0	0	0	0	0	0	0	0	0	0	0	0	0	0	0	0
HEIGHT	13 *	0	0	0	0	0	0	0	0	0	0	0	0	0	0	0	0
(metres)	12.5 *	0	0	0	0	0	0	0	0	0	0	0	0	0	0	0	0
	12 *	0	0	0	0	0	0	0	0	0	0	0	0	0	0	0	0
	11.5 *	0	0	0	0	0	0	0	0	0	0	0	0	0	0	0	0
	11 *	0	0	0	0	0	0	0	0	0	0	0	0	0	0	0	0
	10.5 *	0	0	0	0	0	0	0	0	0	0	0	0	0	0	0	0
	10 *	0	0	0	0	0	0	0	0	0	0	0	0	0	0	0	0
	9.5 *	0	0	0	0	0	0	0	0	0	0	0	0	0	0	0	0
	9 *	0	0	0	0	0	0	0	0	0	0	0	0	0	0	0	0
	8.5 *	0	0	0	0	0	0	0	0	0	0	0	0	0	0	0	0
	8 *	0	0	0	0	0	0	0	0	0	0	0	0	0	0	0	0
	7.5 *	0	0	0	0	0	0	0	0	0	0	0	0	0	0	0	0
	7 *	0	0	0	0	0	0	0	0	0	0	0	0	0	0	0	0
	6.5 *	0	0	0	0	0	0	0	0	0	0	0	0	0	0	0	0
	6 *	0	0	0	0	0	0	0	0	0	0	0	0	0	0	0	0
	5.5 *	0	0	0	0	0	0	0	0	0	0	0	0	0	0	0	0
	5 *	0	0	0	0	0	0	0	0	0	0	0	0	0	0	0	0
	4.5 *	0	0	0	0	0	0	0	0	0	0	0	0	0	0	0	0
	4 *	0	0	0	0	0	0	0	0	0	0	0	0	0	0	0	0
	3.5 *	0	0	0	0	0	0	0	2	0	0	0	0	0	0	0	2
	3 *	0	0	0	0	0	0	4	2	0	0	0	0	0	0	0	6
	2.5 *	0	0	0	0	0	0	11	0	0	0	0	0	0	0	0	11
	2 *	0	0	0	0	0	25	2	0	0	0	0	0	0	0	0	27
	1.5 *	0	0	0	0	13	35	0	0	0	0	0	0	0	0	0	48
	1 *	0	0	0	0	37	0	0	0	0	0	0	0	0	0	0	37
	0.5 *	0	0	0	22	8	0	0	0	0	0	0	0	0	0	0	30
	0 *	0	0	0	25	0	0	0	0	0	0	0	0	0	0	0	25
		1	2	3	4	5	6	7	8	9	10	11	12	13	14	15	
		ZERO UP-CROSSING PERIOD (seconds)															

Table 4.3 - Directional table plot for waves between 45^0 - 67.5^0

SCATTER TABLE FOR WAVE DIRECTION BETWEEN 67.5 - 90 DEG.																	Total
SIG.	14 *	0	0	0	0	0	0	0	0	0	0	0	0	0	0	0	0
WAVE	13.5 *	0	0	0	0	0	0	0	0	0	0	0	0	0	0	0	0
HEIGHT	13 *	0	0	0	0	0	0	0	0	0	0	0	0	0	0	0	0
(metres)	12.5 *	0	0	0	0	0	0	0	0	0	0	0	0	0	0	0	0
	12 *	0	0	0	0	0	0	0	0	0	0	0	0	0	0	0	0
	11.5 *	0	0	0	0	0	0	0	0	0	0	0	0	0	0	0	0
	11 *	0	0	0	0	0	0	0	0	0	0	0	0	0	0	0	0
	10.5 *	0	0	0	0	0	0	0	0	0	0	0	0	0	0	0	0
	10 *	0	0	0	0	0	0	0	0	0	0	0	0	0	0	0	0
	9.5 *	0	0	0	0	0	0	0	0	0	0	0	0	0	0	0	0
	9 *	0	0	0	0	0	0	0	0	0	0	0	0	0	0	0	0
	8.5 *	0	0	0	0	0	0	0	0	0	0	0	0	0	0	0	0
	8 *	0	0	0	0	0	0	0	0	0	0	0	0	0	0	0	0
	7.5 *	0	0	0	0	0	0	0	0	0	0	0	0	0	0	0	0
	7 *	0	0	0	0	0	0	0	0	0	0	0	0	0	0	0	0
	6.5 *	0	0	0	0	0	0	0	0	0	0	0	0	0	0	0	0
	6 *	0	0	0	0	0	0	0	0	0	0	0	0	0	0	0	0
	5.5 *	0	0	0	0	0	0	0	0	0	0	0	0	0	0	0	0
	5 *	0	0	0	0	0	0	0	0	0	0	0	0	0	0	0	0
	4.5 *	0	0	0	0	0	0	0	0	0	0	0	0	0	0	0	0
	4 *	0	0	0	0	0	0	0	0	0	0	0	0	0	0	0	0
	3.5 *	0	0	0	0	0	0	0	0	0	0	0	0	0	0	0	0
	3 *	0	0	0	0	0	0	1	0	0	0	0	0	0	0	0	1
	2.5 *	0	0	0	0	0	0	1	0	0	0	0	0	0	0	0	1
	2 *	0	0	0	0	0	8	1	0	0	0	0	0	0	0	0	9
	1.5 *	0	0	0	0	2	6	0	0	0	0	0	0	0	0	0	8
	1 *	0	0	0	1	20	1	0	0	0	0	0	0	0	0	0	22
	0.5 *	0	0	0	28	10	0	0	0	0	0	0	0	0	0	0	38
	0 *	0	0	0	11	0	0	0	0	0	0	0	0	0	0	0	11
		1	2	3	4	5	6	7	8	9	10	11	12	13	14	15	
		ZERO UP-CROSSING PERIOD (seconds)															

Table 4.4 - Directional scatter table for waves between 67.5^0 - 90^0

SCATTER TABLE FOR WAVE DIRECTION BETWEEN 90 - 112.5 DEG.																	Total
SIG.	14 *	0	0	0	0	0	0	0	0	0	0	0	0	0	0	0	0
WAVE	13.5 *	0	0	0	0	0	0	0	0	0	0	0	0	0	0	0	0
HEIGHT	13 *	0	0	0	0	0	0	0	0	0	0	0	0	0	0	0	0
(metres)	12.5 *	0	0	0	0	0	0	0	0	0	0	0	0	0	0	0	0
	12 *	0	0	0	0	0	0	0	0	0	0	0	0	0	0	0	0
	11.5 *	0	0	0	0	0	0	0	0	0	0	0	0	0	0	0	0
	11 *	0	0	0	0	0	0	0	0	0	0	0	0	0	0	0	0
	10.5 *	0	0	0	0	0	0	0	0	0	0	0	0	0	0	0	0
	10 *	0	0	0	0	0	0	0	0	0	0	0	0	0	0	0	0
	9.5 *	0	0	0	0	0	0	0	0	0	0	0	0	0	0	0	0
	9 *	0	0	0	0	0	0	0	0	0	0	0	0	0	0	0	0
	8.5 *	0	0	0	0	0	0	0	0	0	0	0	0	0	0	0	0
	8 *	0	0	0	0	0	0	0	0	0	0	0	0	0	0	0	0
	7.5 *	0	0	0	0	0	0	0	0	0	0	0	0	0	0	0	0
	7 *	0	0	0	0	0	0	0	0	0	0	0	0	0	0	0	0
	6.5 *	0	0	0	0	0	0	0	0	0	0	0	0	0	0	0	0
	6 *	0	0	0	0	0	0	0	0	0	0	0	0	0	0	0	0
	5.5 *	0	0	0	0	0	0	0	0	0	0	0	0	0	0	0	0
	5 *	0	0	0	0	0	0	0	0	0	0	0	0	0	0	0	0
	4.5 *	0	0	0	0	0	0	0	0	0	0	0	0	0	0	0	0
	4 *	0	0	0	0	0	0	0	0	0	0	0	0	0	0	0	0
	3.5 *	0	0	0	0	0	0	0	0	0	0	0	0	0	0	0	0
	3 *	0	0	0	0	0	0	0	0	0	0	0	0	0	0	0	0
	2.5 *	0	0	0	0	0	0	0	0	0	0	0	0	0	0	0	0
	2 *	0	0	0	0	0	3	0	0	0	0	0	0	0	0	0	3
	1.5 *	0	0	0	0	2	1	0	0	0	0	0	0	0	0	0	3
	1 *	0	0	0	0	18	0	0	0	0	0	0	0	0	0	0	18
	0.5 *	0	0	0	12	8	0	0	0	0	0	0	0	0	0	0	20
	0 *	0	0	0	11	0	0	0	0	0	0	0	0	0	0	0	11
		1	2	3	4	5	6	7	8	9	10	11	12	13	14	15	
		ZERO UP-CROSSING PERIOD (seconds)															

Table 4.5 - Directional scatter table for waves between 90^0 - 112.5^0

SCATTER TABLE FOR WAVE DIRECTION BETWEEN 112.5 - 135 DEG.																	Total
SIG.	14 *	0	0	0	0	0	0	0	0	0	0	0	0	0	0	0	0
WAVE	13.5 *	0	0	0	0	0	0	0	0	0	0	0	0	0	0	0	0
HEIGHT	13 *	0	0	0	0	0	0	0	0	0	0	0	0	0	0	0	0
(metres)	12.5 *	0	0	0	0	0	0	0	0	0	0	0	0	0	0	0	0
	12 *	0	0	0	0	0	0	0	0	0	0	0	0	0	0	0	0
	11.5 *	0	0	0	0	0	0	0	0	0	0	0	0	0	0	0	0
	11 *	0	0	0	0	0	0	0	0	0	0	0	0	0	0	0	0
	10.5 *	0	0	0	0	0	0	0	0	0	0	0	0	0	0	0	0
	10 *	0	0	0	0	0	0	0	0	0	0	0	0	0	0	0	0
	9.5 *	0	0	0	0	0	0	0	0	0	0	0	0	0	0	0	0
	9 *	0	0	0	0	0	0	0	0	0	0	0	0	0	0	0	0
	8.5 *	0	0	0	0	0	0	0	0	0	0	0	0	0	0	0	0
	8 *	0	0	0	0	0	0	0	0	0	0	0	0	0	0	0	0
	7.5 *	0	0	0	0	0	0	0	0	0	0	0	0	0	0	0	0
	7 *	0	0	0	0	0	0	0	0	0	0	0	0	0	0	0	0
	6.5 *	0	0	0	0	0	0	0	0	0	0	0	0	0	0	0	0
	6 *	0	0	0	0	0	0	0	0	0	0	0	0	0	0	0	0
	5.5 *	0	0	0	0	0	0	0	0	1	0	0	0	0	0	0	1
	5 *	0	0	0	0	0	0	0	1	0	0	0	0	0	0	0	1
	4.5 *	0	0	0	0	0	0	0	0	0	0	0	0	0	0	0	0
	4 *	0	0	0	0	0	0	0	0	0	0	0	0	0	0	0	0
	3.5 *	0	0	0	0	0	0	0	0	0	0	0	0	0	0	0	0
	3 *	0	0	0	0	0	0	3	0	0	0	0	0	0	0	0	3
	2.5 *	0	0	0	0	0	0	2	0	0	0	0	0	0	0	0	2
	2 *	0	0	0	0	0	2	0	0	0	0	0	0	0	0	0	2
	1.5 *	0	0	0	0	3	4	0	0	0	0	0	0	0	0	0	7
	1 *	0	0	0	2	16	0	0	0	0	0	0	0	0	0	0	18
	0.5 *	0	0	0	7	7	0	1	0	0	0	0	0	0	0	0	15
	0 *	0	0	0	7	0	1	2	0	0	0	0	0	0	0	0	10
		1	2	3	4	5	6	7	8	9	10	11	12	13	14	15	
		ZERO UP-CROSSING PERIOD (seconds)															

Table 4.6 - Directional scatter table for waves between 112.5^0 - 135^0

SCATTER TABLE FOR WAVE DIRECTION BETWEEN 135 - 157.5 DEG.																	Total
SIG.	14 *	0	0	0	0	0	0	0	0	0	0	0	0	0	0	0	0
WAVE	13.5 *	0	0	0	0	0	0	0	0	0	0	0	0	0	0	0	0
HEIGHT	13 *	0	0	0	0	0	0	0	0	0	0	0	0	0	0	0	0
(metres)	12.5 *	0	0	0	0	0	0	0	0	0	0	0	0	0	0	0	0
	12 *	0	0	0	0	0	0	0	0	0	0	0	0	0	0	0	0
	11.5 *	0	0	0	0	0	0	0	0	0	0	0	0	0	0	0	0
	11 *	0	0	0	0	0	0	0	0	0	0	0	0	0	0	0	0
	10.5 *	0	0	0	0	0	0	0	0	0	0	0	0	0	0	0	0
	10 *	0	0	0	0	0	0	0	0	0	0	0	0	0	0	0	0
	9.5 *	0	0	0	0	0	0	0	0	0	0	0	0	0	0	0	0
	9 *	0	0	0	0	0	0	0	0	0	0	0	0	0	0	0	0
	8.5 *	0	0	0	0	0	0	0	0	0	0	0	0	0	0	0	0
	8 *	0	0	0	0	0	0	0	0	0	0	0	0	0	0	0	0
	7.5 *	0	0	0	0	0	0	0	0	0	0	0	0	0	0	0	0
	7 *	0	0	0	0	0	0	0	0	0	0	1	0	0	0	0	1
	6.5 *	0	0	0	0	0	0	0	0	0	0	0	0	0	0	0	0
	6 *	0	0	0	0	0	0	0	0	1	2	0	0	0	0	0	3
	5.5 *	0	0	0	0	0	0	0	0	2	1	0	0	0	0	0	3
	5 *	0	0	0	0	0	0	0	0	3	1	0	0	0	0	0	4
	4.5 *	0	0	0	0	0	0	0	4	8	1	0	0	0	0	0	13
	4 *	0	0	0	0	0	0	0	9	10	1	0	0	0	0	0	20
	3.5 *	0	0	0	0	0	0	1	15	7	2	0	0	0	0	0	25
	3 *	0	0	0	0	0	0	8	29	7	0	0	0	0	0	0	44
	2.5 *	0	0	0	0	0	0	37	24	5	0	0	0	0	0	0	66
	2 *	0	0	0	0	0	28	38	12	9	6	0	0	0	0	0	93
	1.5 *	0	0	0	0	11	59	25	11	4	2	0	0	0	0	0	112
	1 *	0	0	0	7	92	47	10	9	4	2	1	0	0	0	0	172
	0.5 *	0	0	0	75	218	95	51	16	9	5	2	0	0	0	0	471
	0 *	0	0	0	53	67	26	10	4	3	0	0	0	0	0	0	163
		1	2	3	4	5	6	7	8	9	10	11	12	13	14	15	
		ZERO UP-CROSSING PERIOD (seconds)															

Table 4.7 - Directional scatter table for waves between 135^0 - 157.5^0

SCATTER TABLE FOR WAVE DIRECTION BETWEEN 157.5 - 180 DEG.																	Total
SIG.	14 *	0	0	0	0	0	0	0	0	0	0	0	0	0	0	0	0
WAVE	13.5 *	0	0	0	0	0	0	0	0	0	0	0	0	0	0	0	0
HEIGHT	13 *	0	0	0	0	0	0	0	0	0	0	0	0	0	0	0	0
(metres)	12.5 *	0	0	0	0	0	0	0	0	0	0	0	0	0	0	0	0
	12 *	0	0	0	0	0	0	0	0	0	0	0	0	0	0	0	0
	11.5 *	0	0	0	0	0	0	0	0	0	0	0	0	0	0	0	0
	11 *	0	0	0	0	0	0	0	0	0	0	0	0	0	0	0	0
	10.5 *	0	0	0	0	0	0	0	0	0	0	0	0	0	0	0	0
	10 *	0	0	0	0	0	0	0	0	0	0	0	0	0	0	0	0
	9.5 *	0	0	0	0	0	0	0	0	0	0	0	0	0	0	0	0
	9 *	0	0	0	0	0	0	0	0	0	0	0	0	0	0	0	0
	8.5 *	0	0	0	0	0	0	0	0	0	0	0	0	0	0	0	0
	8 *	0	0	0	0	0	0	0	0	0	0	0	0	0	0	0	0
	7.5 *	0	0	0	0	0	0	0	0	0	0	0	0	0	0	0	0
	7 *	0	0	0	0	0	0	0	0	0	0	0	0	0	0	0	0
	6.5 *	0	0	0	0	0	0	0	0	0	1	0	0	0	0	0	1
	6 *	0	0	0	0	0	0	0	0	0	2	0	0	0	0	0	2
	5.5 *	0	0	0	0	0	0	0	0	7	1	0	0	0	0	0	8
	5 *	0	0	0	0	0	0	0	0	11	1	0	0	0	0	0	12
	4.5 *	0	0	0	0	0	0	0	5	17	0	0	0	0	0	0	22
	4 *	0	0	0	0	0	0	3	29	2	0	0	0	0	0	0	34
	3.5 *	0	0	0	0	0	0	1	21	2	0	0	0	0	0	0	24
	3 *	0	0	0	0	0	0	43	23	3	0	0	0	0	0	0	69
	2.5 *	0	0	0	0	0	4	76	26	2	0	0	0	0	0	0	108
	2 *	0	0	0	0	1	54	59	14	6	1	0	0	0	0	0	135
	1.5 *	0	0	0	1	22	85	26	14	6	0	0	0	0	0	0	154
	1 *	0	0	0	12	83	60	23	11	1	1	0	0	0	0	0	191
	0.5 *	0	0	0	48	121	77	27	4	1	0	0	0	0	0	0	278
	0 *	0	0	0	62	51	33	7	2	0	0	0	0	0	0	0	155
		1	2	3	4	5	6	7	8	9	10	11	12	13	14	15	
		ZERO UP-CROSSING PERIOD (seconds)															

Table 4.8 - Directional scatter table for waves between 157.5^0 - 190^0

From these tables it was possible to create an offshore 'wave rose' which graphically demonstrates the dominance of the southerly swell in the south Irish sea. This is shown in Fig. 4.1.

4.1.1.2 Bringing the offshore wave inshore

The wave refraction/diffraction computer model used was ROWAVE [46]. This required two input files, the bathymetric file for the area, called the GRID FILE and the CONTROL FILE. The CONTROL FILE contained details on the bathymetric grid (number of grid points, dimensions of grid, addition to water level, etc.) and details of the input wave such as the wave height, period and direction.

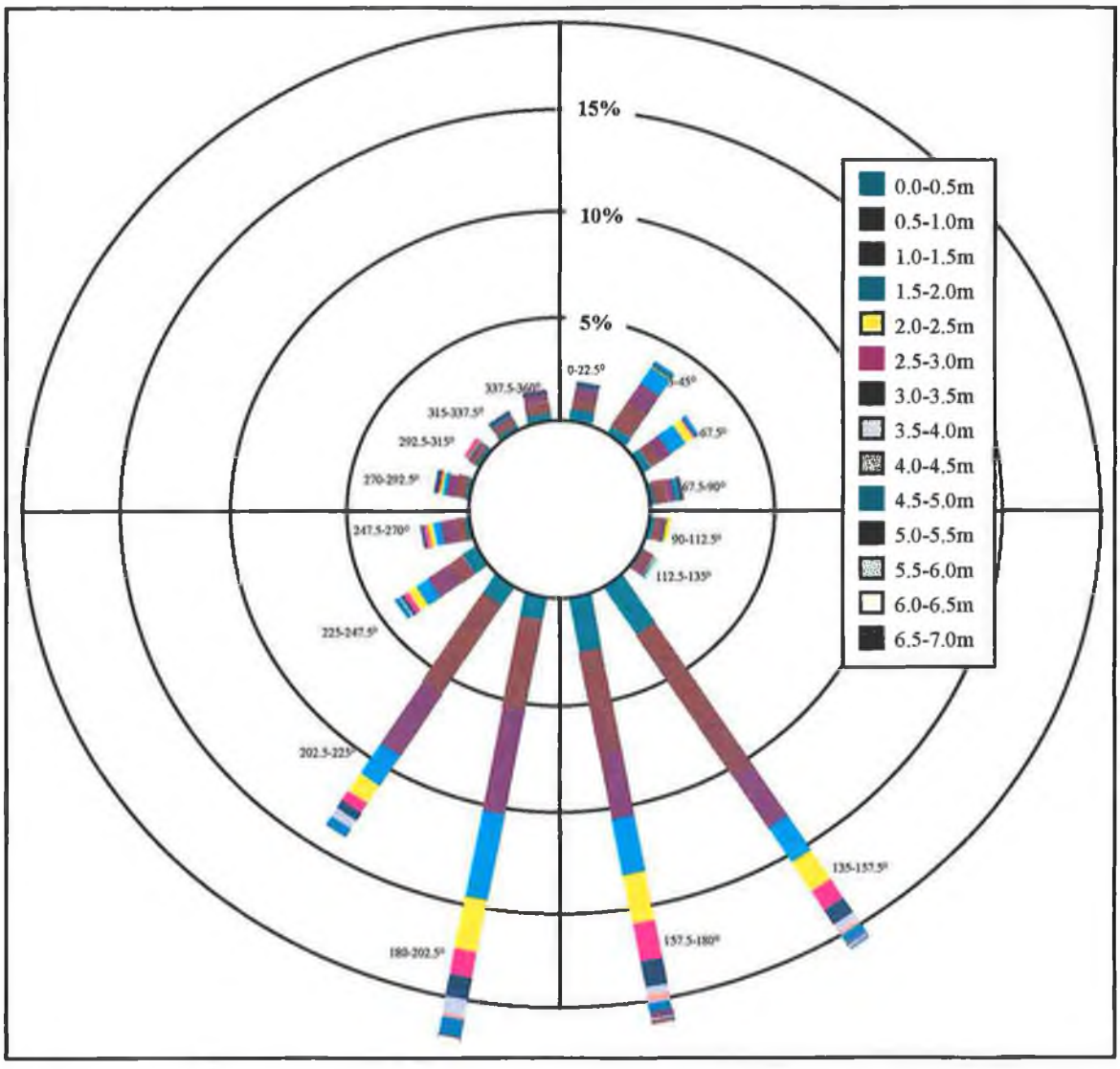

Fig. 4.1 - Wave rose for offshore grid point 52.5N - 6.06W

An individual CONTROL FILE had to be created for each of the wave types in the scatter plots, a total of 181 files. A sample file is given in Fig. 4.2.

The GRID FILE contains the bathymetry for the area and it was created from a bathymetric chart (Admiralty Chart no.1727) by manually inputting water depths. An additional depth of 0.6m was added to simulate mean water level conditions.

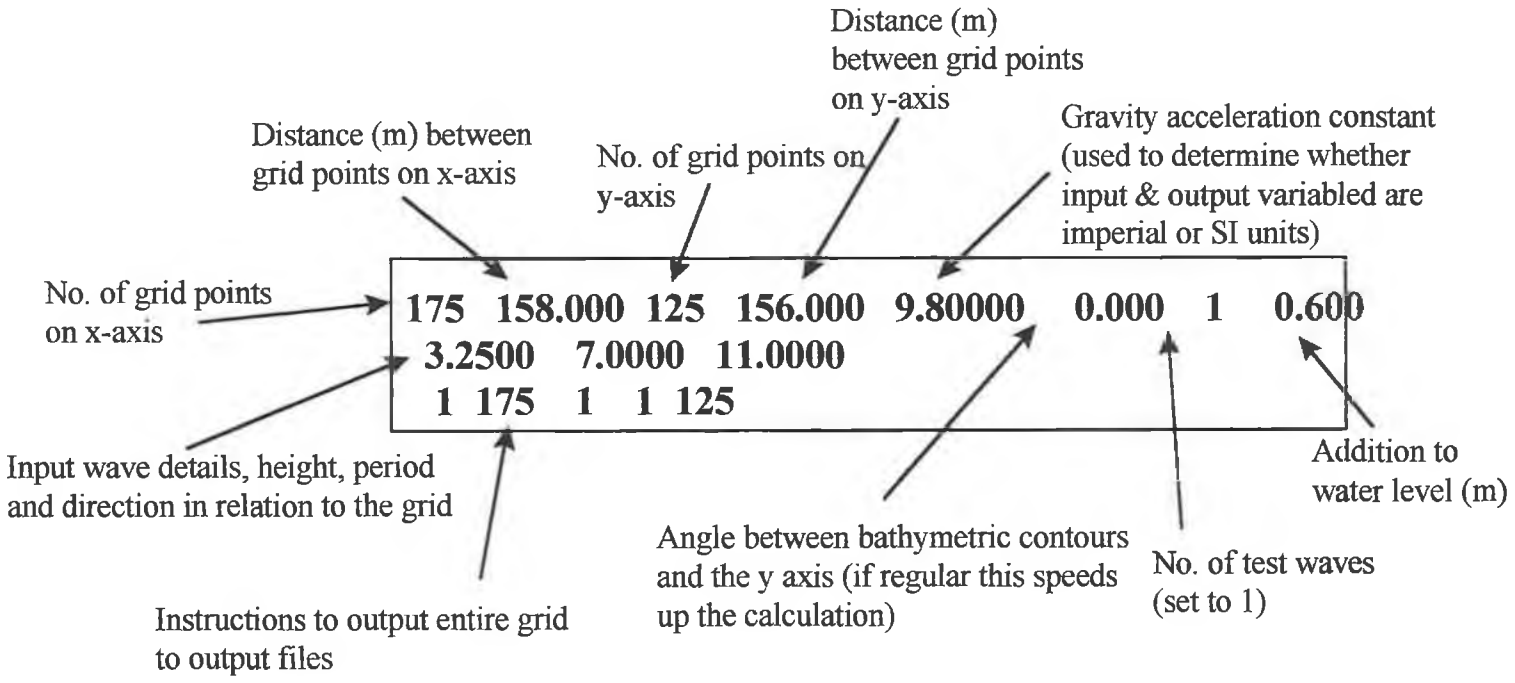

Fig. 4.2 - Control File for wave refraction / diffraction model RCPWAVE

This data was then edited to include nearshore measurements taken during the autumn of 1995 as part of the ECOPRO project [48]. The editing was carried out within the ROWAVE package. The grid covered an area 19.5km x 27.6km and was oriented with the longer x-axis running due north. Fig. 4.3 shows a depth contour map of the grid.

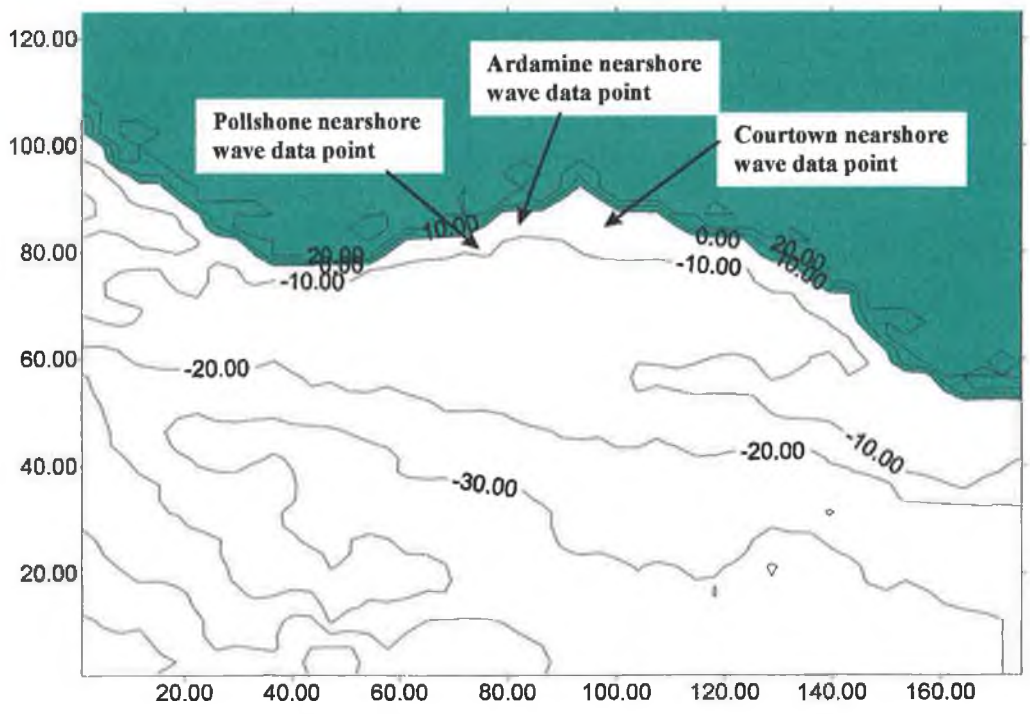

Fig 4.3 - Depth contour map of bathymetric grid

The location of the grid points used to obtain the details of the nearshore wave at each of the three bays is also shown in Fig. 4.2. The water depth at each is approximately 7.9m (including additional 0.6m).

A complication arose when waves of a strongly oblique angle were used as input waves to the model. ROWAVE and the original RCPWAVE along with other wave refraction/diffraction models have difficulty computing wave angles as they approach 90^0 to the grid. To avoid this problem it was necessary to create new grids angled

sufficiently so that the wave angle was always significantly less than 90^0 at all points on the grid. The process of manually inputting water depth data is time consuming so, a BASIC computer program was written which automatically created the new grids. The new grids were angled at 45^0 to the original grid and were resized and shifted to ensure that the new grid edges did not project beyond the original grid dimensions. The outline of the two altered grids is shown in Fig. 4.4 and the BASIC program is listed in the Appendix.

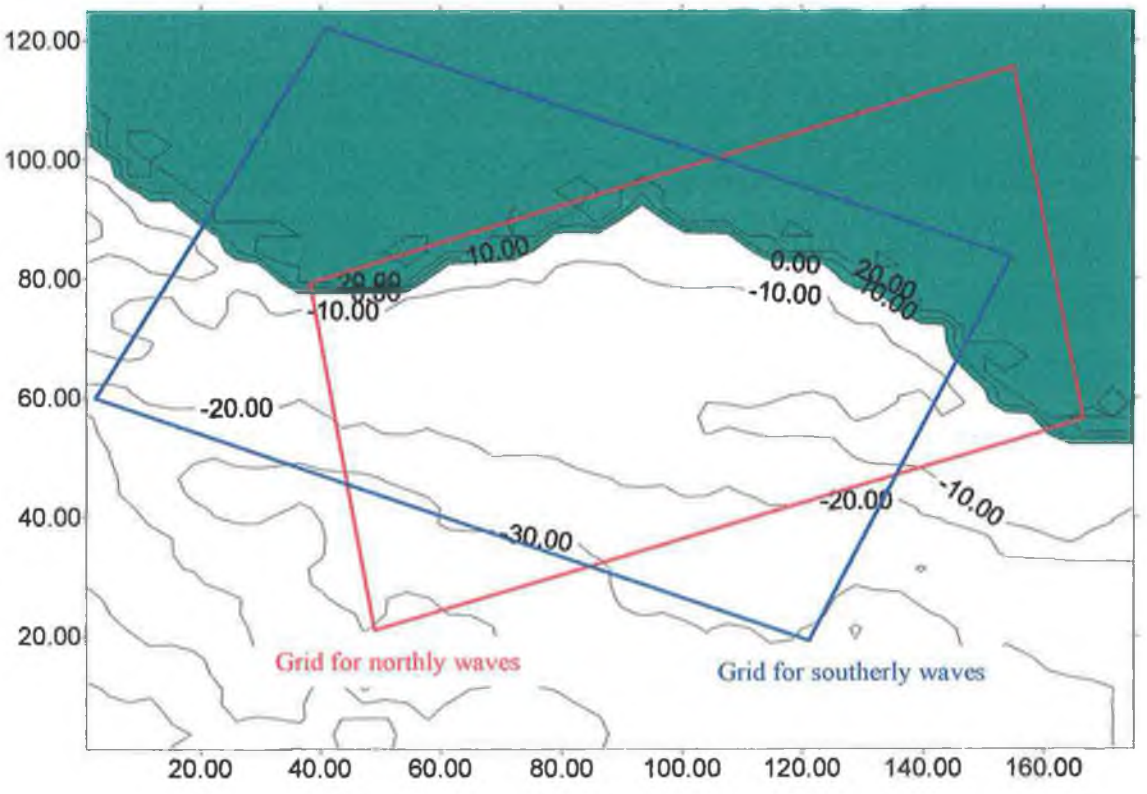

Fig. 4.4 - New bathymetric grids required for northerly and southerly waves

4.1.1.3 Obtaining inshore wave energy data.

With the appropriate CONTROL & GRID FILES each type of offshore wave was propagated towards the shore using the ROWAVE package (Figs. 4.5 to 4.8). The resultant nearshore waves were extracted at points close to the three bays (Fig. 4.3).

Table 4.9 is an example of the tabulated nearshore wave data for offshore waves approaching from 124^0. This represents the effect the bathymetry has on all the wave types tabulated. Similar tables were created for the seven other approach directions. The wave number (k) referred to in these tables is a function of the wave length which is in turn related to the wave period as follows;

$$WaveNumber(k) = \frac{2\pi}{L} \tag{4}$$

$$L = WaveLength = \frac{gT^2}{2\pi}\tanh\left(\frac{2\pi d}{L}\right) \tag{5}$$

where T = Wave period (sec)

d = Water depth (m)

With L on both sides of the wave length formula it is difficult extracting the wave period. However this remains almost constant as the wave propagates shorewards. Using the wave number (k) makes the subsequent wave energy calculations easier.

Substituting k into the wave energy formula (2) allows wave energy for an individual wave (per metre of wave crest) to be calculated as follows;

$$E = \frac{\pi g \rho (Hs)^2}{4k} \tag{6}$$

where E = Energy per metre of wave crest (J)

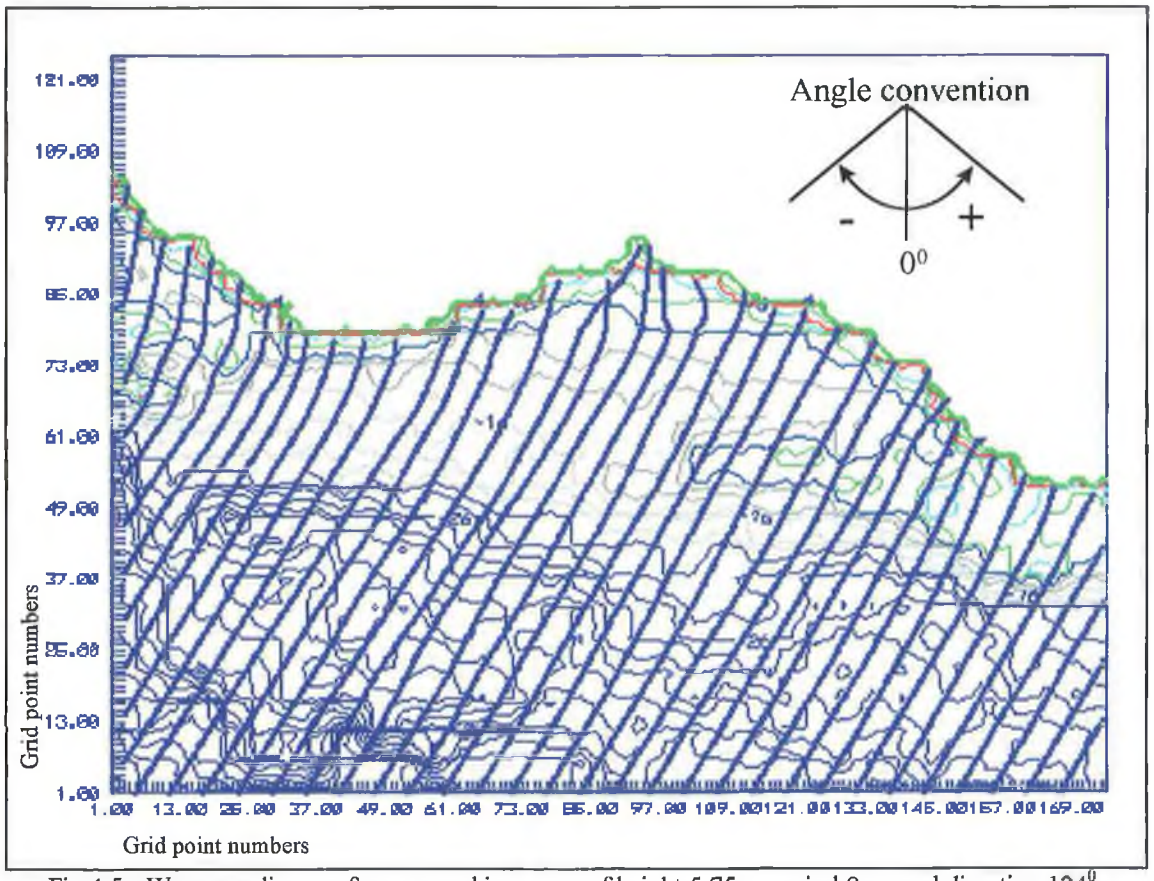

Fig 4.5 - Wave ray diagram for approaching wave of height 5.75m, period 9sec and direction 124^0.

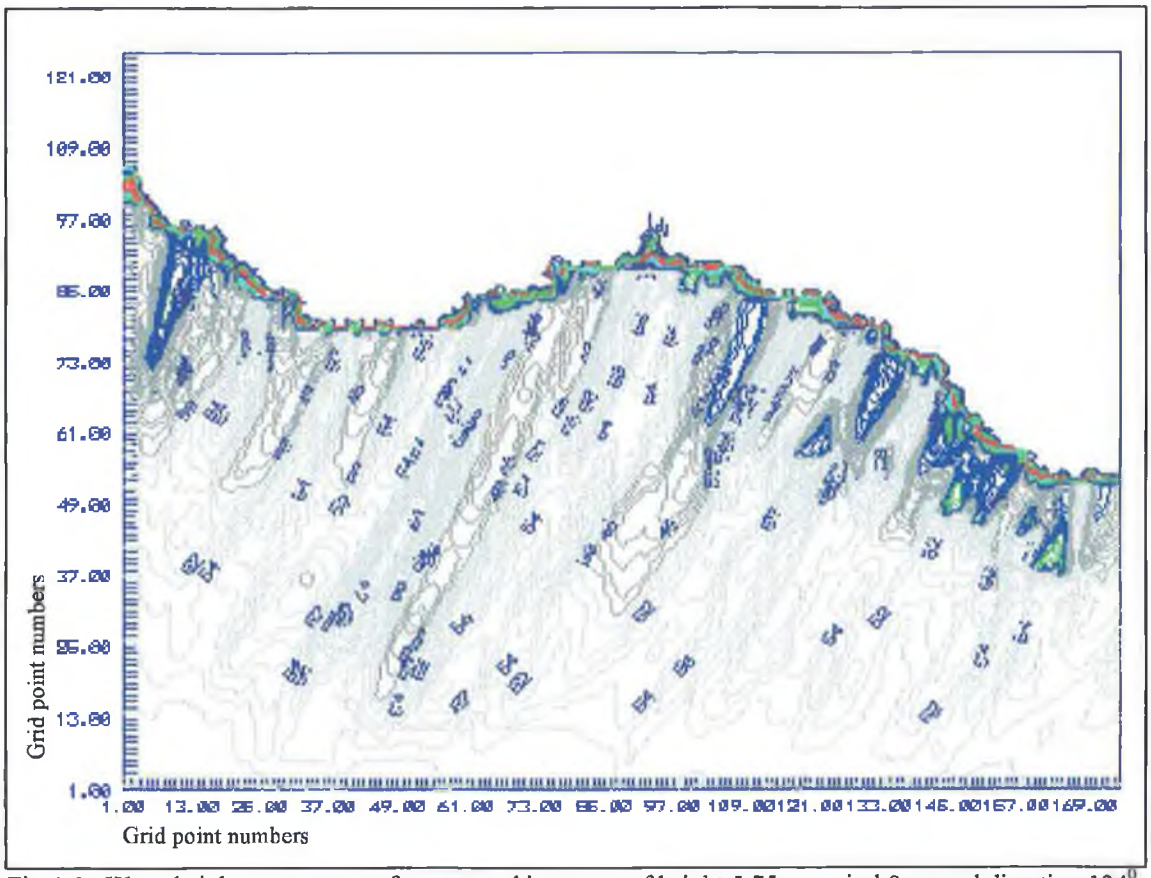

Fig 4.6 - Wave height contour map for approaching wave of height 5.75m, period 9sec and direction 124^0.

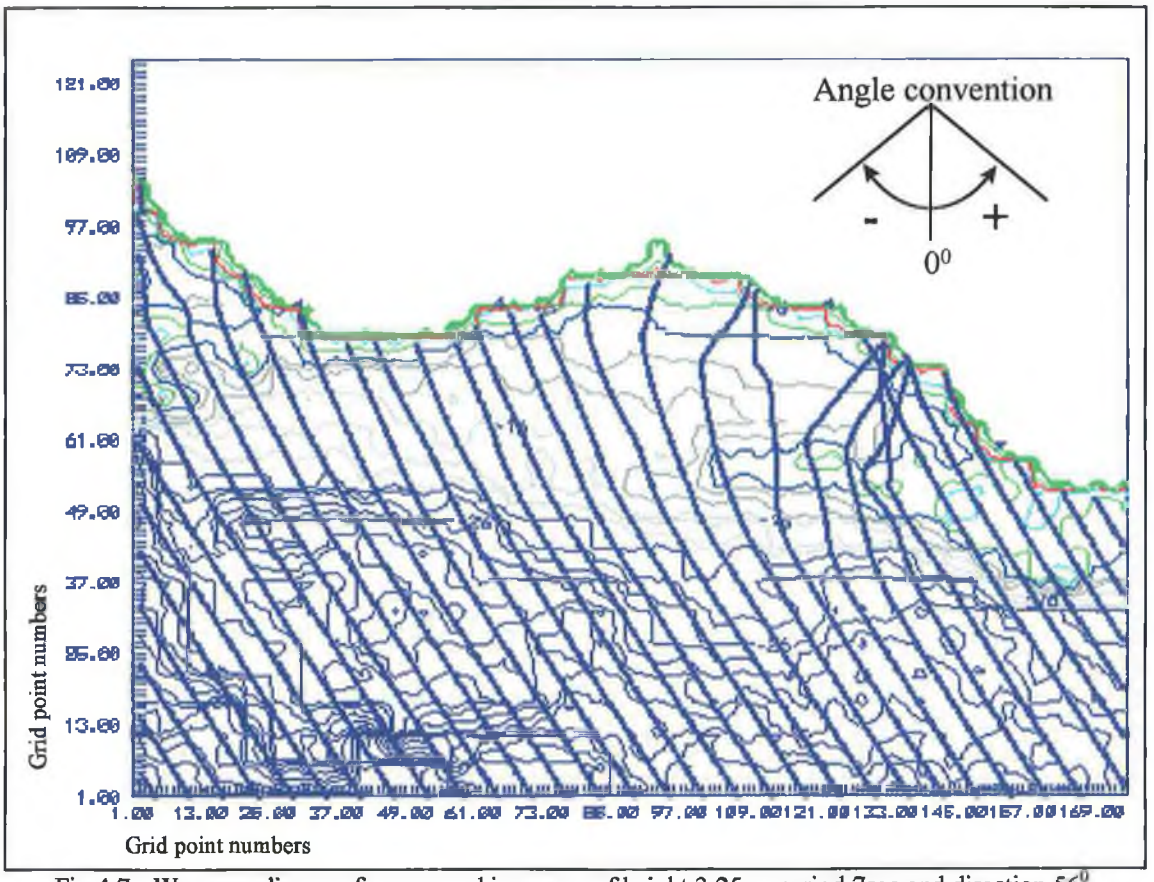

Fig 4.7 - Wave ray diagram for approaching wave of height 3.25m, period 7sec and direction 56^0.

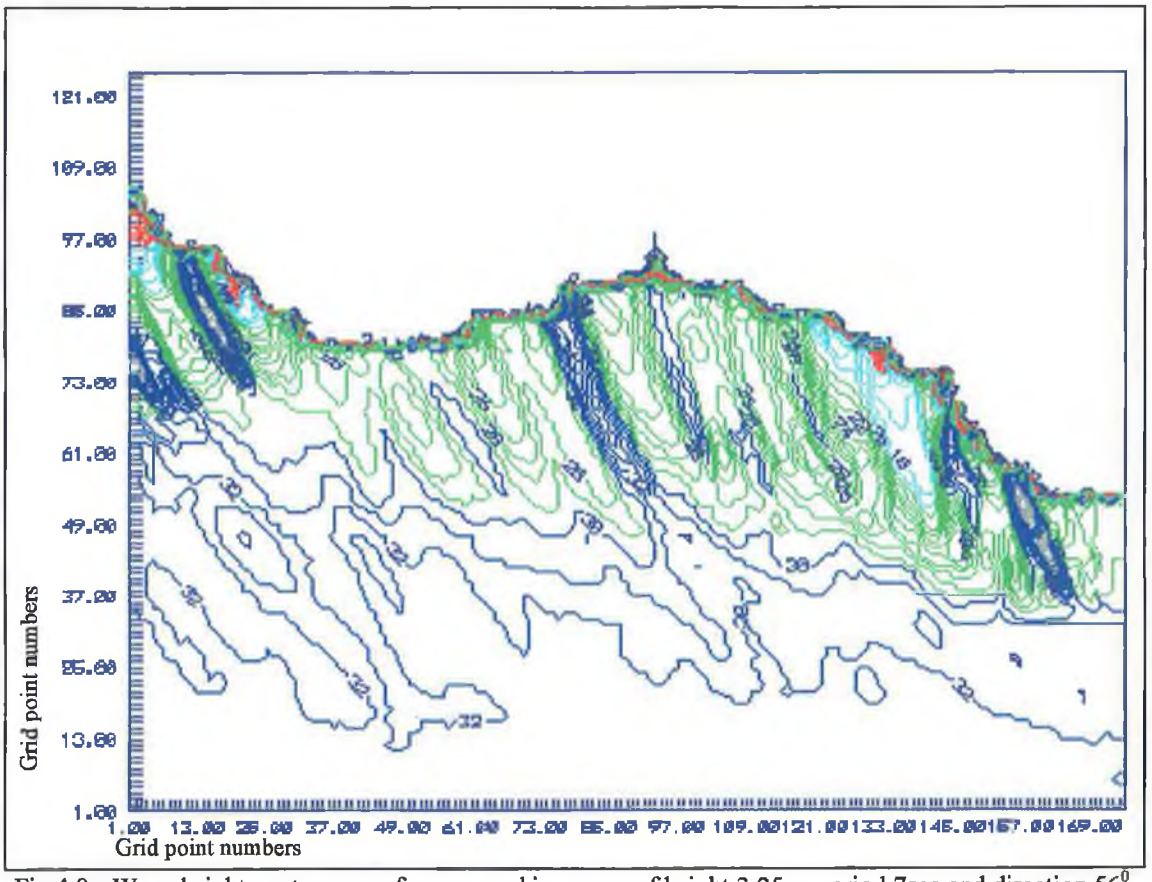

Fig 4.8 - Wave height contour map for approaching wave of height 3.25m, period 7sec and direction 56^0.

REFRACTION/DIFFRACTION OF WAVES FROM 112.5 - 135 DEG.

	INPUT WAVE			GRID			OUTPUT WAVE		
	HS (m)	TZ (sec)	DIR (grid)	X	Y	DEPTH (m)	HS (m)	DIR (grid)	k ($x10^{-3}$)
C.NORTH	5.75	9	-34	97	39	-7.9	5.6	-28	85
ARDAMINE	5.75	9		87	39	-7.7	5.1	-20	86
POLLSHONE	5.75	9		84	40	-7.7	4.4	-21	85
C.NORTH	5.25	8	-34	97	39	-7.9	4.7	-27	98
ARDAMINE	5.25	8		87	39	-7.7	4.4	-21	98
POLLSHONE	5.25	8		84	40	-7.7	4.1	-23	98
C.NORTH	3.25	7	-34	97	39	-7.9	2.8	-31	115
ARDAMINE	3.25	7		87	39	-7.7	2.7	-23	116
POLLSHONE	3.25	7		84	40	-7.7	2.6	-24	115
C.NORTH	2.75	7	-34	97	39	-7.9	2.4	-31	115
ARDAMINE	2.75	7		87	39	-7.7	2.3	-23	116
POLLSHONE	2.75	7		84	40	-7.7	2.2	-24	115
C.NORTH	0.75	7	-34	97	39	-7.9	0.7	-31	115
ARDAMINE	0.75	7		87	39	-7.7	0.6	-23	116
POLLSHONE	0.75	7		84	40	-7.7	0.6	-24	115
C.NORTH	0.25	7	-34	97	39	-7.9	0.2	-31	115
ARDAMINE	0.25	7		87	39	-7.7	0.2	-23	116
POLLSHONE	0.25	7		84	40	-7.7	0.2	-24	115
C.NORTH	2.25	6	-34	97	39	-7.9	1.9	-32	140
ARDAMINE	2.25	6		87	39	-7.7	1.9	-25	141
POLLSHONE	2.25	6		84	40	-7.7	1.8	-26	140
C.NORTH	1.75	6	-34	97	39	-7.9	1.5	-32	140
ARDAMINE	1.75	6		87	39	-7.7	1.5	-25	141
POLLSHONE	1.75	6		84	40	-7.7	1.4	-26	140
C.NORTH	0.25	6	-34	97	39	-7.9	0.2	-32	140
ARDAMINE	0.25	6		87	39	-7.7	0.2	-25	141
POLLSHONE	0.25	6		84	40	-7.7	0.2	-26	140
C.NORTH	1.75	5	-34	97	39	-7.9	1.6	-33	181
ARDAMINE	1.75	5		87	39	-7.7	1.5	-28	182
POLLSHONE	1.75	5		84	40	-7.7	1.5	-29	182
C.NORTH	1.25	5	-34	97	39	-7.9	1.1	-33	181
ARDAMINE	1.25	5		87	39	-7.7	1.1	-28	182
POLLSHONE	1.25	5		84	40	-7.7	1.1	-29	182
C.NORTH	0.75	5	-34	97	39	-7.9	0.7	-33	181
ARDAMINE	0.75	5		87	39	-7.7	0.7	-28	182
POLLSHONE	0.75	5		84	40	-7.7	0.6	-29	182
C.NORTH	1.25	4	-34	97	39	-7.9	1.2	-34	260
ARDAMINE	1.25	4		87	39	-7.7	1.2	-32	261
POLLSHONE	1.25	4		84	40	-7.7	1.2	-32	261
C.NORTH	0.75	4	-34	97	39	-7.9	0.7	-34	260
ARDAMINE	0.75	4		87	39	-7.7	0.7	-32	261
POLLSHONE	0.75	4		84	40	-7.7	0.7	-32	261
C.NORTH	0.25	4	-34	97	39	-7.9	0.2	-34	260
ARDAMINE	0.25	4		87	39	-7.7	0.2	-32	261
POLLSHONE	0.25	4		84	40	-7.7	0.2	-32	261

Table 4.9 - Refraction/diffraction results for waves approaching Grid 1

at an angle of -34^0 (124^0 from true North)

Using this equation (6) and the known number of waves of a particular type and direction it is possible to calculate the total wave power. This is presented in Table 4.10 for waves approaching from 124^0.

NEARSHORE WAVE ENERGY FOR WAVES FROM 112.5 - 135 DEG.

	OUTPUT WAVE			ENERGY		
	HS (m)	DIR (grid)	k ($x10^{-3}$)	(KJ/m crest)	EVENTS	TOTAL(MJ/m crest)
C.NORTH	5.6	-28	85	2911	1	3493
ARDAMINE	5.1	-20	86	2386	1	2864
POLLSHONE	4.4	-21	85	1797	1	2157
C.NORTH	4.7	-27	98	1779	1	2401
ARDAMINE	4.4	-21	98	1559	1	2104
POLLSHONE	4.1	-23	98	1353	1	1827
C.NORTH	2.8	-31	115	538	3	2490
ARDAMINE	2.7	-23	116	496	3	2295
POLLSHONE	2.6	-24	115	464	3	2147
C.NORTH	2.4	-31	115	395	2	1220
ARDAMINE	2.3	-23	116	360	2	1110
POLLSHONE	2.2	-24	115	332	2	1025
C.NORTH	0.7	-31	115	34	1	52
ARDAMINE	0.6	-23	116	24	1	38
POLLSHONE	0.6	-24	115	25	1	38
C.NORTH	0.2	-31	115	3	2	8
ARDAMINE	0.2	-23	116	3	2	8
POLLSHONE	0.2	-24	115	3	2	8
C.NORTH	1.9	-32	140	203	2	732
ARDAMINE	1.9	-25	141	202	2	727
POLLSHONE	1.8	-26	140	183	2	657
C.NORTH	1.5	-32	140	127	4	913
ARDAMINE	1.5	-25	141	126	4	907
POLLSHONE	1.4	-26	140	110	4	795
C.NORTH	0.2	-32	140	2	1	4
ARDAMINE	0.2	-25	141	2	1	4
POLLSHONE	0.2	-26	140	2	1	4
C.NORTH	1.6	-33	181	112	3	723
ARDAMINE	1.5	-28	182	98	3	632
POLLSHONE	1.5	-29	182	98	3	632
C.NORTH	1.1	-33	181	53	16	1823
ARDAMINE	1.1	-28	182	52	16	1813
POLLSHONE	1.1	-29	182	52	16	1813
C.NORTH	0.7	-33	181	21	7	323
ARDAMINE	0.7	-28	182	21	7	321
POLLSHONE	0.6	-29	182	16	7	236
C.NORTH	1.2	-34	260	44	2	236
ARDAMINE	1.2	-32	261	44	2	235
POLLSHONE	1.2	-32	261	44	2	235
C.NORTH	0.7	-34	260	15	7	281
ARDAMINE	0.7	-32	261	15	7	280
POLLSHONE	0.7	-32	261	15	7	280
C.NORTH	0.2	-34	260	1	7	23
ARDAMINE	0.2	-32	261	1	7	23
POLLSHONE	0.2	-32	261	1	7	23
						39963

Table 4.10 - Nearshore wave energy results for waves approaching Grid 1 at an angle of -34^0 (124^0 from true North)

To create vector plots of the nearshore wave energy for the three sites both the energy input and its direction are needed. These are tabulated in Table 4.11 for a specified wave approach direction for each of the three sites. The resultant values are also given.

C.NORTH (112.5 - 135)				ARDAMINE(112.5 - 135)				POLLSHONE(112.5 - 135)			
ANG	ENERGY	X	Y	ANG	ENERGY	X	Y	ANG	ENERGY	X	Y
298	3493	-3085	1640	290	2864	-2691	979	291	2157	-2013	773
297	2401	-5224	2730	291	2104	-4656	1734	293	1827	-3695	1487
301	2490	-7358	4013	293	2295	-6768	2630	294	2147	-5657	2360
301	1220	-8404	4641	293	1110	-7791	3064	294	1025	-6593	2777
301	52	-8448	4667	293	38	-7825	3079	294	38	-6628	2792
301	8	-8455	4672	293	8	-7833	3082	294	8	-6635	2796
302	732	-9076	5060	295	727	-8492	3390	296	657	-7226	3084
302	913	-9851	5544	295	907	-9314	3773	296	795	-7941	3433
302	4	-9854	5546	295	4	-9318	3775	296	4	-7945	3434
303	723	-10461	5940	298	632	-9876	4071	299	632	-8498	3741
303	1823	-11990	6933	298	1813	-11476	4922	299	1813	-10083	4620
303	323	-12261	7109	298	321	-11760	5073	299	236	-10290	4734
304	236	-12456	7241	302	235	-11959	5198	302	235	-10489	4859
304	281	-12689	7398	302	280	-12197	5346	302	280	-10727	5007
304	23	-12708	7411	302	23	-12216	5358	302	23	-10746	5019

RES ANG	300
RES ENERGY	14711

RES ANG	294
RES ENERGY	13340

RES ANG	295
RES ENERGY	11860

Table 4.11 - Nearshore wave energy results and resultant angles for waves approaching Grid 1 at an angle of -34^0 (124^0 from true North)

The wave energy vector diagrams were created using this resultant energy and angle data. A summation of all the results from the three sites is given in Table 4.12. The overall resultant values shown at the bottom of each 'Resultant Angle' column represent the dominant wave direction as indicated by the two years of offshore wave data. The total amount of wave power available is equivalent to a constant wave power input per linear meter of wave crest of 8.4kw, 7.5kw and 7.2kw for the nearshore sites

at Courtown North, Ardamine and Pollshone respectively. This compares with a typical value of 70kw for the offshore area off the west coast of Ireland.

	Courtown North		Ardamine		Pollshone	
Approach wave direction	Res. Angle	Res. Energy (MJ)	Res. Angle	Res. Energy (MJ)	Res. Angle	Res. Energy (MJ)
0-22.5	228	3141	228	3141	228	3141
22.5-45	236	15357	232	13745	232	17349
45-67.5	252	40813	246	34125	247	31703
67.5-90	268	10318	260	11717	262	13460
90-112.5	283	5576	278	5380	281	4879
112.5-135	300	14711	294	13340	295	11860
135-157.5	312	264675	300	254912	309	186298
157.5-180	320	177597	307	139119	315	182046
Resultant	307	493816	295	447974	303	413961

Table 4.12 - Nearshore wave energy results

The vector diagrams of wave energy are shown in Fig 4.9 to Fig. 4.11. The similarity between the wave energy plots and the shape of the bays has been highlighted by Mashima [36] who noted a similar relationship between the wave energy rose for a site and the bay shape.

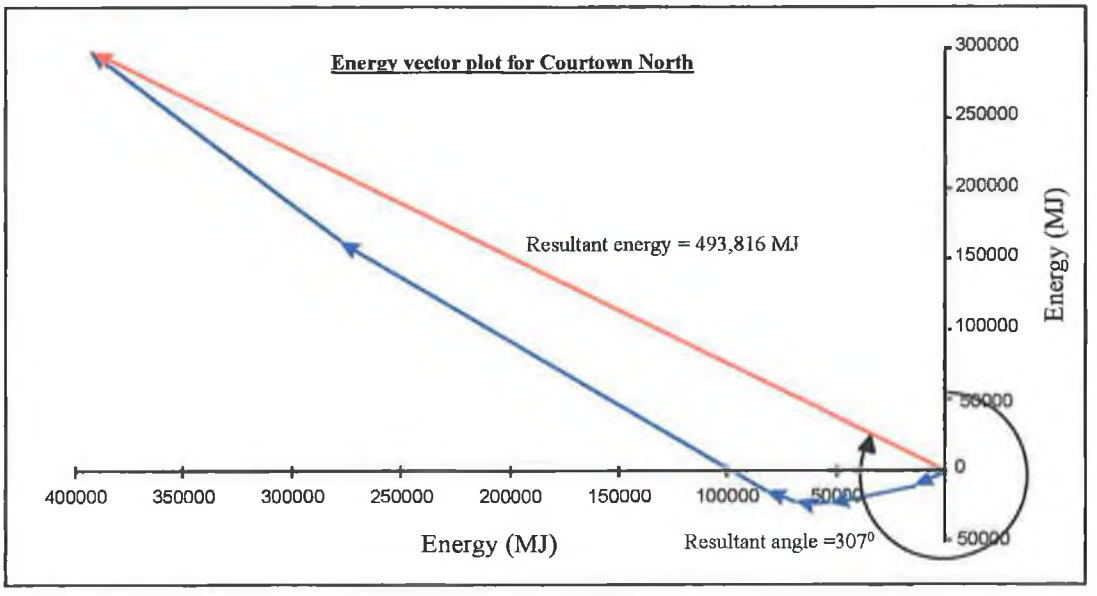

Fig 4.9 - Wave energy vector plot for point off Courtown North

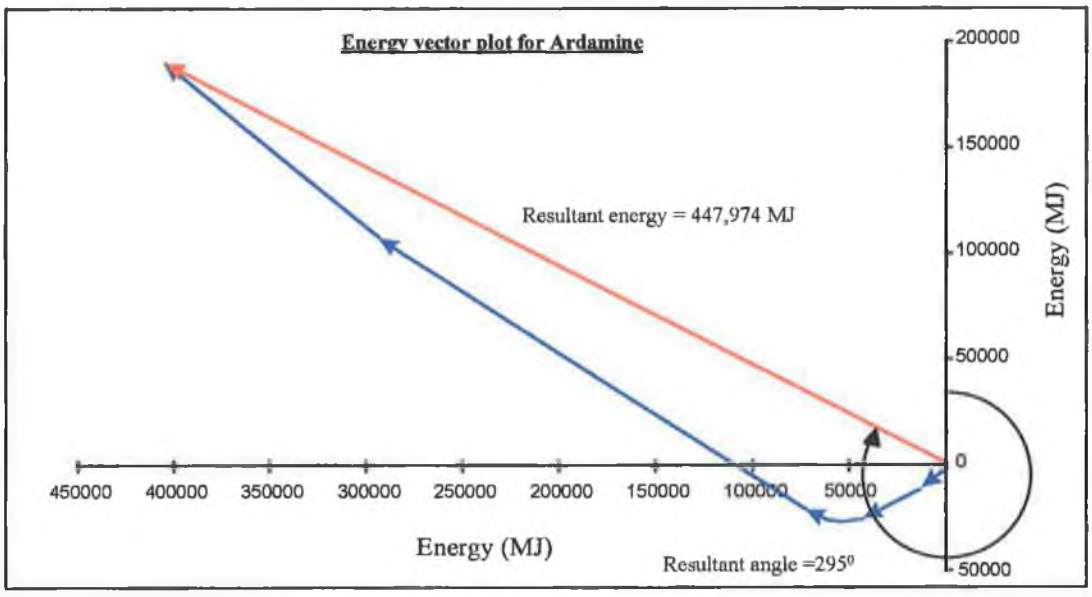

Fig 4.10 - Wave energy vector plot for point off Ardamine

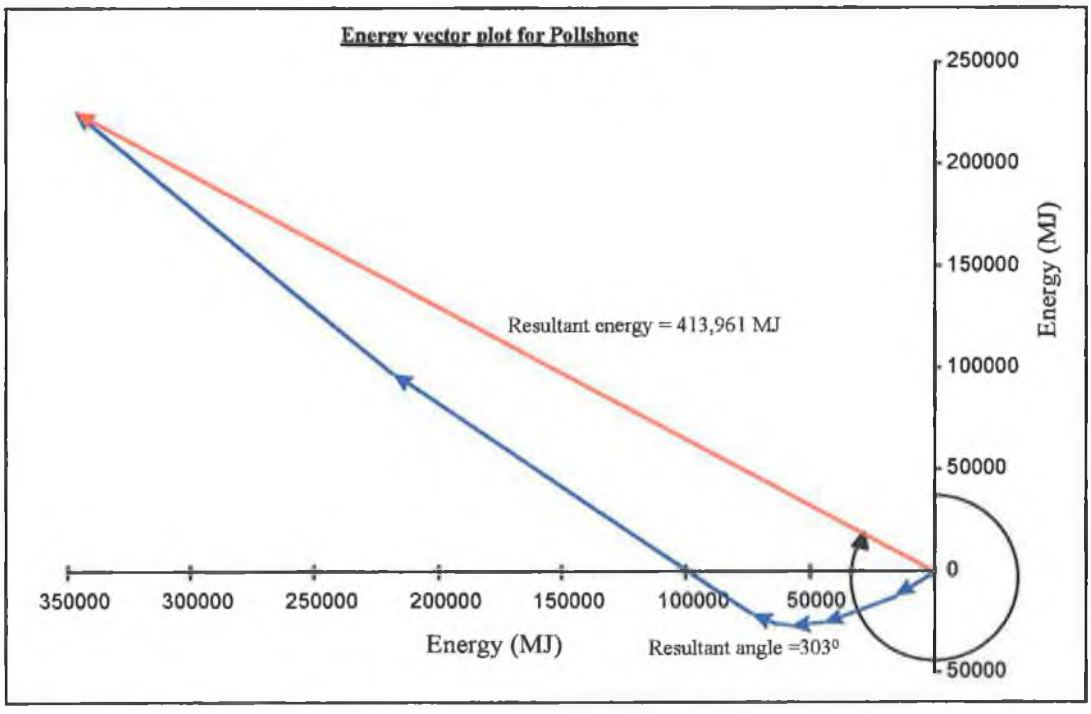

Fig 4.11 - Wave energy vector plot for point off Pollshone

The resultant angle from these plots indicates the dominant wave direction (Fig 4.12). The variation of 13^0 between the lowest and highest value is significant and is primarily due to the difference in the bathymetric profiles between the -20m and -10m contour lines. In the case of Pollshone the relatively deep water close to shore allows the

southerly waves to maintain their path until they are quite near to the shore. The short distance that remains means that the waves do not veer westward as much as they do at Ardamine. The lower energy values at Pollshone may be attributed to the effect of the headlands to the south.

The nearshore bathymetry off Courtown North beach runs almost parallel to the coast. As the contours veer eastward the southerly waves intercept these lines at a less oblique angle. The turning effect on these waves is therefore less, and the dominant wave angle here is more southerly than either Pollshone or Ardamine.

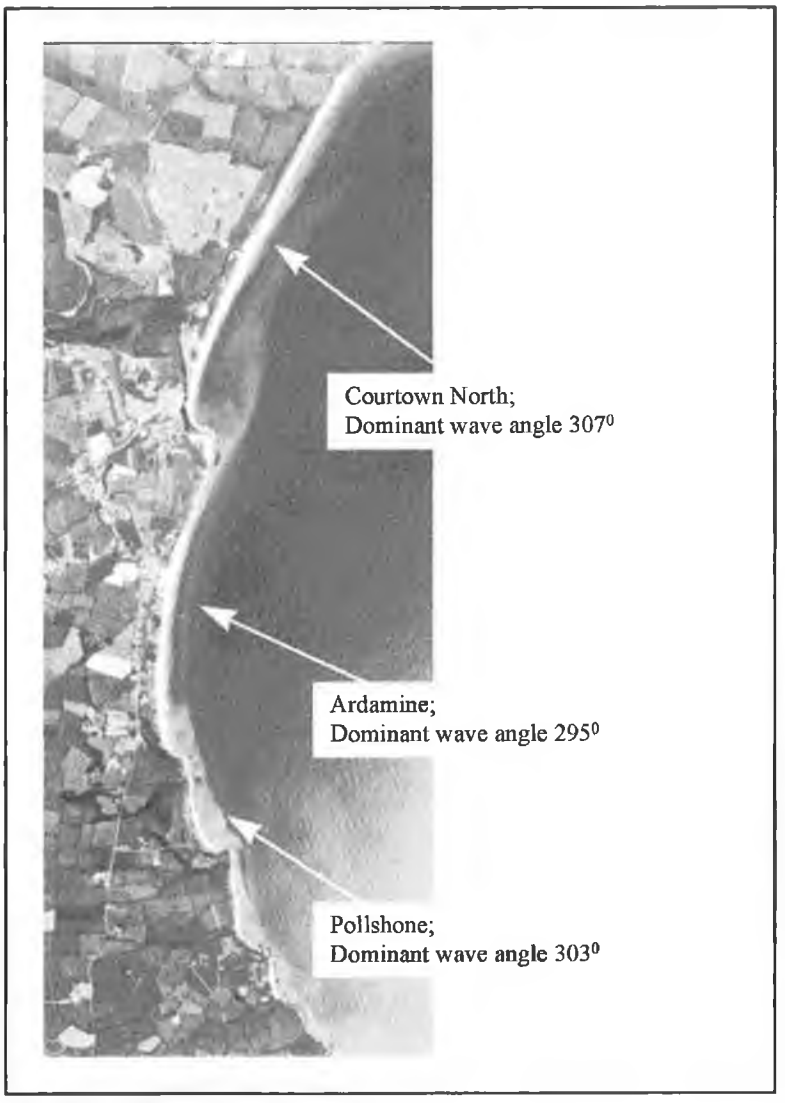

Fig 4.12 - Dominant wave angle as calculated from offshore wave data

4.1.2 Dominant wave direction from coastline planform

This technique is to measure the angle of the coastline at the tangential section of the bay close to the downcoast control point (Fig. 3.4). In order to make accurate angular measurements of the coastline, acetates were laid over the aerial photographs of the area and the coastline was sketched. The photographs used were black and white images taken in 1988 by the Ordnance Survey Office from a flying height of 10,000 feet. In the case of Pollshone it was possible to use photographs taken from 5,000 feet in 1989. A line was drawn along the tangential section of the bay and the angle this makes with the line of true North was measured. The line indicating true North was extracted from the 6 inch Ordnance Survey maps of the area.

4.1.2.1 The tangential section of Courtown North Beach

As the tangential section of this bay is very long and straight the downcoast control point must exist somewhere within the bay rather than at the downcoast headland, Duffcarrick Rocks. This headland is 2.7km from the upcoast control point and is too remote to exert any controlling influence on the bay shape [30]. As discussed in section 3.2.2.1, finding the location of this point is only possible by selecting a number of possible points and drawing the SEP's for each. The angle β between the tangential section of the bay and the control line will change slightly.

Because of the straightness of the tangential section, the selection of various downcoast control points within the bay will not affect the angle the tangential section makes with the line of true North. Fig. 4.13, which was made from a composite of two aerial

photographs, shows this tangential section with a line drawn along it. The angle this line makes with the line of true North was measured at 24^0. This gives a wave approach angle of 294^0. The coastline is remarkably straight along this part of the bay with the only deviations due to the presence of river and stream outlets.

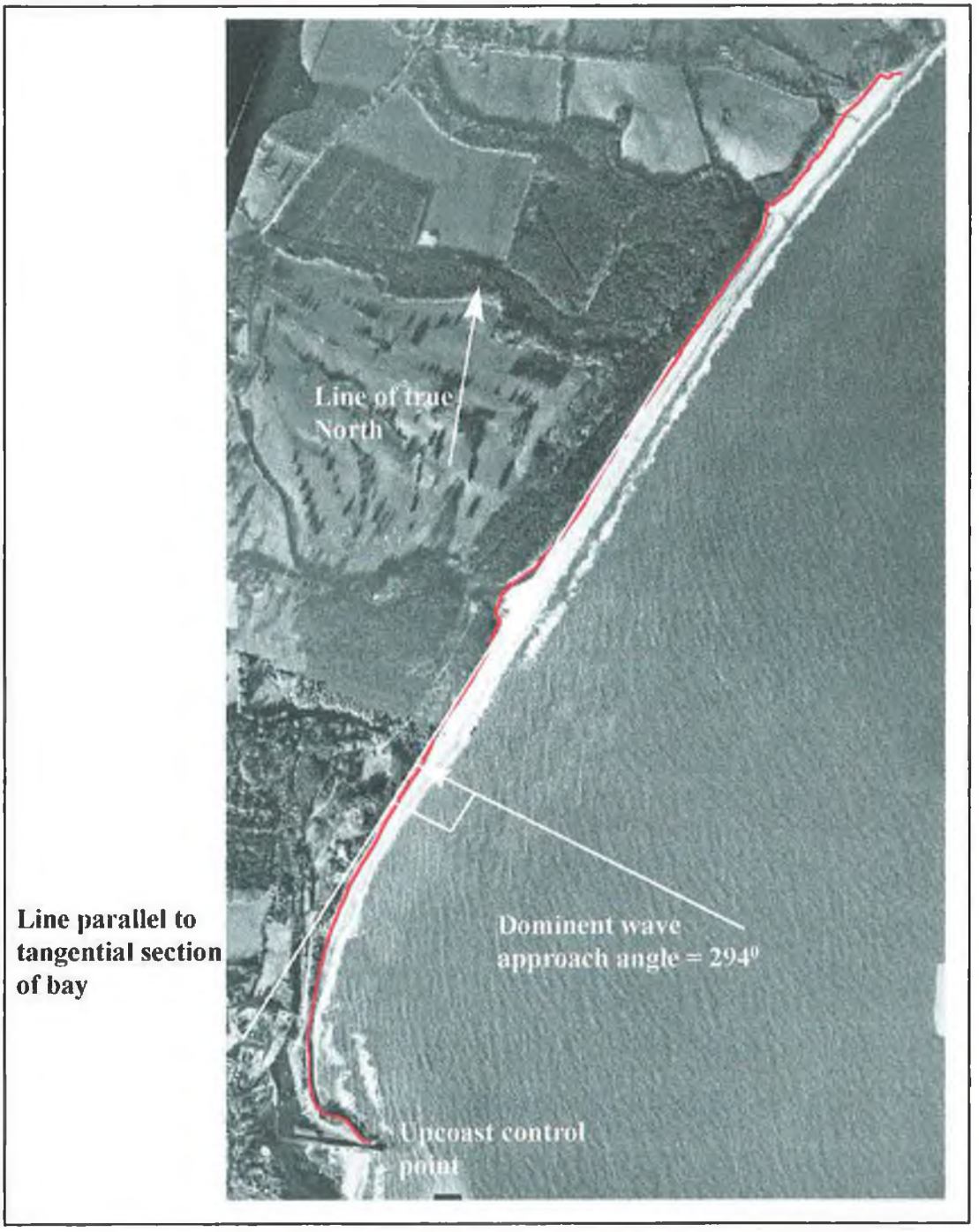

Fig. 4.13 - The tangential section of Courtown North Beach.

Since the line along the tangential section of the bay is drawn manually there exists a possible source of error. However, because of the straightness of this section the error is considered small as lines drawn with a deviation of $\pm 1^0$ are obviously inaccurate.

4.1.2.2 The tangential section of Ardamine Beach

The downcoast control point for Ardamine is clearly evident as a rock outcrop at the northern end of the bay. The tangential section is largely straight except for a deviation along the section adjacent to the large caravan parks at the northern end. Here, because of recreational use, the sand dune system has been damaged and much of it denuded of vegetation. This will affect its ability to repair itself in the aftermath of damaging storms. There is surprisingly little curvature in the coastline at the southern end of the bay.

Fig. 4.14 shows the bay and the tangential section line for Ardamine Beach. The angle this makes with the line of true North was found to be 9^0 giving an approaching wave direction of 279^0.

Two distinct tangential lines can be drawn in the vicinity of the downcoast control point. Apart from the line shown, a line at an angle of 19^0 may be drawn along the short length of coastline adjacent to the downcoast control point. It is difficult to determine which of these two lines is the true indicator of dominant wave direction especially since much of this bay's coastline has been artificially hardened over the years. However, the 9^0 line is preferred as it is representative of the larger portion of the tangential section. In addition, the glacial clay cliff along the smaller 19^0 line is much higher than the clay cliff and sand dunes along the major part of the bay so its

lateral erosion rate would be much slower than the rest of the bay. This would distort the coastline at this location.

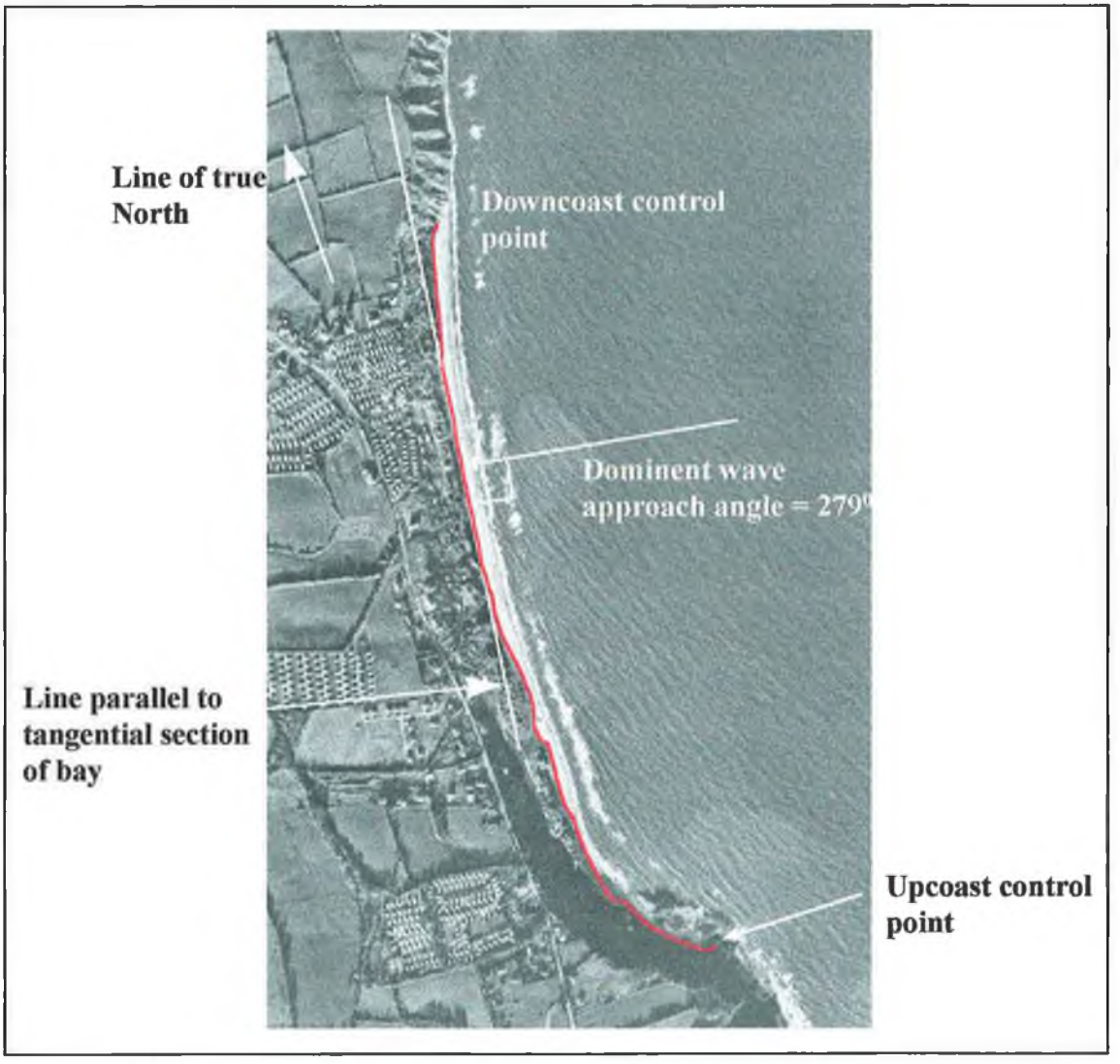

Fig. 4.14 - The angle of the tangential section of Ardamine.

4.1.2.3 The tangential section of Pollshone

This is the smallest of the three bays and both the upcoast and downcoast control points are clearly evident from the aerial photographs. The tangential section of the bay is also obvious. Because of the proximity of houses to the sea, much of the bay has been artificially hardened with rock. This would be expected to cause a distortion in the

planform of the bay though it is likely that the placement of rock in the late 1980's followed the natural curvature of the bay. While the narrow beach along the tangential section suggests that the bay curve is not quite in equilibrium, the low historical erosion rates for Pollshone indicate that the bay is reasonably stable. It is assumed, therefore that the present planform is primarily the result of sculpting by the sea.

The angle between the tangential section line and the line of true North, shown in Fig. 4.15, was found to be -13^0. This gives an dominant wave direction of 257^0.

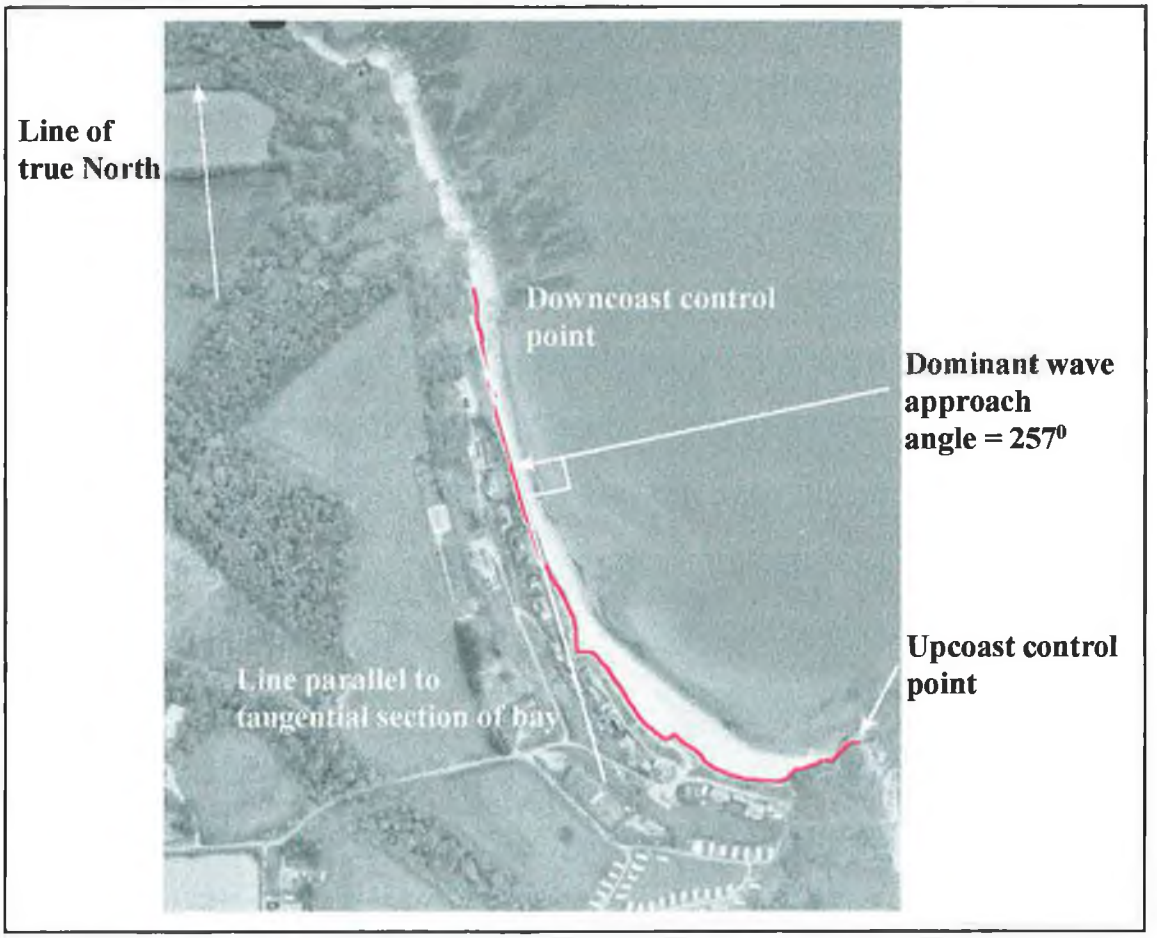

Fig. 4.15 - The angle of the tangential section of Pollshone.

4.1.3 Comparison of the two techniques for determining the dominant wave direction

The dominant wave directions as calculated and measured for each of the three bays are listed in Table 4.13.

Bay	Dominant wave direction	
	Using refracted offshore wave	Using bay planform
Courtown North	307^0	294^0
Ardamine	295^0	279^0
Pollshone	303^0	257^0

Table 4.13 - Dominant wave directions for the three bays

There is a considerable difference between the results of the two techniques. A number of possible reasons for these are given below.

1. There may be some under estimation of the effect of nearshore bathymetry on wave refraction. More accurate modelling of this effect would require much more detailed bathymetric measurements. Within this nearshore zone sand bars develop, move and disappear over time so their effect on wave transformation would be very difficult if not impossible to ascertain. In addition, the non-linear wave transformation processes involved in this wave breaking zone are currently poorly understood.

The variation in the difference between the results for the three bays would seem to confirm this assumption as the margin of difference is much less for Courtown North. From the wave model results, refraction was least for this bay. It seems that the model was unable to replicate the true amount of refraction particularly for the two more southern bays where refraction tended to be higher.

2. There is the possibility that the bay planform is the result of the effect of a select type of wave rather than the accumulative result of the effect of all waves. Perhaps bays are shaped more by waves that occur over the longest duration rather that by the sudden high energy storm events or possibly the waves in the immediate aftermath of storms are of more importance. A weighting system might be more appropriate when analysing the effect of waves rather than the straightforward energy calculation method used.

3. It is known that the bays are not in a state of static equilibrium as sediment is passing alongshore. This drift of sediment suspends the evolution of the coastline and the existing coastline position is dependant on the influx of sediment for its stability.

The result of this comparison highlights the problems commonly associated with modelling natural processes. The initial conditions are not fully known and the processes involved are extremely complex. Errors or lack of detail in the initial conditions (i.e. offshore & nearshore bathymetry and input waves) are compounded by the inaccuracies in the model itself.

As the prediction of the SEP using the Silvester & Hsu [30] method depends on just two variables, the dominant wave direction and the location of the control point, it is critical to accurately determine both of these. The dominant wave direction as indicated by the bay planform is considered the most accurate because of the reasons given above but there are sources of error primarily the fact that the bays are in a state of dynamic and not static equilibrium due to the passing sediment.

4.2 Plotting the Static Equilibrium Position of the Coastline

4.2.1 Determining the Control Points and drawing the Static Equilibrium Position of the Coastline

Along with the approaching wave direction, the upcoast and downcoast control points determine the overall shape of the bay. The upcoast point is usually a hard point, either natural or manmade, where wave diffraction occurs. The downcoast point may also be a hard point although in longer bays this control point may exist somewhere within the soft coast of the bay. The Control Line joins these two points (Fig. 3.4).

4.2.1.1 The Control Points for Courtown North

There are three possible upcoast control points for this bay, the southernmost headland (Breanoge Head), the remains of the 19th century breakwater extending from this headland and the harbour piers constructed in the mid 19th century. The method used to

determine which of the three controls the shape of the bay has been detailed in Section 3.3.1.

Using the bay planform dominant wave direction, Fig. 4.16 shows that the harbour pier has the major effect on the bay with the approaching waves being diffracted about this point.

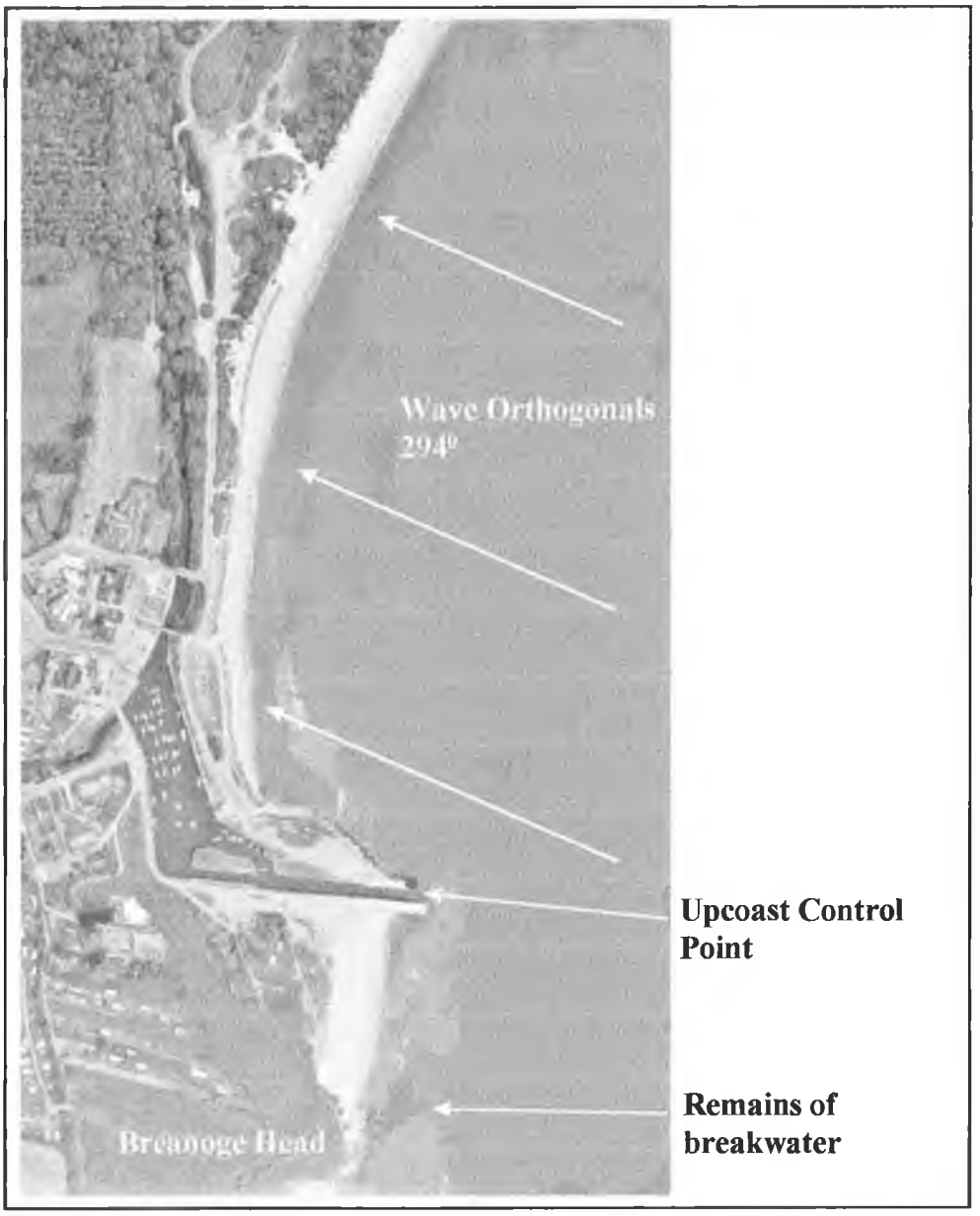

Fig. 4.16 - Upcoast control point for Courtown North

The beach south of the harbour should also exhibit the crenellate curve shape however the partially submerged remains of the breakwater has altered the nearshore wave climate here and so distorted the bay shape.

The downcoast control point for Courtown North exists within the bay as the hard point to the north, Duffcarrick Rocks, is too far distant to exert any controlling influence. According to Silvester and Hsu [30] the only way to determine where this point is located is by plotting the SEP for various points and by comparing these with the existing coastline configuration, an accurate location can be achieved.

The points selected are shown in Fig. 4.17. The southernmost point was located at a point where the largely straight tangential section begins to curve. From here, two more points, equally-spaced along the tangential section were chosen. The final precise location of the downcoast control point was based on the fine tuning of the SEP's for these initial points.

4.2.1.3 The Static Equilibrium Position for Courtown North

A Microsoft EXCEL© spreadsheet was created which solves the polynomial expression developed by Hsu and Evans [38]. This uses a table of values for each of the three coefficient curves employed in the formula (Fig 3.6). These were obtained from data given by Hsu and Evans and from digitising the curves. The SEP was drawn using the XY Radial plot function within EXCEL©.

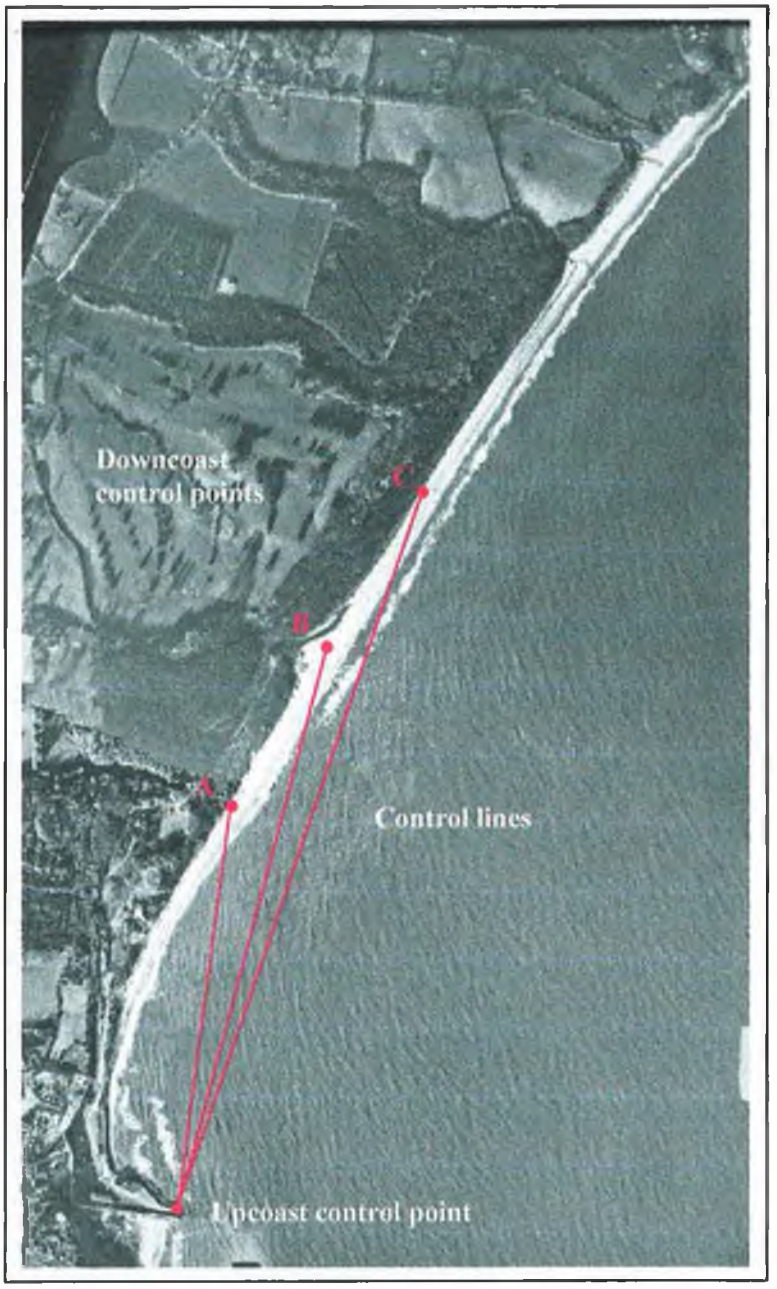

Fig. 4.17 - Initial Downcoast Control Points and Control Lines for Courtown North

The SEP's were drawn for each of the three control lines initially selected and for both dominant wave approach directions as calculated using the offshore wave refraction and bay planform methods. For higher accuracy, the angle β (Fig. 3.6) between the control line and the tangential section line was measured using the aerial photograph acetate overlays. The values of β for each case are given in Table 4.14.

	Measured values of β	
	Dominant wave direction using refracted offshore waves	**Dominant wave direction using bay planform**
Control line for downcoast control point A	**38^0**	**25^0**
Control line for downcoast control point B	**30^0**	**17^0**
Control line for downcoast control point C	**25.5^0**	**12.5^0**

Table 4.14 - Values of β for different control lines and wave directions for Courtown North

The SEP's for each control line and dominant wave direction is shown in Fig. 4.18. It is obvious that the SEP's for the dominant wave direction calculated using the wave refraction method do not represent the current evolutionary state of the coastline. This is most likely due to inaccuracies in the technique and the fact that the longshore drift of sediment is maintaining the coastline in a state of dis-equilibrium. This is discussed further in Section 4.2.2.

The SEP's for the three points drawn using the bay planform method are much closer to the current coastline position and all follow roughly the same bay curve. As observed by Silvester and Hsu [30], this effect is due to the angle β undergoing a compensatory change as the control line varies. After further investigation a control line connecting a point close to point **B** to the upcoast control point was found to give an SEP which most accurately follow the general curvature of the bay.

As much of the coastline adjacent to the harbour has been artificially hardened with a seawall and rock revetments, this area can no longer erode over the short term and will be in a continued state of dis-equilibrium. Only the soft coast, sand dunes, etc., will be able to adopt the SEP. This is shown in Fig. 4.18 and the curved connecting line

between the end of the revetment and the SEP has been drawn manually sympathetic with the general nature of the crenellate curve. The dashed lines represent the SEP that the coastline would adopt if all the bay coastline was soft.

Fig. 4.19 shows the historical evolution of the southern portion of the bay. There was very little erosion in the area northwards. The base map is the Ordnance Survey map of 1921 and the coastlines for 1950, 1988 and 1990 were obtained by tracing the vegetation line from aerial photographs of the area. There are inaccuracies in the survey map, the aerial photographs (they have not been rectified) and in the manual tracing of the vegetation line, however, the trend and general degree of erosion is considered sufficiently accurate for this application.

Using the vegetation line as an indicator of the coastline position is preferred to using the high water mark as the exact condition of the tide at the time of the aerial photographs is not known. In any event the meteorological situation at the time can also play a significant role as water levels are higher when the barometric pressure is low (10mm rise per 1hPa fall in pressure) and onshore winds will also raise water levels. The vegetation line is, nevertheless, affected by forces other than marine erosion. Recreational users of the beach and grazing by animals can severely damage the dune vegetation leading to bare sand areas which can then suffer from wind erosion. Because of the popularity of Courtown and Ardamine as seaside resorts it is likely that much of the recession of the vegetation line is due to recreational pressure, particularly in areas of heavy usage such as access routes. This has been taken into account when estimating the true amount of marine erosion.

Fig. 4.18 - The SEP's for Courtown North Beach.

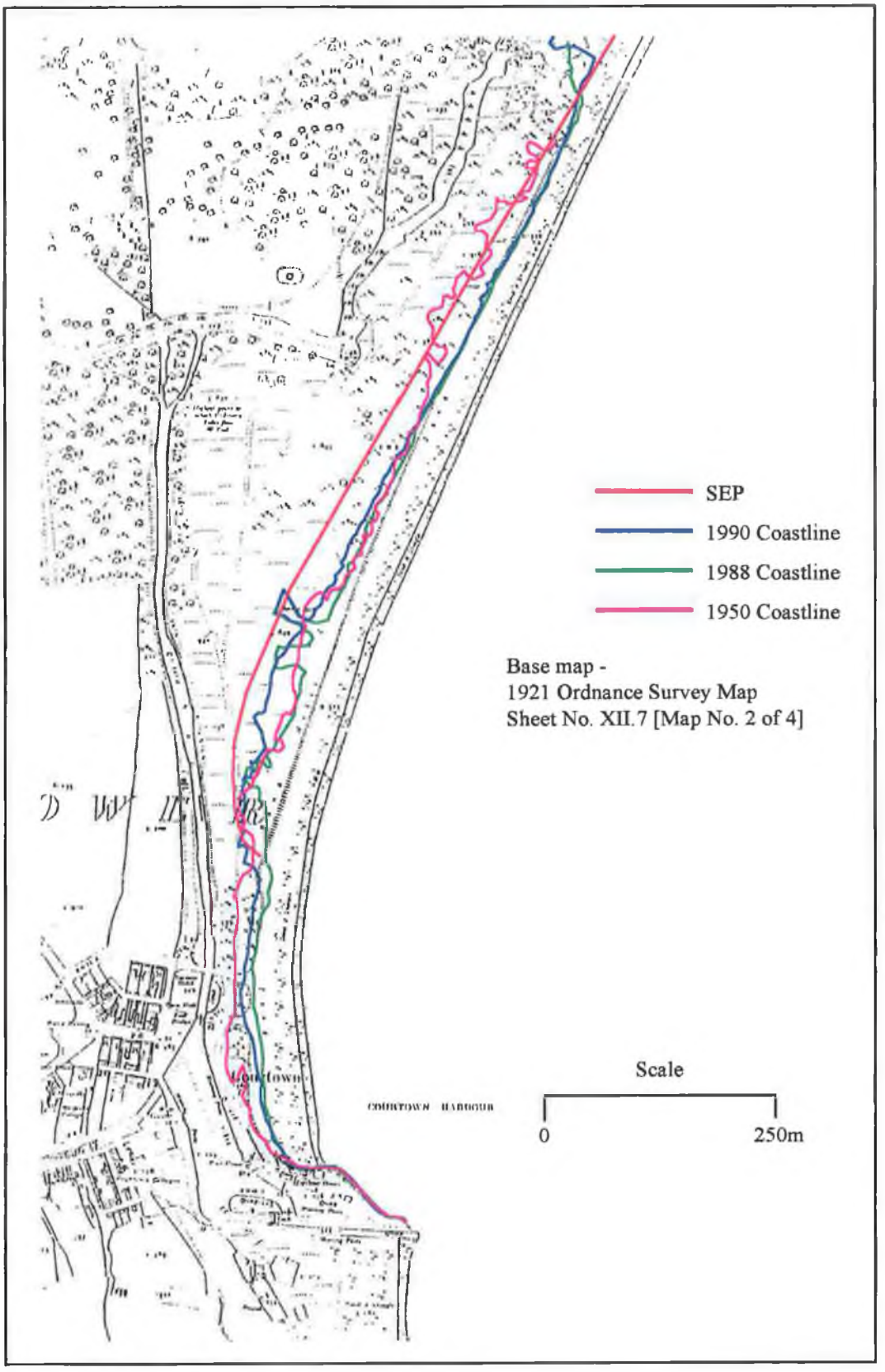

Fig. 4.19 - Historical position of coastline and vegetation lines for Courtown North Beach.

Between the years 1921 and 1950 there was considerable recession of the vegetation line along the southern portion of the bay. This was concentrated in areas where pedestrian access routes funnelled people to the beach. There was, also, considerable marine erosion particularly adjacent to the harbour area. This prompted the placement of concrete blocks on the beach in an attempt to protect this area. This was successful up to the 1980's when they became undermined and were subsequently replaced with a rock revetment. The coastline of 1950 also shows vegetation line recession at the northern end of this section of coast. It is considered that this is entirely due to recreational pressure as, at this time, this area consisted of sand dunes, easily accessible from an approach track to the rear. In later years a thorny shrub, sea buckthorn, spread to this area and the thorny bushes made the site unusable.

The coastline of the late '80 shows much of this northern section has been revegetated with buckthorn and trees. The coastal defences in the southern section near the harbour had recovered much of the land loss evident in the 1950 photograph. There was, however, continued recession of the vegetation line around the mid portion of the bay which by now has become the most vulnerable section as it is the area of soft coastline furthest from the equilibrium position predicted by the SEP.

Between 1988 and 1990 there was extensive recession of the vegetation line along this mid section. This period was characterised by one of the stormiest periods this century, the winter of '89/'90. Most of the recession was due to marine erosion with many frontal sand dunes slumping onto the beach. It is interesting to note that the northern section remained largely unaffected by these storms and that the 1990 coastline has begun to adopt the curvature of the predicted SEP. Since 1990 the protection works

near the harbour have been extended making the unprotected area further north more vulnerable to erosion.

4.2.1.4 The Control Points for Ardamine

The upcoast and downcoast control points for Ardamine are shown in Fig. 4.20 and are connected by the control line. The upcoast point is a rock outcrop and, from aerial photographs, wave diffraction can be seen to be taking place about this point.

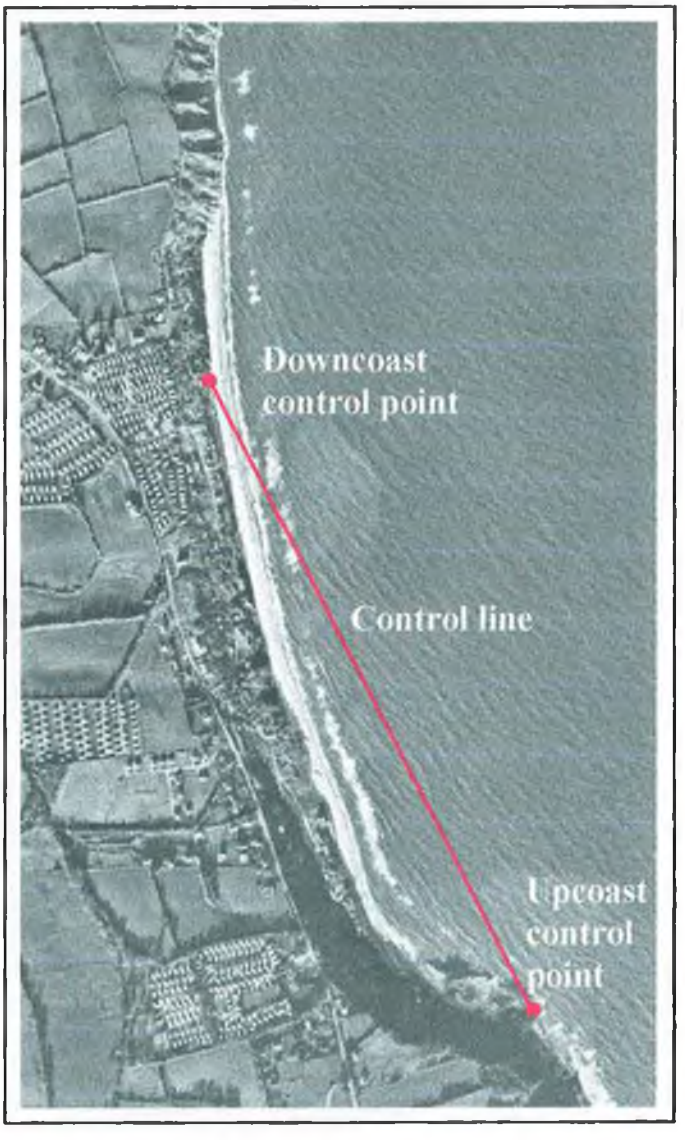

Fig. 4.20 - Control Points and Control Line for Ardamine.

The downcoast point is taken as the point where the coastline begins to deviate from the relatively straight tangential section at the point where the coastal cliff begins to rise. Selecting a downcoast control point further north, at the end of the bay, would not have greatly altered the position of the SEP, however, it is felt that the point chosen is more accurate as the higher glacial clay cliff would distort the lateral movement of the coastline.

4.2.1.5 The Static Equilibrium Coastline for Ardamine

Again, the SEP's were drawn for both calculated and measured dominant wave directions using the EXCEL© XY radial plot function. The values of β are given in Table 4.15 and an acetate overlay on the aerial photograph was used to measure β.

	Measured values of β	
	Dominant wave direction using refracted offshore waves	**Dominant wave direction using bay planform**
Control line for downcoast control point Ardamine	**31^0**	**15^0**

Table 4.15 - Values of β for Ardamine

The SEP's are shown in Fig. 4.21 and the difference between the curves drawn using the different values of β is immediately obvious. The comments made on the similar disparity between Courtown North SEP's is also valid here and is discussed further in Section 4.2.2. The SEP drawn using the dominant wave angle as exhibited by the bay planform is considered more representative of the current evolutionary condition of the bay.

As much of the bay has been artificially hardened by coastal protection works (mainly rock revetments), the bay is restricted in adopting the SEP. By 1990 the areas most vulnerable to marine erosion, as indicated by the distance of the coastline from the SEP, had been hardened, Indeed, since then, the rock revetments have been greatly extended and it is likely that the entire bay will be protected by rock in the near future.

Fig. 4.21 shows the 1988 situation. The connecting line between the hardened coastline and the SEP has been drawn manually. The position of the SEP shows that the bay is quite close to equilibrium as determined using the bay planform method. As the hardened coastline is extended northward the areas vulnerable to erosion will be pushed further north. However, the SEP indicates that their vulnerability will become less as the line of the revetment begins to approach and eventually follow the line of the SEP.

The historical evolution of the bay is shown in Fig. 4.22. Again, the coastlines extracted from the aerial photographs are, in fact, the vegetation line. However, because much of the area behind the beach is in private ownership, the vegetation line is regarded as a true indicator of marine erosion since degradation of vegetation from recreational users is restricted to the small number of beach access routes.

The period between 1921 and 1950 appears to account for most of the recession of the coastline. There may be some inaccuracies in the original ordnance survey map and the lines extracted from the aerial photographs but the overall level of erosion is considered correct. From the indented nature of the 1950 vegetation line it would appear that the beach was more popular with visitors during this period and that more access routes and recreational areas in the sand dunes were available to the public.

The 1988 and 1990 vegetation line shows the impact of the coastal protection works in the southern portion of the bay. The bulge, one third of the way up from the southern headland, marks a projecting rock revetment and the terminus of the coastal protection works at that time. Subsequently, the rock revetment was extended.

Fig. 4.21 - The SEP's for Ardamine

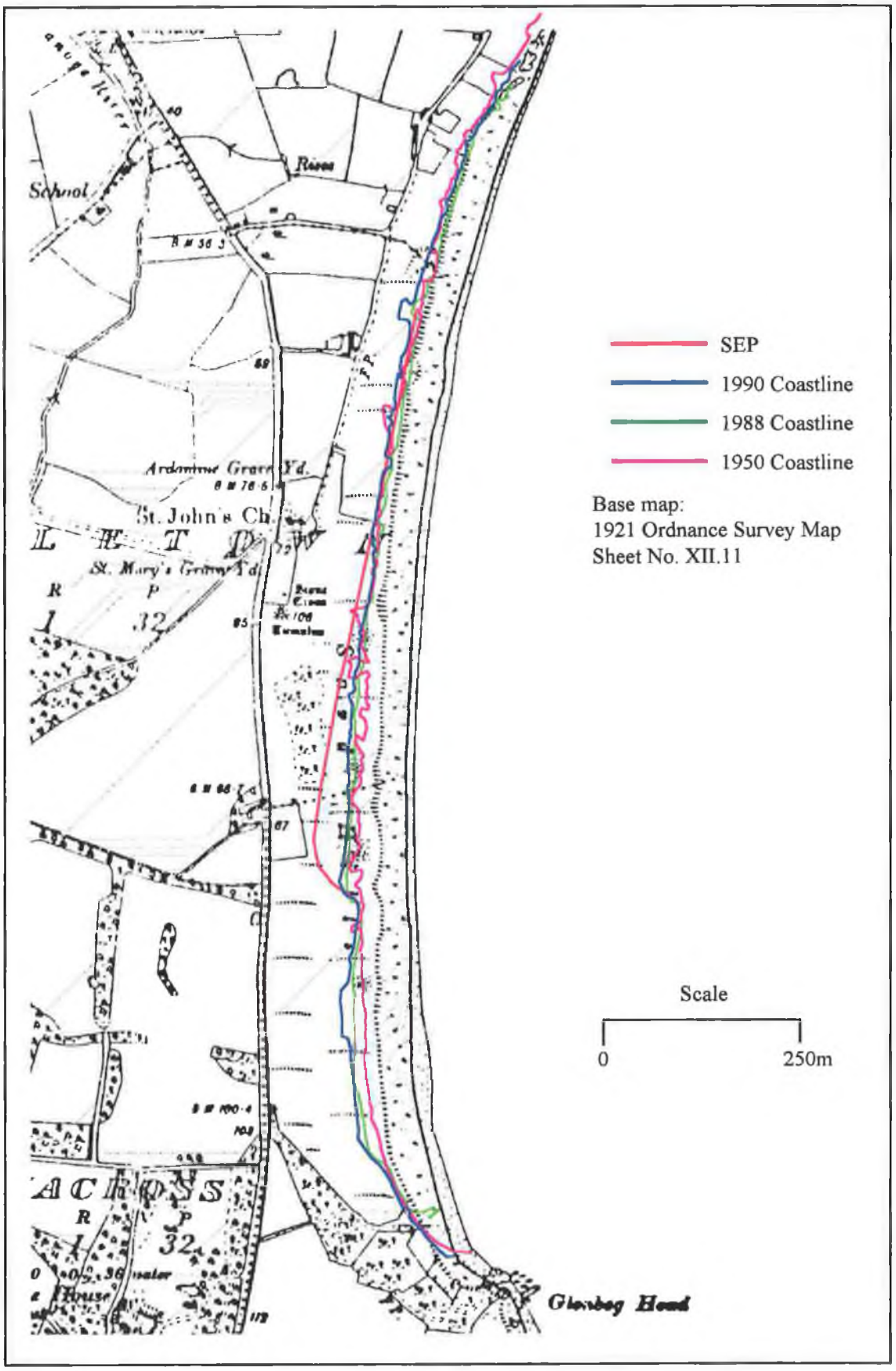

Fig. 4.22 - Historical position of the coastline and vegetation lines at Ardamine

4.2.1.6 The Control Points for Pollshone

Fig. 4.23 shows the control points and control line for Pollshone. This bay exhibits the classic characteristics of a relatively stable crenellate curve bay. This stability is highlighted by the close proximity of buildings to the beach. Unfortunately this proximity means that no fluctuation of the coastline can be tolerated and has resulted in the construction of coastal defences.

The upcoast control point is situated on a out crop of rock at the southernmost headland and wave diffraction about this point can be seen in aerial photographs. The downcoast point is located at the point where the soft coast meets the emerging rock at the northern end.

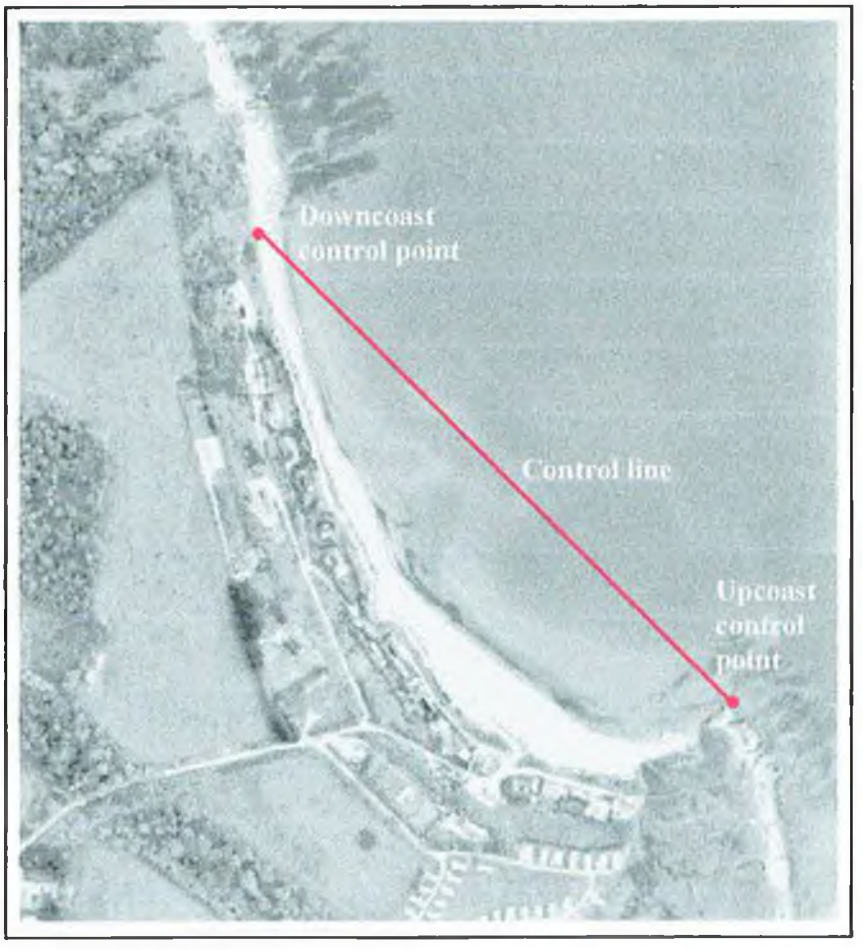

Fig. 4.23 - The Control Points and Control Line for Pollshone

4.2.1.7 The Static Equilibrium Coastline for Pollshone

The SEP's were drawn for both calculated and measured dominant wave directions using the EXCEL© XY radial plot function and the values of β are given in Table 4.16. Again, an acetate overlay on the aerial photograph was used to measure β.

	Measured values of β	
	Dominant wave direction using refracted offshore waves	**Dominant wave direction using bay planform**
Control line for downcoast control point Ardamine	75^0	29^0

Table 4.16 - Values of β for Pollshone

The SEP's are shown in Fig. 4.24 and, as with the other two bays, there is a large difference between the SEP's for the two values of β. The difference here is even more pronounced because of the 46^0 variation in the two wave approach angles. This difference is discussed further in Section 4.2.2. Almost all of the bay had been protected with rock revetments by the time this photograph was taken in 1989 and it is only a small portion close to the downcoast control point that remains soft. Fortunately, the line chosen for the protection works follows closely the bay planform SEP for much of it's path but begins to deviate from the mid point of the bay. This area will be the most vulnerable to undermining of the rock and to erosion in the future.

The coastal cliff in Pollshone is high and uniform with a steep slope down to the beach. This may have contributed to the rather uniform erosion rate along the bay with the

coastline following the planform SEP. This would explain why the rock revetment, which was placed at the base of the bluff, lies along the SEP.

Fig. 4.25 shows the historical evolution of the bay. The extracted vegetation line from the aerial photograph taken in 1973 should closely follow the position of the coastline as recreational damage of the vegetation is not considered a factor here due to the steepness of the coastal cliff. The line extracted from the 1989 photograph mainly follows the rock revetment coastal defence.

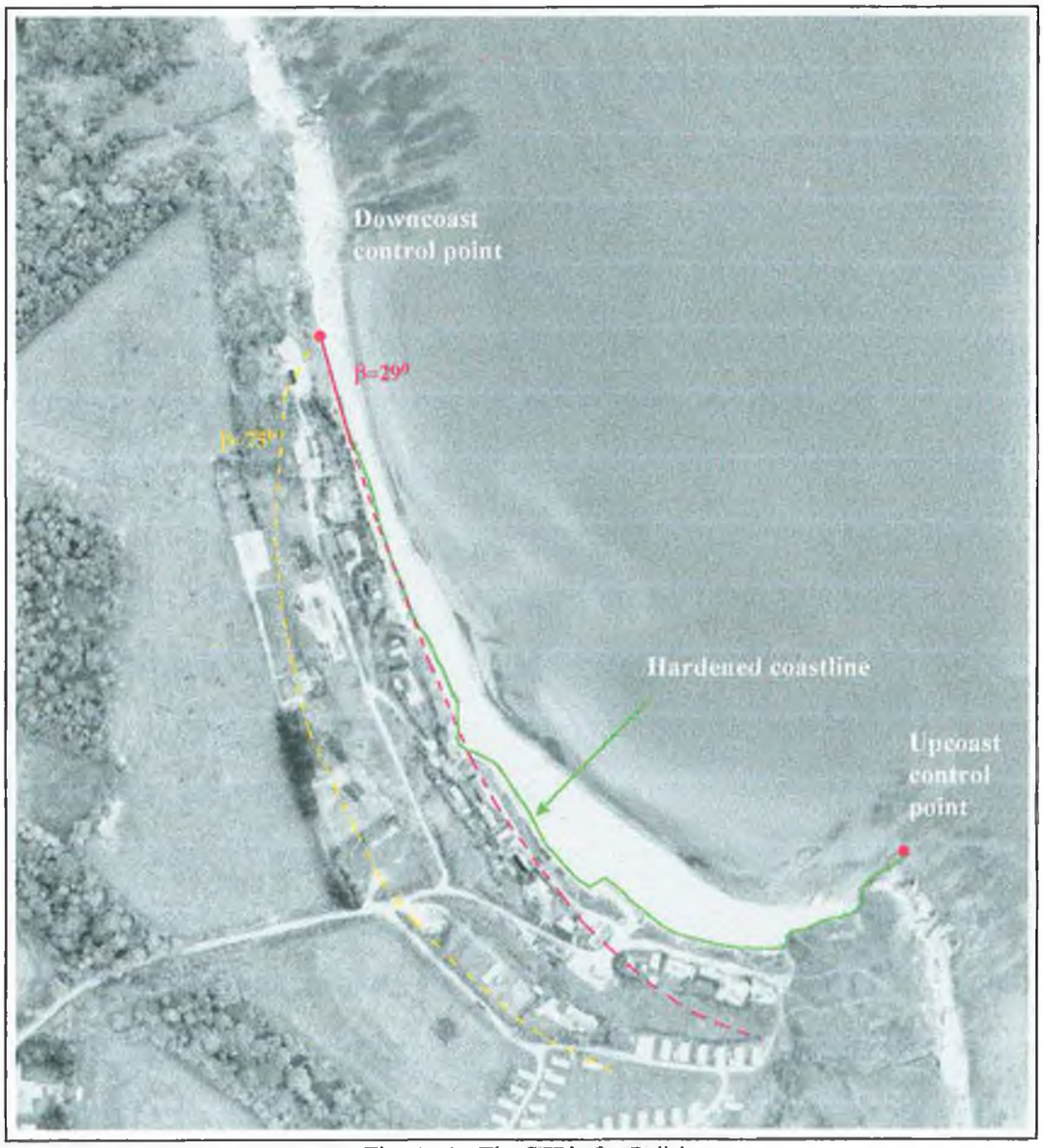

Fig. 4.24 - The SEP's for Pollshone

The vegetation line obtained from the 1973 photograph indicates that there was considerable accretion in the bay since the ordnance survey of 1921 particularly at the northern end. Although it is likely that there was some accretion the amount indicated in Fig. 4.25 may be exaggerated because of inaccuracies in the original ordnance survey map and in the manual tracing of the line from the aerial photograph. The 1973 line does, however, show erosion occurring around the middle of the bay with a number of houses and a road being threatened. It was this that prompted the construction of the first rock revetment.

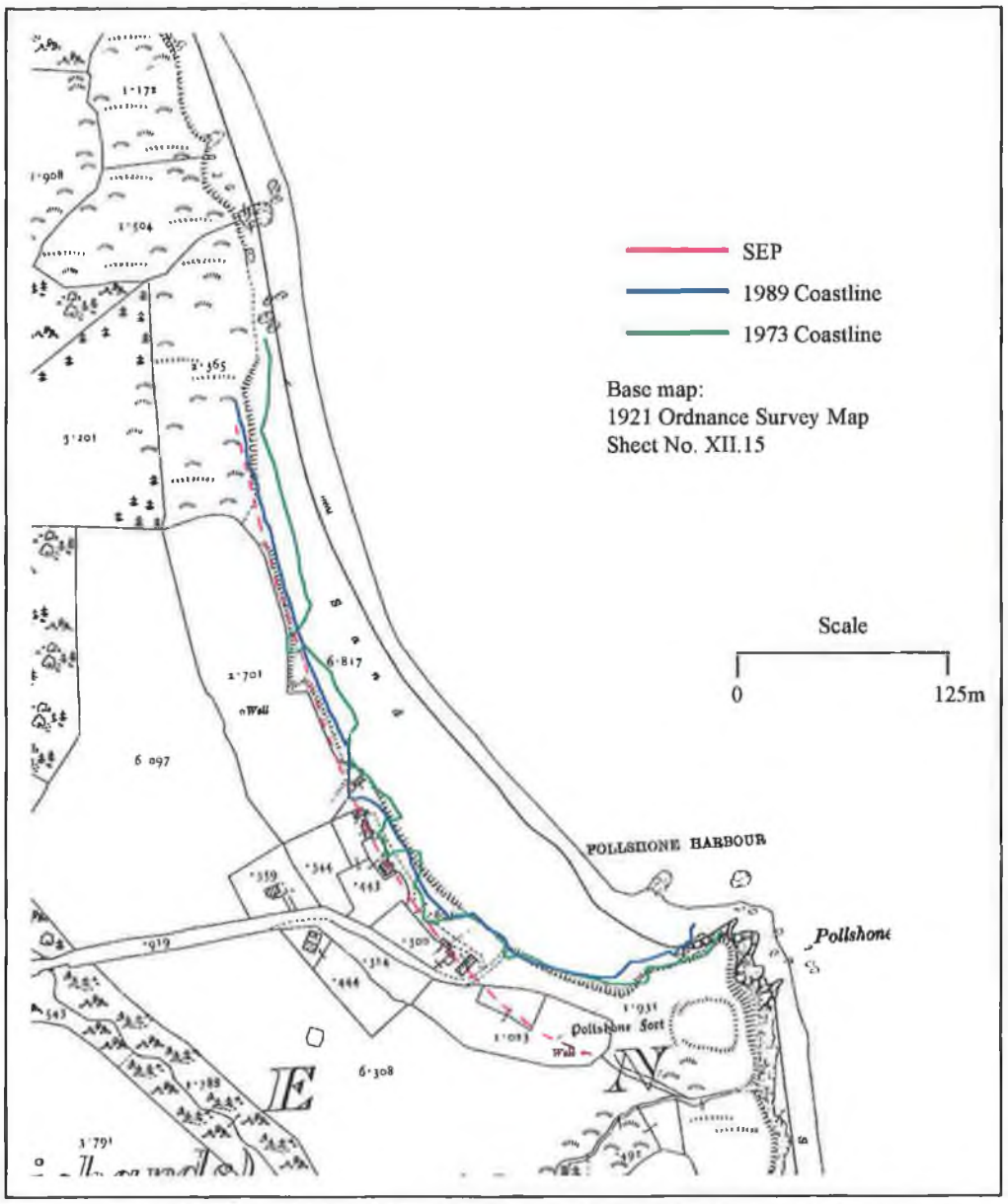

Fig. 4.25 - Historical position of coastline and vegetation lines at Pollshone

The 1989 vegetation line shows the coastline after the construction of the coastal defences in the 1980's. It follows closely the SEP up to the mid point of the bay and it is also very close to the original Ordnance Survey coastline from 1921.

4.2.2 Comparing the different SEP's

The difference between the values of the dominant wave approach angle β as calculated and measured using the two techniques results in widely different predictions for the SEP's of the three bays. The angle measured from the existing bay planforms indicate that the dominant waves come from a more easterly direction than was calculated using the refracted offshore waves method. The possible reasons for this discrepancy have been discussed in Section 4.1.3

The SEP's for the more southerly calculated wave direction cause the coastline to be more indented as the tangential section of the bay attempts to align itself normal to the approaching wave crests. In nature, however, there is usually not enough sediment to completely fill an indented bay and the coast retreats to a point where the bay is able to maintain a coastline position that is determined by waves which are diffracted about a prominent headland. These pocket bays are common on the higher energy western and southern coastlines of Ireland.

It should be noted that the downcoast control points selected for Courtown North were chosen on the basis of the present plan of the bay. This point would be located further north, probably at the northern headland, had the much altered bay, as predicted by the calculated wave direction, been used. The maximum indentation of this bay would

have been slightly greater than that indicated by the SEP drawn for downcoast control point **B** (Fig. 4.18).

The SEP's from the calculated wave values may indicate the extreme limit of coastal recession in the event of a complete cessation of longshore drift of sediment and in this regard it has it's use as a possible limit line for future developments. This scenario is, thankfully, far into the future and when it finally occurs the eastern seaboard will look more like the indented and headland controlled southern and western coasts.

For the shorter and medium term the SEP's based on the measured values of β are much more useful. They indicate the natural curvature of the bay, if nature is allowed to take it's course. The placement of rock revetments along lines that are inherently in dis-equilibrium cause their eventual failure as the beach in front narrows and the revetments become undermined. Continual maintenance and repair will be necessary to keep them effective.

4.3 The Effect of Climate Change and Coastal Protection Measures

4.3.1 Climate change

This section examines the effect of changes in the dominant wave direction caused by changes in storm pattern. From the wave rose (Fig. 4.1) and the wave energy plots (Figs. 4.9, 4.10, 4.11) it is clear that the coastline is dominated by waves from the south. The planform of the bays agree, with the control line of each bay being intercepted by a dominant wave direction from the south.

From the analysis of recent wind data there has been an increase in the number of severe storms and general storminess over the North Atlantic [52, 53]. With global warming, this is likely to continue. It is also possible that the tracks storms take will also alter. If the storms take a more southerly route then the anti-clockwise rotation of winds associated with these depressions will result in more south, south-easterly and easterly gales hitting the east coast [48].

However, the dominant swell in the south Irish sea will still enter along the St. George's Channel although the local winds will tend to turn it towards the west. This will result in the dominant wave direction shifting more towards the east then it would otherwise. Figs. 4.20, 4.21 and 4.22 show the effect this will have in the three bays.

The realignment of the coastline at Courtown North, shown in Fig. 4.20, indicates that the vulnerability to erosion of the southerly section of the bay will lessen as the dominant wave direction swings eastward and the angle β decreases from 17^0 to 13^0.

It is likely that the sediment required to realise this realignment will be obtained from the longshore drift as there will be a localised reversal of the predominant northward drift of sediment. This process will, however, take many years to complete. Indeed, over one hundred years have passed since the bay was thrown into dis-equilibrium by the construction of the harbour and the present coastline has not yet reached a balanced state. Admittedly, coastal protection measures have suspended the process somewhat.

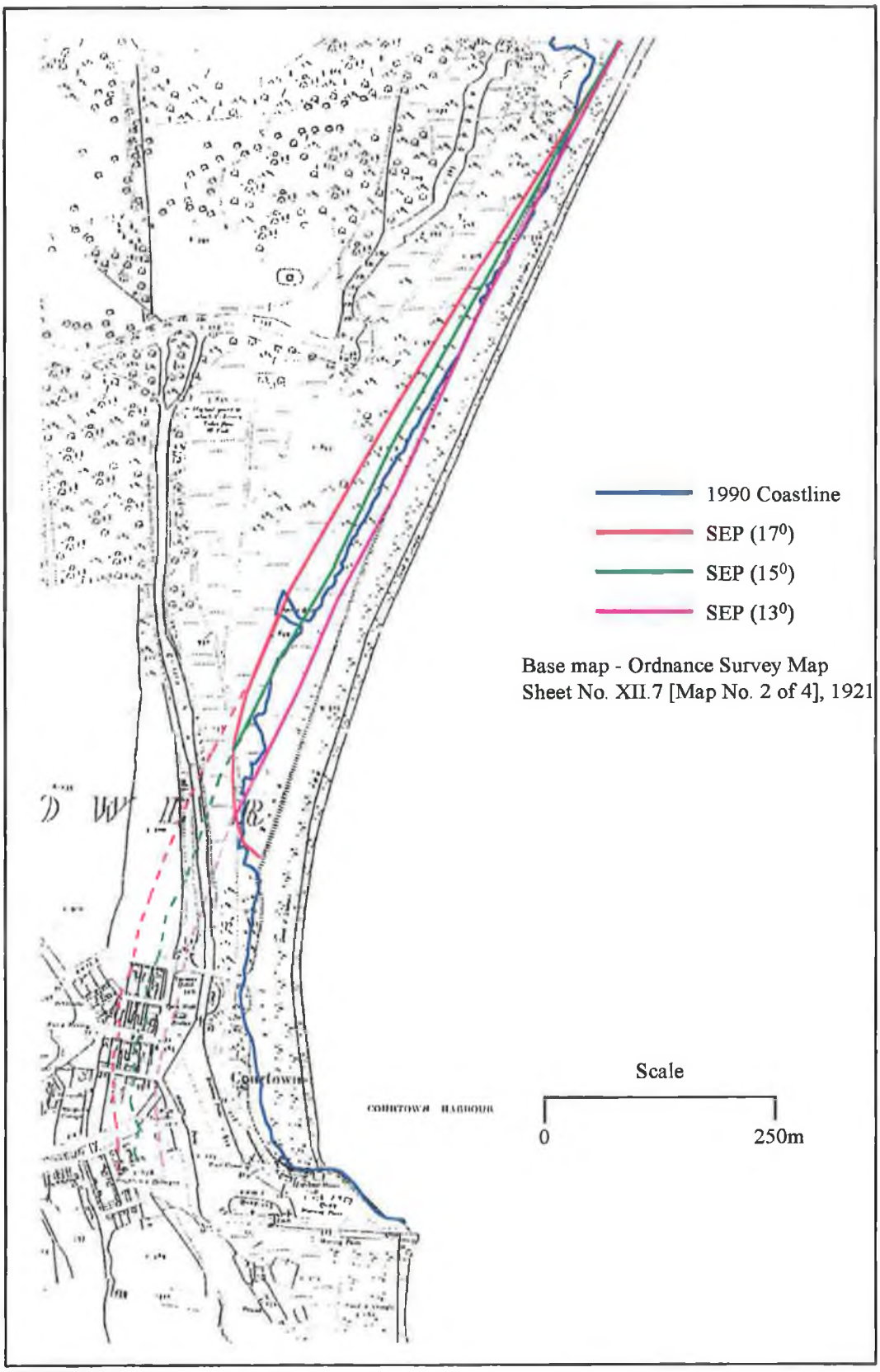

Fig. 4.26 - Realignment of Courtown North caused by changing dominant wave direction

The realignment will not be a steady one-directional process and it is likely that there will be continued events of storm erosion from time to time but averaged over a number of decades the coastline will first stabilise about a norm and gradually, in halted steps, advance seaward at the southern section.

Eventually, there will be less pressure on the coastal defences north of Courtown Harbour but areas in the extreme north of the bay may recede if they are seaward of the new SEP. Realignment of this tangential section will be the first evidence of a change in the dominant wave direction and this could be used as an indicator that change is occurring.

Fig. 4.27 shows a similar situation for Ardamine. As with Courtown North the downcoast control point may move northwards but this will be restricted by the nearby headland. Again the result of an easterly shift in the dominant wave direction will be the lessening of the vulnerability to erosion of the middle to southern sections of the bay.

Fig. 4.28 shows the situation for Pollshone. Here, because of the original more easterly approach of waves the effect of a further swing to the east is less pronounced. The difference between the maximum indentation of the coastline between the SEP for $\beta=29^0$ and $\beta=25^0$ is less than 10m. This will, however, lessen the vulnerability to erosion of the middle and southern sections of the bay.

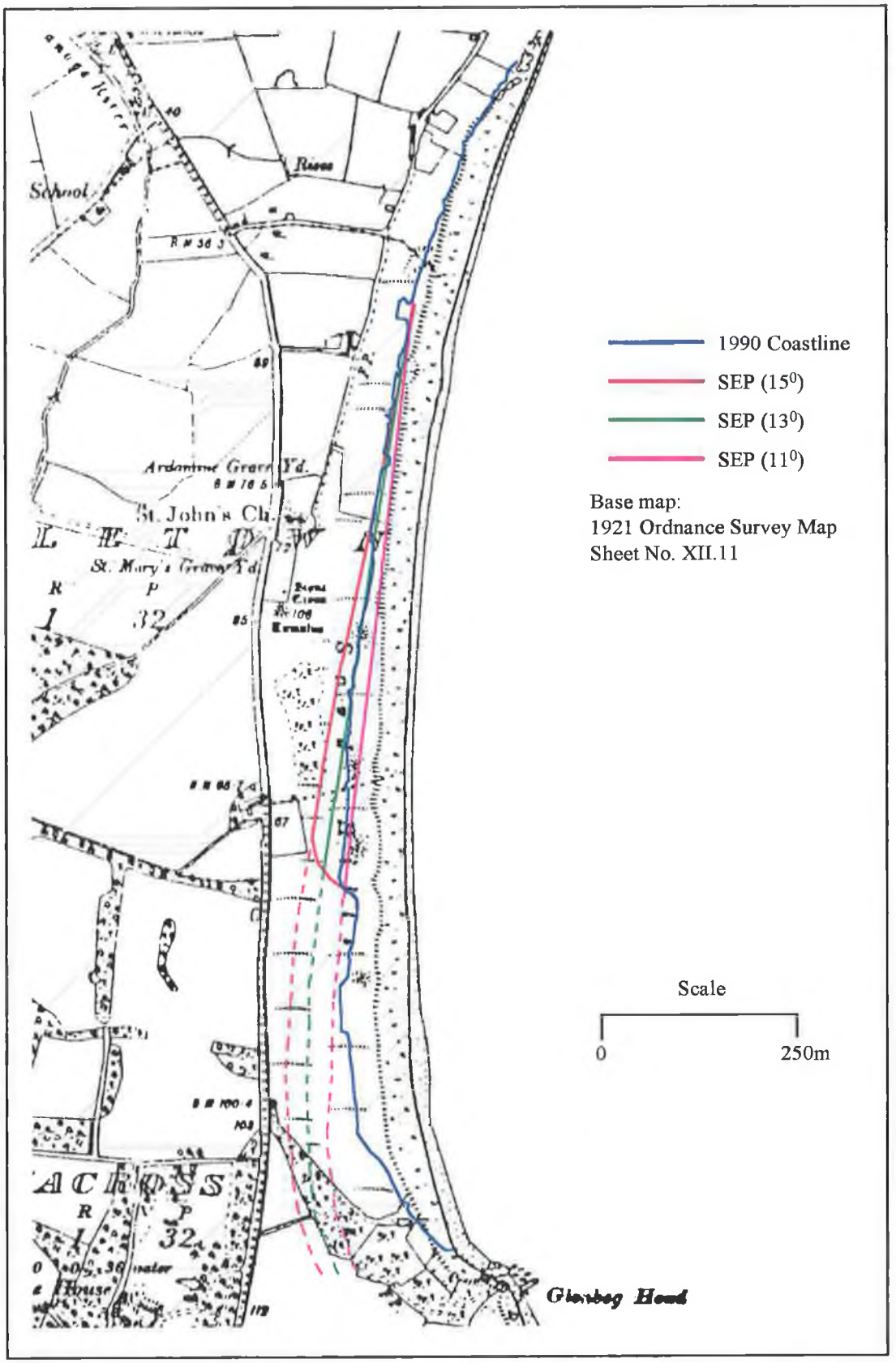

Fig. 4.27 - Realignment of Ardamine caused by changing dominant wave direction

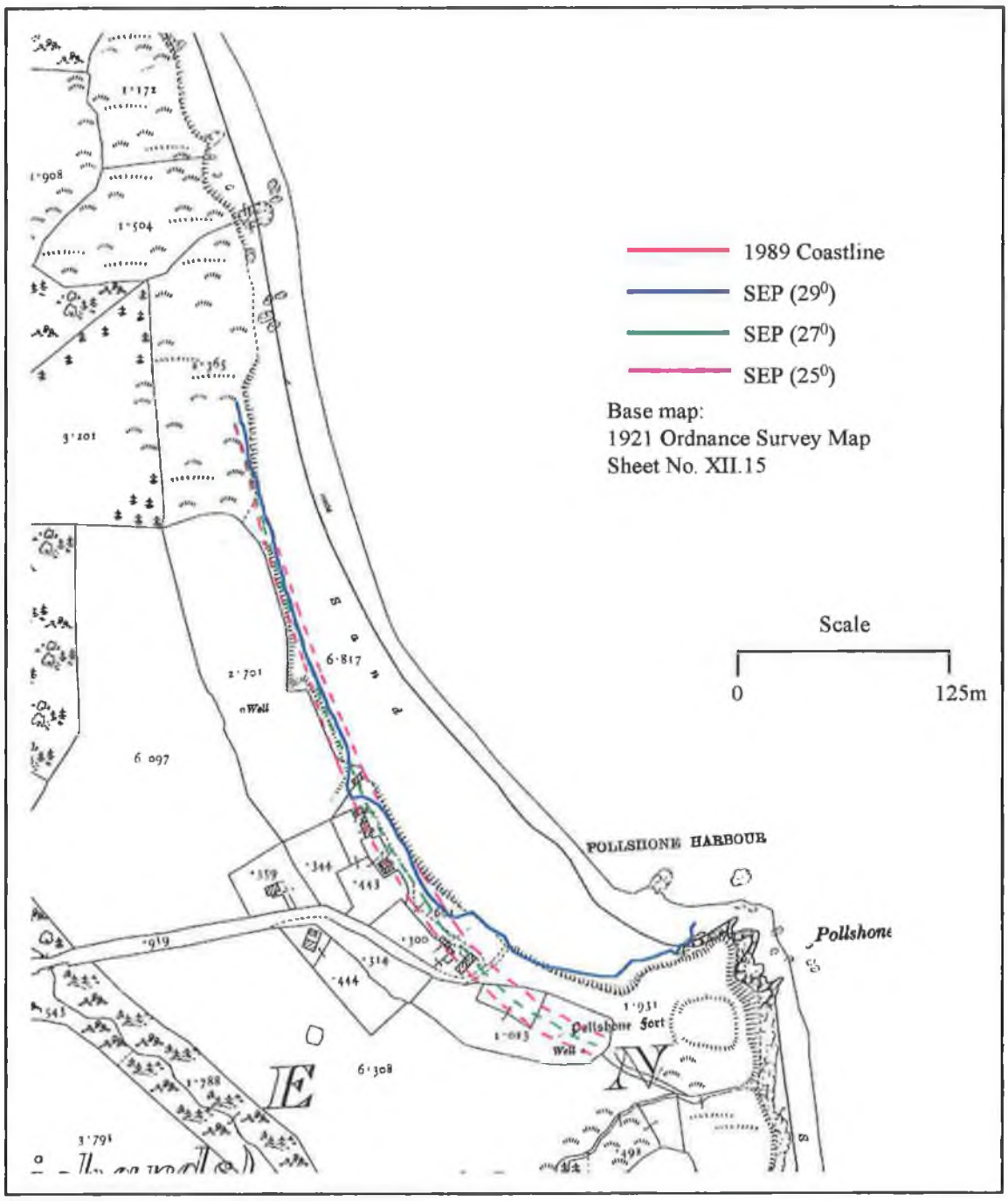

Fig. 4.28 - Realignment of Pollshone caused by changing dominant wave direction

4.3.2 Coastal protection measures

The impact of humans on the erosion patterns in the three bays is already evident particularly in Courtown North where the shift in the position of the upcoast control point caused by the building of the harbour walls has caused the coastline to realign

itself. In Ardamine, the placement of rock revetments along a line that is inherently in dis-equilibrium with present day forces may have accelerated the erosion rate of unprotected downcoast areas.

The current policy of the local authority to continue to chase the erosion problem downcoast will eventually mean that all of the soft coast within the bays will be protected with rock. If the line adopted is seaward of the predicted SEP then the beach in front will narrow and the rock will be in danger of being undermined. The example set by the coastal protection works in Pollshone should be followed as the line chosen follows closely the present day SEP.

The other major effect of humans is from recreational usage of the sand dune areas and the heavier usage of access routes. Areas denuded of vegetation are vulnerable to wind erosion which, by blowing sand inland, reduces the amount available to act as a buffer against the sea. This sand is extremely effective at remaining within the coastal system as it has been sorted over the millennia to be the optimum grain size for the local wave energy field. As such it is the ideal medium to move between sand bar, beach and dune. Vegetation, particularly marram grass, collects the sand blown from the beach and builds firstly, embryo dunes and eventually full sand dune systems.

Courtown North exhibits the effect of recreational pressure with the heavily used southern section of the bay showing the greatest vegetation line retreat. As the sand from these areas has been blown inland the inherent instability in the present coastline position has been exploited by the sea and the coastline has retreated. The ability of these areas to self repair in the aftermath of storms where dislodged clumps of marram

would restart the building of the dunes is severely curtailed by the dearth of vegetation. Although coastal recession in this area is inevitable the rate of erosion has probably been accelerated as a result.

The species of vegetation is also a factor in the rate of coastal erosion. Marram and other grasses are the only vegetation capable of building dunes. A thorny shrub, sea buckthorn, was introduce to this area at the beginning of this century and has spread extensively in Courtown North. While this plant prevents people from using the dunes thus protecting the area from trampling, it is incapable of trapping sand and creating dunes. Therefore, when an area is eroded by the sea there is little chance of it being naturally rebuilt. These plants have also concentrated people onto the few access routes remaining and the effect of this can be seen in the bare sand areas of Courtown North (Fig. 4.16) and Ardamine (Fig. 4.20).

4.4 General Discussion

The parabolic curve method of predicting the equilibrium position of the coastline tested in this study is essentially the result of a curve fitting statistical exercise applied to data obtained under laboratory conditions. The resultant formula, although potentially very useful to coastal engineers, is limited in its application because of the governing condition that there should be no longshore drift of sediment and that the bay is in a state of static equilibrium. Dynamic equilibrium bays where there is a longshore drift will have a coastline seaward of the predicted SEP but, to date, there is no method by which the amount of longshore drift can be used to indicate the amount of

dislocation of the coastline position. Nor, conversely, can the dislocation be used to estimate longshore drift although, in theory, both should be possible.

Applying the technique to conditions for which it was not designed leads to difficulties in identifying what is the true cause of discrepancies in the results. The wave approach angles as indicated by the planforms for each bay differ from one another to a much greater degree than can be explained by wave refraction. This is probably due to variations in longshore drift rate in the bays or the sediment may be by-passing sections of the bays. The presence of offshore bars, particularly in Courtown north and Ardamine, created by the longshore drift further complicates the problem.

If the planform of the bay cannot be used as a true indication of wave approach angle because of these problems, the question arises as to whether the offshore wave analysis method is a more accurate technique. This method has as many if not more complications. It firstly relies heavily on the accuracy of the wave data itself. Hindcast wave data generated by a computer is only as accurate as the original input data and the computational process will allow. The timespan covered may not include significant storm events which often alter the coastline to such a degree that their effect can still be observed decades later. Bringing the offshore data inshore is another potential source of error. Wave refraction analysis, especially in nearshore and surf zone areas requires accurate bathymetric data which often does not exist or is out of date. Sand bars, for example usually migrate about the bay.

As mentioned previously, there is also the possibility that bays are shaped more by waves that occur over long periods rather than the high energy storm. This would have

the effect of swinging the calculate wave direction towards the east which would more closely match the values obtained from the bay planforms. Further investigation of various weighting systems applied to the wave energy analysis might help to answer these questions.

This problem of the true wave approach angle lies at the heart of a successful application of the technique. In zero longshore drift bays, the planform wave angle can be relied upon. However in longshore drift coastlines there is no precise method currently available. If the bay planform method is used (and it seems the most accurate at present) then there will be an underestimation of how far a bay will erode in the event of cyclical changes in the longshore drift rate. The wave energy method, tested here, does not seem to give valid results, although with further research it should be possible to refine the technique.

It remains to assess the value of the new parabolic curve method in longshore drift coastlines. Firstly it is a simple method of determining whether a bay is following a contemporary 'natural' curve. As has been demonstrated in the present study, the bay curves, predicted by the formula, are easily created using the devised spreadsheet formula and graph. The location of the control points is more difficult but with practice problems can be overcome. Comparing the present coastline position with the predicted coastline allows the current vulnerability of coast to erosion to be gauged by noting the degree of deviation of the present coastline from the predicted 'natural' curve. The reasons why a bay's coastline does not follow its 'natural' curve can be both man-made (structures intruding into the bay such as harbours and training walls or an

inherently unstable coastline position may have been hardened with rock armour or gabions) or natural rock outcrops within the bay.

Secondly the technique can be used to accurately predict the effect structures will have on the coastline. This could be especially useful when considering new harbour developments, harbour extensions or river training walls. As the method has shown, small changes in the location of the upcoast control point can have dramatic implications on the position of the coastline.

Thirdly it can be used to gauge the impact of changes in wave approach angle caused by changes in wind climate. As shown in this study, an increase in easterly storms will make the southern portion of the bays less vulnerable to erosion as the 'natural' curve in this area will advance seaward. However, the resultant increased wave energy now arriving at this end of the bay means that the 'natural' curve line should be attained more quickly.

5. CONCLUSIONS

5.1 Conclusions

- The new parabolic curve technique used to predict the eventual stable position of the coastline examined in this study is limited in its application because of the governing condition that there should be no longshore drift of sediment into or out of the bay.

- If this condition is satisfied then the technique can be used successfully to examine how future changes within the bay will effect the position of the coastline. Such changes may be the construction of coastal protection works or changes in the wind and wave climate.

- In open coastal areas where there is a longshore drift of sediment the technique may be used to predict the 'natural' curvature of a bay created by the existing conditions. This coastline is likely to be unstable in the long term and would be dependent on the continuation of the present supply of sediment to the bay. Deviations from this curve may indicate areas that are vulnerable to erosion.

- The technique is easier to apply than earlier coastline prediction methods and should see more widespread use. It is particularly suitable for determining coastal set back lines and, being based on physical model tests, it is a more scientific approach than the arbitrary selection process used heretofore.

5.2 Recommendations

Although created primarily for crenellate shaped bays the new parabolic curve technique has the potential, at least in theory, to be applicable to all headland controlled bays. This would allow the examination of many of the recessed pocket beaches on the west coast of Ireland and bays enclosing a sand spit formation. Since most of these should be in a static equilibrium condition the curves drawn should accurately predict the present day coastline position. Situations where there is a deviation from this line could be examined and causes investigated. The degree of dislocation from the natural curve could be used to prioritise expenditure on coastal protection works or to determine development control set back lines.

It would be interesting to apply the technique to as many and as varied a number of bays as possible and to document the findings. This, along with the mapping of the historical evolution of the coastline and vegetation line should give a clear insight into the nature of the problem or perceived problem of coastal erosion.

In bays which are in a state of dynamic equilibrium the technique is still valid in determining the current 'natural' curve of the bay. However if the method could be refined to use wave data to determine the true dominant wave direction then the predicted SEP for these bays would be very useful. Dynamic equilibrium bays are much more susceptible to erosion as longshore drift rates fluctuate or stop altogether. Knowing where the coastline will eventually settle down would be an extremely valuable piece of information to coastal engineers and local authority planners alike. Further research into this problem using weighting schemes or filters on the wave data

might be the way forward and is something that could be completed within a relatively short time. It may not, however, be possible to create a generic formula for all bay types although with an 'expert' computer system to assist, a multi-formula method could be made user friendly.

LIST OF REFERENCES

1. EOLAS, (1992). Coastal Management - A case for action. On behalf of the County and City Engineers Association. Eolas [Forbairt], Glasnevin, Dublin 9, Ireland.
2. Silvester, R. and Ho, S-K. (1972). Proceedings from the 13th Coastal Engineering Conference, , American Society of Civil Engineers, New York, USA, pp. 1347-1364.
3. Inman, D. L. (1974). 'Ancient and Modern Harbors: A Repeating Phylogeny'. Proceedings from the 14th Coastal Engineering Conference, American Society of Civil Engineers, New York, USA, pp. 2049-2067.
4. Brunn, P. (1972). 'The History and Philosophy of Coastal Protection'. Proceedings from the 13th Coastal Engineering Conference, American Society of Civil Engineers, New York, USA, pp. 33-74.
5. Commission of the European Communities, (1992). Towards Sustainability. A European Community Programme of Policy and Action in relation to the Environment and Sustainable Development. Office for Official Publications of the European Communities, Luxembourg.
6. Carter, R. W. G., (1988). Coastal Environments - An Introduction to the Physical, Ecological and Cultural Systems of Coastlines, Academic Press, London.
7. CERC, Coastal Engineering Research Center, US Army Corps of Engineers, (1973). Shore Protection Manual, 2nd edition. Government Printing Office, Washington, D. C., USA.
8. Kamphuis, J. W., Davies, M.H., Nairn, R.B. & Sayao, O.J. (1986). 'Calculation of littoral sand transport rate'. Coastal Engineering, vol. 10 pp. 1-21.

9. Van Hijum, E. & Pilarczyk, K.W. (1982). 'Equilibrium profile and longshore transport of coarse material under regular and irregular wave attack'. Publication No. 274, Delft Hydraulic Laboratory, Netherlands.

10. May, J. P., and Tanner, W. F., (1973). 'The littoral power gradient and shoreline changes'. In Coastal Geomorphology, edited by D. R. Coates, New York: Binghamptom. State University, pp 43-61.

11. Lowry, P. and Carter, R.W.G. (1982). 'Computer simulation and the delimitation of littoral power cells on the south coast of Co. Wexford'. In Journal of Earth Science, Royal Dublin Society, vol.4, pp. 121-132.

12. Johnson, T. W., (1984). 'Longterm Sediment Supply, Sediment Transport and Shoreline Evolution on 'Open' and 'Closed' Cellular Coasts'. PhD Thesis, The University of Ulster.

13. Davies, J.L. (1974). Australian Geographical Studies. 12, pp. 139-151.

14. Harlow, D.A. (1979). Quart. Journal of English Geology. 12, pp. 257-265.

15. McCave, J.N. & Geiser, A. C. (1978). 'Megaripples, ridges and runnels on intretidal flats of The Wash, England'. Sedimentology 26, 353-369.

16. Stapor, F.W. Jr. and May, J.P. (1983). Marine Geology, 51, pp. 217-237.

17. Davies, J.L. (1972). Geographical Variation in Coastline Development. Oliver and Boyd, Edinburgh.

18. Lewis, V.W. (1938). 'The Formation of Dungeness Foreland'. Geographical Journal 80, pp. 309-324.

19. Jennings, N. (1955). 'The Influence of Wave Action on Coastal Outline in Plan'. The Australian Geographer, Vol. 6, pp. 36-44.

20. Davies, J.L. (1958). 'Wave Refraction and the Evolution of Shoreline Curves'. Geophysical Studies, Vol. 5, pp. 1-14.

21. Komar, P.D. (1973). 'Computer models of delta growth due to sediment input from rivers and longshore transport'. Bulletin of the Geological Society of America 84, pp. 2217-26.

22. Hanson, H. & Kraus, N.C. (1989). 'GENESIS - a Generalised Shoreline Change Numerical Model'. Journal of Coastal Research, vol. 5 No. 1, pp. 1-27.

23. Bakker , W.T., Klein Breteler, E.H.J. & Roos, A. (1970). 'The dynamics of a coast with a groyne system'. Proceedings from the. 12th Coastal Engineering Conference, American Society of Civil Engineers, New York, USA, pp. 1001-1020.

24. Perlin, M. & Dean, R.G. (1983). 'A Numerical Model to Simulate Sediment Transport in the Vicinity of Coastal Structures'. Misc. report No. 83-10, Coastal Engineering Research Centre US Army Corps of Engineers.

25. Berenguer, J.M. & Enriques, J. (1988). 'Design of pocket beaches: the Spanish case'. Proceedings from the 21st Int. Coastal engineering Conference, , American Society of Civil Engineers, New York, USA.

26. Krumbein, W.C. (1944). 'Shore processes and beach characteristics'. Technical Memorandum No.3. U.S. Corps of Engineers, Beach Erosion Board,.

27. Silvester, R., Tsuchiya and Shibano (1980). 'Zeta Bays, Pocket Beaches and Headland Control'. Proceedings from the 17th Coastal Engineering Conference, American Society of Civil Engineers, New York, USA, 1981, Part 2, Chapter 79, pp. 1306-1319.

28. Yasso, W. E., (1965). 'Plan Geometry of Headland Bay Beaches'. Journal of Geology, Vol. 73, pp. 702-714.

29. Silvester, R. (1974). Coastal Engineering II. Elsevier, Amsterdam, Netherlands.

30. Silvester, R. and Hsu, J.R.C. (1993). Coastal Stabilisation. P.T.R. Prentice Hall, Inc., N.J., USA.

31. Rea, C.C. and Komar, P.D. (1975). 'Computer simulation models of a hooked beach shoreline configuration'. Journal of Sedimentary Petroleum, vol.45, pp. 866-872.

32. Walton, T.L. (1977). 'Equilibrium shores and coastal design'. Coastal Sediments '77. , American Society of Civil Engineers, New York, USA, pp. 1-16.

33. LeBlond, P.H. (1979). 'An explanation of the logarithmic spiral plan shape of headland-bay beaches'. Journal of Sedimentary Petrology, vol.49, No. 4, pp. 1093-1100.

34. LeBlond, P.H. (1980). 'Model studies of headland-bay beaches'. Proceedings from Canadian Coastal Conference, Burlington, Ontario, pp. 353-366.

35. Phillips, D. A. (1985). 'Headland-Bay Beaches Revisited: An Example From Sandy Hook, New Jersey'. Marine Geology, Vol. 65, pp. 21-31.

36. Mashima, Y., (1961). Stable configuration of coastline. Coastal Engineering in Japan 4: 47-59.

37. Ho, S-K., (1971). 'Crenulate shaped bays'. Master Eng. Thesis, No. 346, Asian Institute of Technology.

38. Hsu, J.R.C. and Evans, C., (1989). 'Parabolic bay shapes and applications'. Proceedings from the Institution of Civil Engineers, vol.87: pp. 557-70.

39. Kirk, McClure, Morton, Consulting Engineers, Belfast (1996). 'Courtown/Ardamine Beach Study'. Report prepared for Wexford County Council.

40. Dollard, Brendan (1997). 'Erosion assessment and protection measures using ECOPRO guidelines at two demonstration sites in Ireland'. Report prepared for STOA programme, European Parliament.

41. Ebersole, B. A., Cialone, A., & Prater, M. D., Coastal Engineering Research Centre, Corps of Engineers, US, 1986. Regional Coastal Processes Numerical Modelling System. Department of the Army, US Army Corps of Engineers, Washington, DC.

42. Ross, C.H. Meteorological Office, U.K.,(1988). Operational numerical weather prediction system - The operational wave models. Unpublished paper, doc. paper 5.1.

43. Khandekar, M.L., (1989). 'Operational Analysis and Prediction of Ocean Wind Waves'. Coastal and Estuarine Studies, No. 33. Springer-Verlag New York.

44. The Sea Wave Modelling Project (SWAMP) Group, J. H. Allender, T. P. Barnett, L. Bertotti, J. Bruinsma, C. V. Cardone, J. Ephraums, B. Golding, A. Greenwood, J. Guddal, H. Günter, S. Hasselmann, K. Hasselmann, P. Joseph, S. Kawai, G. J. Komen, L. Lawson, H. Linne, R. B. Long, M. Lybanon, E. Maeland, W. Rosenthal, Y. Toba, T. Uji and W. J. P. de Voogt, (1985). Ocean Wave Modelling - Principal Results and Conclusions. Plenum Press, New York.

45. WAMDIG: The WAM (Wave Model) Development and Implementation Group, S. Hasselmann, K. Hasselmann, E. Bauer, L. Bertotti, C. V. Cardone, J. A. Ewing, J. A. Greenwood, A Guillaume, P. A. E. M. Janssen, G. J. Komen, P. Lionello, M. Reistad, and L. Zambresky, (1988). 'The WAM Model - a third generation ocean wave prediction model'. Journal of Physical Oceanography, Vol. 18, No. 12, pp. 1775-1810.

46. Murphy, K., Walsh, J., (1991). Development of Sea Wave Propagation System. Final year project, Computer Applications, Dublin City University.

47. Smith, R. and Sprinks, T., (1975). 'Scattering of Surface Waves by a Conical Island'. Journal of Fluid Mechanics, Vol.87, No.WW4, pp. 529-548.

48. Descartes, R., (1637). Snell's Law first published by Descartes in Discours de la méthode pour bien conduire sa raison et chercher la vérité dans les sciences, Leyden.

49. Dollard, B., Forbairt (1996). ECOPRO Environmentally Friendly Coastal Protection - Code of Practice. Government Publications, Ireland.

50. Airy, G. B., (1845), 'On Tides and Waves'. Encyclopedia Metropolitana, London, pp. 241-396.

51. The International Panel for Climate Change, (1990). Climate Change: The IPCC scientific assessment. Cambridge University Press.

52. Devoy, R.J.N., (1990). 'Sea-level changes and Ireland'. In Technology Ireland, 22(5), pp. 24-30.

53. Bacon, S. & Carter, D.J.T., 1991. 'Wave Climate Changes in the North Atlantic and North Sea'. International Journal of Climatology, 11, 1991.

54. Deutscher Wetterdienst, 1994. Annual Bulletin of Climatology. WMO region VI. Deutscher Wetterdienst, Hamburg, Germany.

APPENDIX

SCATTER Programme - Creates Hs-Tz scatter tables from wave data

```
01  !*************************************************************************
    !***   CALCULATION OF HS V TZ SCATTER TABLES USING DIRECTION    ***
    !***          PERIOD AND SIG. WAVE HEIGHT                 ***
    !*************************************************************************
    !*************************************************************************

05  !*************************************************************************
    !***                INITIALISE                       ***
    !*************************************************************************

    DIM HS(8000) \DIM TZ(8000) \DIM DIR(8000)
    DIM HS1(8000) \DIM TZ1(8000) \DIM DIR1(8000)
    DIM SC(30,30)
    ON ERROR GOTO 10000


10  !*************************************************************************
    !***                  INPUTS                         ***
    !*************************************************************************

    PRINT ESC;"[2J"
    FOR AST=1 TO 80 \PRINT '*'; \NEXT AST

    FOR AST=1 TO 80 \PRINT '*'; \NEXT AST
    PRINT\PRINT\PRINT

!   INPUT 'FILENAME                          ';FILE$
    FILE$="CO9394.PRN"
    INPUT 'RANGE OF WAVE DIRECTION TO BE ANALYSED  (FROM)';DIR1
    INPUT '                        (TO INCL.)';DIR2
    PRINT
    FOR AST=1 TO 80 \PRINT '*'; \NEXT AST

20  !*************************************************************************
    !***            OPEN AND DIMENSION FILE                ***
    !*************************************************************************
    M=1 \Z=1
    OPEN FILE$ FOR INPUT AS FILE #1%
21   LINPUT #1%,TXT$
!       print txt$
    HS(M)=VAL(SEG$(TXT$,1,8))
    TZ(M)=VAL(SEG$(TXT$,9,17))
    DIR(M)=VAL(SEG$(TXT$,18,25))
!       PRINT HS(M),TZ(M),DIR(M)
    N=M \M=M+1
22   GOTO 21

30  !*************************************************************************
    !***      CREATE HS & TZ ARRAYS FOR SPECIFIC DIRECTION      ****
    !*************************************************************************
    M=1
    FOR NO=1 TO N
        IF DIR(NO)=0 THEN GOTO 40 \END IF
        IF DIR(NO)>DIR1 AND DIR(NO)<=DIR2 THEN
        TZ1(M)=TZ(NO) \HS1(M)=HS(NO) \DIR1(M)=DIR(NO)
        TOT=M \ M=M+1 \END IF
40   NEXT NO
50   !FOR Z=1 TO TOT
!       PRINT DIR1(Z),TZ1(Z),HS1(Z)
    !NEXT Z
100 !*************************************************************************
    !***            CALCULATE HS - TZ SCATTER             ****
    !*************************************************************************
```

```
    X=1

    FOR X=1 TO TOT
        FOR T=0 TO 28
            IF HS1(X)>=(T/2) AND HS1(X)<((T/2)+0.5) THEN 110
            ELSE 150
110           FOR W=1 TO 28
                IF TZ1(X)=>(W-1) AND TZ1(X)<(W)
                THEN SC(T,W)=SC(T,W)+1
                END IF
            NEXT W
150       NEXT T
    NEXT X

500 !*************************************************************************
    !***              PRINT  HEADER                    ****
    !*************************************************************************
!   INPUT 'SET PRINTER TO TOP OF FORM';RET$ \SLEEP 3%
    PRINT\PRINT\PRINT
    FOR AST=1 TO 80 \PRINT '*'; \NEXT AST \PRINT
    PRINT TAB(5);'SCATTER DIAGRAM  -  FOR WAVE DIR. BETWEEN ';DIR1;' & ';DIR
2;' DEGREES'
    FOR AST=1 TO 80 \PRINT '*'; \NEXT AST \PRINT
    PRINT 'SIG.';TAB(6);'*'
    PRINT 'WAVE';TAB(6);'*'
    P=0
    FOR T=28 TO 0 STEP -1
        PRINT T/2;TAB(6);'*';
        FOR W=1 TO 15
            PRINT TAB(P+10);SC(T,W);
            P=P+4
        NEXT W
        P=0
        PRINT
    NEXT T
    FOR AST=1 TO 80 \PRINT '*'; \NEXT AST \PRINT
    PRINT TAB(11);'1';
    FOR W=1 TO 14
        PRINT TAB(P+14);(W+1);
        P=P+4
    NEXT W

    PRINT\PRINT TAB(26);'ZERO UP-CROSSING PERIOD'
550   PRINT\PRINT\PRINT
    FOR AST=1 TO 80 \PRINT '*'; \NEXT AST \PRINT
    PRINT TAB(5);'SCATTER DIAGRAM  -  FOR WAVE DIR. BETWEEN ';DIR1;' & ';DIR
2;' DEGREES'
    FOR AST=1 TO 80 \PRINT '*'; \NEXT AST \PRINT
    PRINT 'SIG.';TAB(6);'*'
    PRINT 'WAVE';TAB(6);'*'
    P=0
    FOR T=28 TO 0 STEP -1
        PRINT T/2;TAB(6);'*';
        FOR W=15 TO 28
            PRINT TAB(P+10);SC(T,W);
            P=P+4
        NEXT W
        P=0
        PRINT
    NEXT T
    FOR AST=1 TO 80 \PRINT '*'; \NEXT AST \PRINT
    PRINT TAB(11);'15';
    FOR W=15 TO 27
        PRINT TAB(P+14);(W+1);
        P=P+4
    NEXT W
```

```
    PRINT\PRINT TAB(26);'ZERO UP-CROSSING PERIOD'
    PRINT\PRINT\PRINT 'TOTAL NUMBER OF WAVES FROM THIS DIRECTION.....';
TOT
    pRINT\PRINT 'TOTAL NUMBER OF WAVES IN DATASET.....';N
600   GOTO 10010
10000 !*****************************************************************************
    !***              ERROR HANDLER                    ***
    !*****************************************************************************

    IF ERR=11 AND ERL=21 THEN M=1 \RESUME 30
    END IF
    PRINT ERT$(ERR);'AT LINE ';ERL


10010 !*****************************************************************************
    !***              PROGRAMME END                    ***
    !*****************************************************************************

    END
```

ALTER Programme - Creates new bathymetry grid from existing grid.

```
10        ON ERROR GOTO 10000
REM REM  THIS PROGRAM PROVIDES A METHOD FOR INTERPOLATING BATHYMETRY
REM REM  FROM ONE GRID TO ANOTHER.  FOR FULL INSTRUCTIONS SEE RCPWAV
REM REM  OPERATING MANUAL.
REM REM
REM REM  ************************************************************
15        DIM REAL OLD(300,300)
          DIM REAL NEW(300,300)

20     INPUT "OLD GRID X VALUES"; M
21     INPUT "OLD GRID Y VALUES"; N
22     INPUT "NEW GRID X VALUES"; M2
23     INPUT "NEW GRID Y VALUES"; N2
24     INPUT "ANGLE OF ROTATION (+ COUNTERCLOCK)"; ANG
25     INPUT "XSHIFT"; XSHIFT
26     INPUT "YSHIFT"; YSHIFT
27     INPUT "OLD GRID CELL SIZE - X DIRECTION"; DX
28     INPUT "OLD GRID CELL SIZE - Y DIRECTION"; DY
29     INPUT "NEW GRID CELL SIZE - X DIRECTION"; DX2
30     INPUT "NEW GRID CELL SIZE - Y DIRECTION"; DY2
          ANG=(ANG/180)*PI

100    INPUT "FILENAME FOR INPUT..."; FILIN$
120    INPUT "FILENAME FOR OUTPUT.."; FILOUT$
130    OPEN FILIN$ FOR INPUT AS #1
140    OPEN FILOUT$ FOR OUTPUT AS #2
rem                 map (lin)
rem                           line$=80%
REM      141    OPEN "FILTEST.DAT" FOR OUTPUT AS #3

142       G=N/10


149    FOR T = 1 TO N
150          LINPUT #1, LIN0$
151          C = 1
152          FOR I = 1 TO 20
155                LINPUT #1, LIN$
156             P = 1
160             FOR H = 1 TO 10
170                OLD(C,T)=VAL(MID$(LIN$,P,8))
                                IF C=M THEN 200
                                END IF
                           C = C + 1
                           P = P + 8
                   NEXT H
180          NEXT I
200    NEXT T


REM      201    FOR T = 1 TO N
REM            FOR C = 1 TO M
REM              PRINT #3, OLD(C,T)
REM           NEXT C
REM      202    NEXT T

REM      *******************************
REM      CREATE NEW XY GRID IN RELATION TO OLD XY GRID
REM      *******************************

300       S=0
```

```
350     FOR T=1 TO N2
            FOR G=2 TO M2
351             IF S=0 THEN X2=XSHIFT
                Y2=YSHIFT
                NEW(1,1)=OLD(X2,Y2)
                S=1
                END IF
                X2=X2+COS(ANG)
                Y2=Y2-SIN(ANG)
                NEW(G,T)=OLD(INT(X2),INT(Y2))
            NEXT G
            X2=XSHIFT + (SIN(ANG)*(T+1))
            Y2=YSHIFT + (COS(ANG)*(T+1))
            NEW(1,(T+1))=OLD(INT(X2),INT(Y2))
400     NEXT T

        MARGIN #2%, 80%

500     FOR T=1 TO N2
            PRINT #2%
            C=1
            FOR G=1 TO 20
                FOR H=1 TO 10
                    PRINT #2% using '######.##';NEW(C,T);
                    IF C=M2 THEN GOTO 600
                    END IF
                    C=C+1
                NEXT H
550         NEXT G
600         print #2%
        NEXT T

610     PRINT 'OK'
        GOTO 20000

10000   print 'error AT',ERL
        RESUME 20000

20000   end
```